SEMMELWEIS EGYETEM

DOKTORI ISKOLA

Ph.D. értekezések

2838.

SCHVARCZ CSABA ANDRÁS

A vérkeringési rendszer normális és kóros működésének mechanizmusai
című program

Programvezető: Dr. Benyó Zoltán, egyetemi tanár

Témavezető: Dr. Hamar Péter, egyetemi tanár

MULTIPLEX ASSESSMENT OF MODULATED ELECTRO-HYPERTHERMIA INDUCED LOCAL ACUTE-PHASE PROTEIN PRODUCTION IN MOUSE TNBC MODEL

PhD thesis

Csaba András Schvarcz

Doctoral School of Theoretical and Translational Medicine

Semmelweis University

Supervisor: Péter Hamar, MD, D.Sc

Official reviewers: Gyöngyvér Szentmártoni, MD, Ph.D

Éva Borbély, MD, Ph.D

Head of the Complex Examination Committee: György Reusz, MD, D.Sc

Members of the Complex Examination Committee: Tamás Radovits, MD, Ph.D

Ákos Jobbágy, PhD, D.Sc

Budapest
2023

List of content

Abbreviations

AC:	Alternating Current
AAT:	Alpha-1 Antitrypsin
AIF:	Apoptosis Inducing Factor
APPs:	Acute-Phase Proteins
APR:	Acute-Phase Response
ATP:	Adenosine Triphosphate
BC:	Breast Cancer
BL1:	Basal Like 1
BL2:	Basal Like 2
BW:	Body weight
cC3:	cleaved caspase-3
Cfb:	Complement factor B
Cfd:	Complement factor D (adipsin)
Cfp:	Complement factor P
CHPP:	Continuous Hyperthermic Peritoneal Perfusion
CR:	Complete Response
C1s1:	Complement component 1, s subcomponent 1
C4b:	Complement component 4B (Chido blood group)
DAB:	3,3′-diaminobenzidine
DAMP:	Damage-associated Molecular Pattern
DCIS:	Ductal Carcinoma in situ
DC:	Dendritic Cell
DCR:	Disease Control Rate
DE:	Differentially expressed
DMSO:	Dimethyl sulfoxide
DNA:	Deoxyribonucleic acid
ECM:	Extracellular Matrix
EMF:	Electromagnetic field
EMT:	Epithelial-mesenchymal Transition
ER:	Estrogen Receptor
Fb:	Fibrin
FC:	Fold Change
Fgb:	Fibrinogen beta chain
FGF:	Fibroblast Growth Factor
Fgg:	Fibrinogen gamma chain
FSH:	Follicle-stimulating Hormone
GO:	Gene Ontology
GPI:	Glucose-6-phosphate Isomerase
Hc:	Hemolytic complement
HCC:	Hepatocellular Carcinoma
HCD:	Higher-energy Collisional Dissociation
H&E:	Hematoxylin and Eosin
Her2:	Human epidermal growth factor receptor 2
HIFU:	High-Intensity Focused Ultrasound
HIPEC:	Hyperthermic Intraperitoneal Chemotherapy
Hp:	Haptoglobin

Hsf-1:	Heat shock factor-1
Hspa1a:	Heat shock 70 kDa protein 1A
Hspa1b:	Heat shock 70 kDa protein 1B
Hspb1:	Heat shock protein beta-1
Hsph1:	Heat shock protein 105 kDa
Hsp70:	70 kilodalton heat shock protein
HSR:	Heat Shock Response
IHC:	Immunohistochemistry
IM:	Immunomodulatory
Itih2:	Inter-alpha-trypsin inhibitor heavy chain H2
Itih4:	Inter-alpha-trypsin inhibitor heavy chain H4
LAR:	Luminal Androgen Receptor
LCIS:	Lobular Carcinoma in situ
LFQ:	Label-free Quantification
LPS:	Lipopolysaccharides
LR:	Local Response
mEHT:	modulated Electro-Hyperthermia
M:	Mesenchymal
MS:	Mass Spectrometry
MAC:	Membrane Attack Complex
MBL:	Mannose-Binding Lectin
MET:	Mesenchymal-epithelial Transition
mRNA:	messenger Ribonucleic Acid
MSL:	Mesenchymal Stem-like
NGS:	Next Generation Sequencing
NSCLC:	Non-small Cell Lung Cancer
PBS:	Phosphate Buffered Saline
PFS:	Progression-free Survival
PMN:	Polymorphonuclear Granulocyte
PR:	Progesteron Receptor
PRe:	Partial Response
p-TEFb:	positive Transcription Elongation Factor b
Ptx3:	Pentraxin related gene
RF:	Radiofrequency
RR:	Response Rate
rMA:	Relative mask area
RT PCR:	Reverse Transcription Polymerase Chain Reaction
SAR:	Specific Absorption Rate
SCID:	Severe Combined Immunodeficiency
SD:	Stable Disease
SEM:	Standard Error of the Mean

Serpina3c:	Serine (or cysteine) peptidase inhibitor, clade A, member 3C
Serpina3m:	Serine (or cysteine) peptidase inhibitor, clade A, member 3M
Serpina3n:	Serine (or cysteine) peptidase inhibitor, clade A, member 3N
TDR:	Tumor Destruction Ratio
TE:	Tris-EDTA
TME:	Tumor Microenvironment
TMM:	Trimmed Mean of M values
TNBC:	Triple-negative Breast Cancer
TPM:	Transcripts Per Million
US:	Ultrasound
UNS:	Unstable
WBH:	Whole Body Hyperthermia

1. Introduction

1.1. Hyperthermia in oncology

1.1.1. Principles of hyperthermia

Hyperthermia in oncological disease was first utilized by Hippocrates, when he successfully applied it to breast cancer patients (1). The primary application of medical hyperthermia is complementary, adjuvant treatment of tumors nowadays (2). Other applications include the eradication of parasites like Leishmania (3), the treatment of rheumatic autoimmune diseases like ankylosing spondylitis and fibromyalgia (4), autoimmune skin diseases like psoriasis (5) or Peyronie's disease (6).

Oncological hyperthermia means the heating of malignant tissues in the 40-48 °C range with curative or palliative intention. Higher temperatures can be used in oncological processes for coagulation (>50 °C) or thermal ablation (60-90 °C) (7), which are not discussed in detail in this dissertation. Based on the extension of heating, systemic and local/regional hyperthermia are distinguished. Blood is heated up during systemic hyperthermia, which conductively warms up the malignant tissue (8). On the other hand, during local/regional hyperthermia, energy/heat is applied directly to the tumor, while the rest of the body remains at body temperature, including blood, therefore blood flow acts as a cooling medium (8). Heat can be transmitted via conduction (diffusion), convection (invasive or semi-invasive) or radiation (infrared heating, microwaves or radiowaves) (9) or can be generated by mechanical waves (ultrasound) (7).

Hyperthermia can induce numerous biological processes in tumors on tissue, cellular and molecular levels. *On the tissue level*, the higher basal metabolism of tumors than healthy tissues and local blood-flow regulation are the basis of hyperthermia effects. Tumor heating elevates the already high metabolic rate. The oxygen and nutrient supply cannot keep up with the enhanced demand, resulting in hypoxia and anaerobic metabolism. This leads to the accumulation of acidic metabolic intermediates and consequent acidosis within the tumor. Similarly, in expanded tumors, the poorly vascularized central regions do not get enough oxygen leading to spontaneous hypoxic necrosis. The aimed temperature by tumor heating is critical regarding blood flow: over 42 ^{o}C, blood flow is reported to decrease, whereas below 42 ^{o}C, blood flow is

demonstrated to increase (10) in tumors. *On the cellular and molecular level*, hyperthermia is reported to induce

- DNA repair inhibition by the denaturation of DNA repair proteins (10)
- heat shock response (11)

The DNA-repair inhibition and exhaustion of the heat shock response become irreversible after a certain point leading to

- cell cycle arrest (12)
- different types of cell death (such as necrosis, apoptosis (extrinsic and intrinsic) and other types of cell death) (13).

One of the main challenges of hyperthermia treatment is the focus of treatment and the transfer of heat to malignancies localized in deeper tissues.

Hyperthermia in oncological treatment is used as a complementary treatment in general: it can enhance and complete the effects of conventional oncological treatments like chemo- (14), radio- (15), targeted (16) and immunotherapy (17). Intravenously administered chemotherapeutic drugs are most effective in the well-vascularized areas, where the bioavailability of the drug is the highest, while hyperthermia is more effective in hypoxic, low-vascularized regions of the tumor (9). Moreover, hyperthermia agents exert their effects in the S phase of the cell cycle, while widely used chemotherapeutic agents, like taxanes and anthracyclines are more likely to act in the M and G_2 phases (18). The vasodilatation effect of hyperthermia can enhance drug delivery of intravenously applied chemotherapeutic agents by increasing blood flow (19) and even the absorption of drugs can be improved by hyperthermia via electro-osmosis (20). Radiotherapy efficacy is also higher in well-oxygenized parts of the tumor, where oxygen supports the formation of DNA-damaging free radicals. The increased cell killing effect of hyperthermia + radiotherapy combinational therapy is primarily due to an increase in the PO_2 in tumors by hyperthermia-induced vasodilatation (21). Furthermore, similarly to chemotherapy, radiotherapy acts during proliferation in the M and G_1 phases of the cell-cycle, whereas hyperthermia in the S phase (18). The mechanisms of synergism between hyperthermia and chemo- or radiotherapy are listed in Table 1.

Table 1. Synergistic mechanisms between hyperthermia and chemo-/radiotherapy. Modified from the original table from Szasz et al., 2011 (8).

Modality / Effect	Hyperthermia	Chemotherapy	Radiotherapy
Effect on cell cycle	effective in S phase 'push out' cell from G_0 phase	effective in M + G_2 phase no activity in G_0 phase	effective in M + G_1 phase
pH dependency	effective in acidic environment	-	effective in alkaline environment
Oxygenation, vascularization	effective in hypoxic regions, further from vessels	effective in regions, close to vessels	effective in well-oxygenized regions
Drug absorption	enhanced by electro-osmosis	low, due to high pressure	-
Drug metabolism	enhanced	normal	-
Reaction rate	enhanced	normal	-

Regarding the expansion of heating, three main types of medical hyperthermia are used: Whole body hyperthermia (WBH), regional and local hyperthermia.

1.1.2. Whole-body hyperthermia

Whole-body hyperthermia (WBH) is mostly used in metastatic cancer diseases. It is diffuse heating of the patient's body. Thermal chambers, hot water blankets or infrared radiation are used to warm up the whole body at around 41.8-42.2 °C. The procedure is usually performed under anesthesia for 3-4 hours (39.5-41.0 °C) or for 2 hours as an intensive (42 °C), short treatment. WBH results in a homogenous thermal distribution; thus it has the most adverse effects of all hyperthermia forms. Adverse effects include nausea, vomiting, diarrhoea and the thermal stress of vital organs such as the heart, the lung, the liver and the brain (22). Further side-effects include disconcertment of blood pressure regulation, blood clotting, systemic skin irritation, etc. WBH is often used in combination with fever generation by IL-2 and/or IFN-γ. The hypothetic beneficial mechanism includes the non-specific activation of the immune system (23).

1.1.3. Regional hyperthermia

Regional hyperthermia means the heating up of extensive body areas containing the tumor. Tumors of the pelvis, thighs (soft tissue sarcomas) or abdominal malignancies (cervical, prostate, bladder, colorectal, ovarian carcinomas) are treated this way. Three subtypes of regional hyperthermia exists: deep-positioned tumors heated with external

applicators; limbs or organs heated by thermal perfusion and continuous hyperthermic peritoneal perfusion (CHPP). External applicators heat up the affected region to 41-42°C, using at least one pair of dipole antennas, positioned around the patient's tumor. The applicators can apply radiofrequency or microwave emission. Regional hyperthermia techniques can perform deep-heating with capacitive or conductive radiofrequency methods. The amplitude and phase parameters of the antennas can be controlled according to the Specific Absorption Rate (SAR) distribution, a physical parameter intended to describe the interaction between the electric field and the stimulated material (see in 1.1.5.). Cumulative Equivalent Minutes at 43°C (CEM43) is the unit used to to calculate the thermal dose during therapeutic hyperthermia.

Regional perfusion is applied in the case of malignancies found in distinct limbs or organs (liver, lung). A large artery of the limb or organ and a draining vein are bypassed and the blood is warmed up extracorporeally. The treatment can be completed by administering chemotherapeutic agents and having less side effects than WBH. Continuous hyperthermic peritoneal perfusion (CHPP) is used perioperatively to deliver heated washing fluid (41.0-42.5°C). CHPP can also be completed by adding chemotherapeutic agents to hyperthermic intraperitoneal chemotherapy (HIPEC). The indication of HIPEC treatment is disseminated tumors in the abdominal cavity, such as carcinomatosis of unknown origin, multifocal ovarian or colorectal metastases, stomach cancer or mesothelioma. The therapeutic strategy includes the resection of the primary tumor and cytoreduction of the extended peritoneal metastases (7).

1.1.4. Local hyperthermia

Local hyperthermia methods - often referred to as loco-regional hyperthermia - communicate energy with the target area, that is transformed into heat locally in the tumor. It is mainly used in small tumors, found in superficial regions of the body, or in approachable locations, like the orifices of the gastrointestinal tract (rectum or esophagus). The great advantage of local hyperthermal treatment, is that just the malignancy-containing volume, a small portion of the body is heated up. Thus, systemic side effects (see in 1.1.2), are reduced. Different approaches are used to focus local hyperthermia, e.g. administration of iron-oxide or gold nanoparticles intravenously or directly to the tumor site. These particles acquire the energy of the heating source and

indirectly transferring the energy to the tumor locally (24). However, even local hyperthermia has side effects: bleeding, infection, local irritation of the skin, muscles or nerves, blistering. For preventing skin-related complications during treatments, water boluses are used, to keep the surface temperature at 37 ^{o}C. Tumors of the skin are the easiest to treat. Superficial applicators or antennas of different forms can be positioned on the tumors. Temperature monitoring during treatment is crucial. For temperature monitoring, needles or tubes are inserted into the tumors after anesthetization. Heating can be generated by electromagnetic waves, like microwaves (300 MHz-300 GHz, (25, 26)) or radio frequency waves (1 – 300 MHz, (27)) or by mechanical waves, like ultrasound (High-Intensity Focused Ultrasound, HIFU, (28)). Intracavital applicators can provide local hyperthermia in certain types of tumors (cervical, vaginal, rectal, oesophagus cancer). Interstitial local hyperthermia is applied in tumors, treated with brachytherapy (head and neck tumors, prostate, breast cancers, brain tumors). For this purpose, microwave antennas, ultrasound transducers or radiofrequency electrodes are inserted into the tumor tissue. Thermoablation is a specific type of interstitial hyperthermia, when the applied temperature exceeds 50 ^{o}C and causes vascular stasis, cellular coagulation and tissue necrosis (7).

Comparison of the three main types of medical hyperthermia is presented in Table 2.

Table 2. Comparison of different types of medical hyperthermia. Based on the publication of Chicheł et al. (7) and Szasz and al. (8).

Type / Aspect	Whole Body Hyperthermia	Regional Hyperthermia	Local Hyperthermia
Area of heating	Whole body	Parts of the body (limbs, abdomen, pelvis)	Small portion of tissue
Tumor site	Disseminated, metastatic	Deep seated, locally advanced	Superficial, intracavital, intraluminal, interstitial
Heat transfer	Conduction	Convection, radiation	Radiation
Adverse effects	Most serious, systemic	Moderate	Least severe, localized, skin symptoms
Focusing	-	Moderate	necessary
Role of blood	Transfer medium	Cooling medium	Cooling medium
Application form	Blankets, hot water, infrared	External applicator, perfusion	Superficial applicators, antennas

1.1.5. Modulated electro-hyperthermia

Modulated electro-hyperthermia (mEHT) is a loco-regional, non-invasive treatment modality, applied in cancer, preferentially in combination with traditional oncological treatments like chemo-, radiotherapy and lately with targeted- and immunotherapy. It uses the electromagnetic method with a capacitively coupled electromagnetic field for heating the targeted, tumorous area (8).

The upmost requirement of anti-cancer modalities is selectivity: to harm the malignant cells but spare the healthy ones. The principle of mEHT is the auto-focusing effect, which is based on the metabolic reprogramming of malignant cells (29) and the consecutive altered impedance of the tumor tissue. Electrical impedance (Z) is the physical parameter, that describes the resistance of a material in an alternating current (AC). Cancer cells prefer to use glucose and favor the less-effective glycolysis instead of oxidative phosphorylation, even in aerobic conditions, which is called the Warburg effect (30). This type of metabolism produces less ATP (2 mol ATP/mol glucose), than oxidative phosphorylation (36 mol ATP/mol glucose) (31). However, it preserves the carbon-carbon bonds of the macromolecules, which supports the biomass production rather than energy production, unlike in healthy tissues. Therefore, the Warburg effect can be interpreted as an adaptation mechanism to support the biosynthetic requirements of uncontrolled proliferation of the tumors (30). However, the role of Warburg effect in cancer metabolism is a disputed, Nobel laureate statement. It is controversial, whether it is a cause or a consequence of the cancer cells' development (31). The concept of Warburg effect is presented in Figure 1.

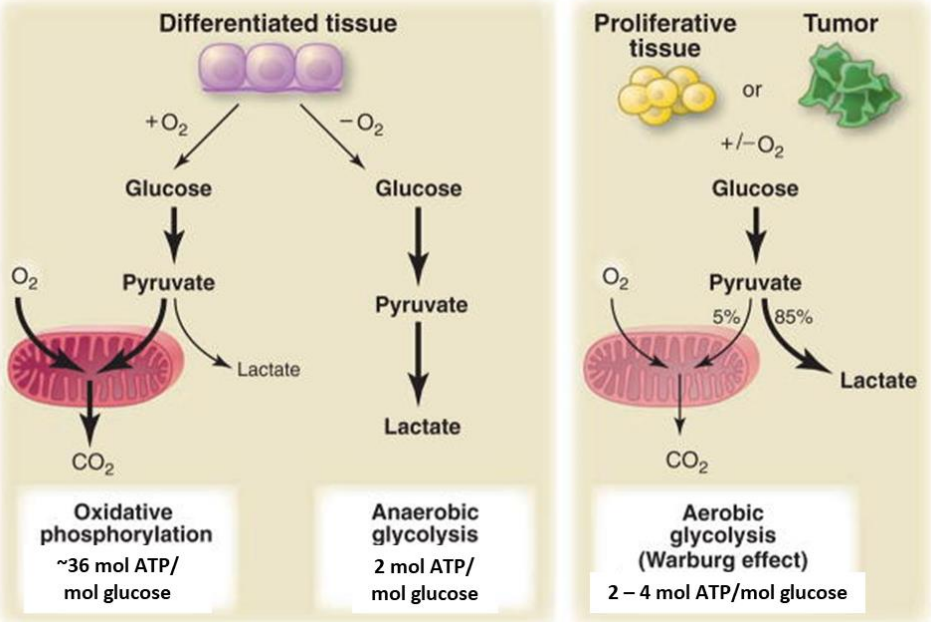

Figure 1. Comparison of Warburg effect to oxidative phosphorylation and anaerobic glycolysis. When oxygen is present, differentiated tissues prefer to metabolize glucose to pyruvate via glycolysis and then completely oxidize most of that pyruvate in the mitochondria to CO_2 during the process of oxidative phosphorylation. Oxygen is indispensable for this process, as the final electron acceptor to completely oxidize the glucose. When oxygen access is limited, cells redirect the pyruvate generated by glycolysis away from mitochondrial oxidative phosphorylation by generating lactate (anaerobic glycolysis). This generation of lactate during anaerobic glycolysis allows glycolysis to continue (by cycling NADH back to NAD+), but results in minimal ATP production when compared with oxidative phosphorylation. According to the Warburg effect, cancer cells tend to convert most glucose to lactate regardless of whether oxygen is present (aerobic glycolysis). Mitochondria remain functional and some oxidative phosphorylation continues. Aerobic glycolysis is less efficient than oxidative phosphorylation for generating ATP. Modified from the original image, published by Heiden et al. (32).

As a result of the altered metabolism, cancer cells produce more lactate and H^+, which reduces the pH in tumor tissue and creates an acidic environment (33). The modified metabolism causes altered bioelectrical properties (elevated permittivity and conductivity) of the tumor tissue (34). Dielectric permittivity (ε) is a physical property which characterizes the degree of electrical polarization, a material experiences under the influence of an external electric field. A material with high permittivity polarizes more and stores more energy in response to an applied electric field than a material with low permittivity. ε is associated with the dipole content of a biological material, which are mainly the water molecules and cytoplasmic, extracellular or membrane-bound macromolecules, e. g. proteins, but not the simple, water-dissolved ions (Na^+, K^+, Ca^{2+},

Cl^-). These dipole molecules tend to rotate due to excitation by an electric field, which causes the dielectric heating of the biological material (35). Conductivity (σ), on the other hand, refers to the free-charged molecules of a biological material, which can drift as the consequence of the electric current (36). In addition, tumor tissues have been described to have elevated water, metal-ion and salt content. All of these factors lead to the decreased complex impedance of the tumors, which is utilized in cancer diagnostics (Electrical Impedance Tomography: EIT), in breast (37), skin (38) and cervix (39) cancer. Moreover, the decreased impedance causes a consequent predisposition of tumor tissues to the excitation by electric fields (40). Setup and color-scaled results of EIT in breast cancer is presented in Figure 2.

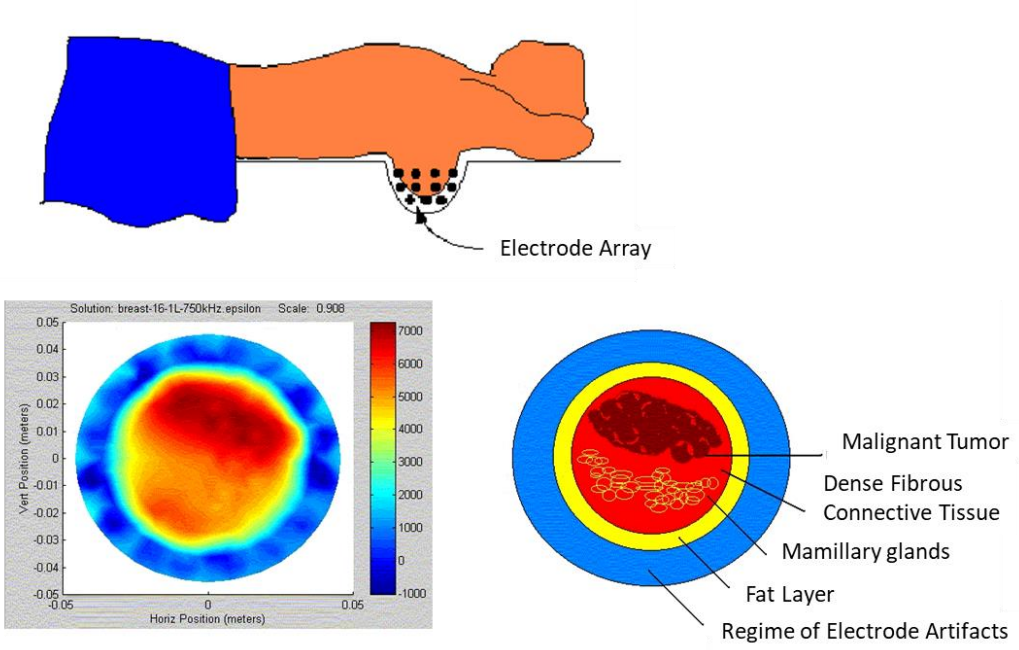

Figure 2. Electrical Impedance Tomography (EIT) examination in breast cancer. EIT electrode setup in breast cancer examination. Absolute permittivity image: Coronal View Breast with malignant tumor at 750 kHz. Modified from the original image, published in the review of Zou et al. (41).

mEHT uses a 13.56 MHz frequency, capacitively coupled, alternative current electromagnetic field (EMF) with 1/frequency (1/f) amplitude modulation to transfer energy and heat to the malignant tissue. Two electrodes are positioned on two sides of the tumorous area, which becomes part of the electric circuit. Because of the aforementioned altered electric properties (reduced complex impedance) of the malignant tissue, the energy of the EMF is mostly absorbed by the tumor.

Applied frequency range (13.56 MHz) was chosen, because the radiofrequency should penetrate deeply into the tissues (<25 MHz) and avoid the neuron excitation range (10 KHz). Also, this frequency doesn't interfere with other electronic devices, therefore no adumbration is needed (8).

mEHT performs inhomogenous heating of the tumor tissue: the energy of the EMF is absorbed chiefly in the extracellular space, where the electric impedance is the lowest. SAR can be used to measure the absorbed energy in a unit of mass (dose), related to the thermal effect of the electromagnetic field. SAR can be calculated by the following formula: $SAR = \Delta T \times C/t$, where ΔT = temperature change, C: specific heat of the biological material [J/K*kg], t: time [s] (35). Capacitance is the ratio of the amount of electric charge stored on a conductor to a difference in electric potential (charge/potential). Cancer cells are insulated from the electric field, as the cell membrane maintains a high resistance related to it's high capacitance values (10 millifarad/square meter (mF/m^2)) (9). The absorbed energy creates a remarkable rise of temperature in the extracellular fluid, which generates a large heat-gradient (~1 kelvin/micrometer (K/μm)) and heat-flow through the cell membranes and consequent ion- (Na^+ (42), Ca^{2+} (43)) and water flow towards the intracellular space. These flows cause the swelling of cells, harm the membrane functions and membrane potential, and lead to cell disintegration (9). Moreover, heat, generated by mEHT is absorbed mostly in the lipid rafts of cancer cells membranes, creating hot spots with peculiarly high energy absorption (nanoheating) (44) and cancer cell membranes have higher rigidity, than healthy cells, makes the tumors more susceptible to mEHT (8). mEHT induced cellular stress initiates cellular death forms, primarily apoptosis and via the release of DAMPs, secondarily Immunogenic Cell Death (ICD).

Besides the thermal effects, the EMF itself exposes own non-thermal effects. During mEHT, an 1/f amplitude-modulation is applied on the carrier EMF, which is in the stochastic resonance frequency range (sometimes referred as pink noise). Since malignant cells are more susceptible to this frequency, it could cause a definite resonant effect on cancer cells, disintegrating enzymatic processes and ionic channels of their membranes (8, 45). Energy of the EMF can also influence DNA function (46) and protein expression (47). Moreover, the EMF creates the motion (electrophoresis) of dielectric particles (48) and the rotation of cells and cell nuclei (49). The EMF has a prominent

effect on cell membranes, like electroporation and electro-permeabilization, which can greatly affect membrane transport mechanisms and membrane integrity (50, 51).

During mEHT treatment the thermal and non-thermal effects amplify each other's cancer cell killing effects, leading to an effective tumor destruction (52). The most important anti-cancer effects of mEHT on cellular level are summarized in Figure 3.

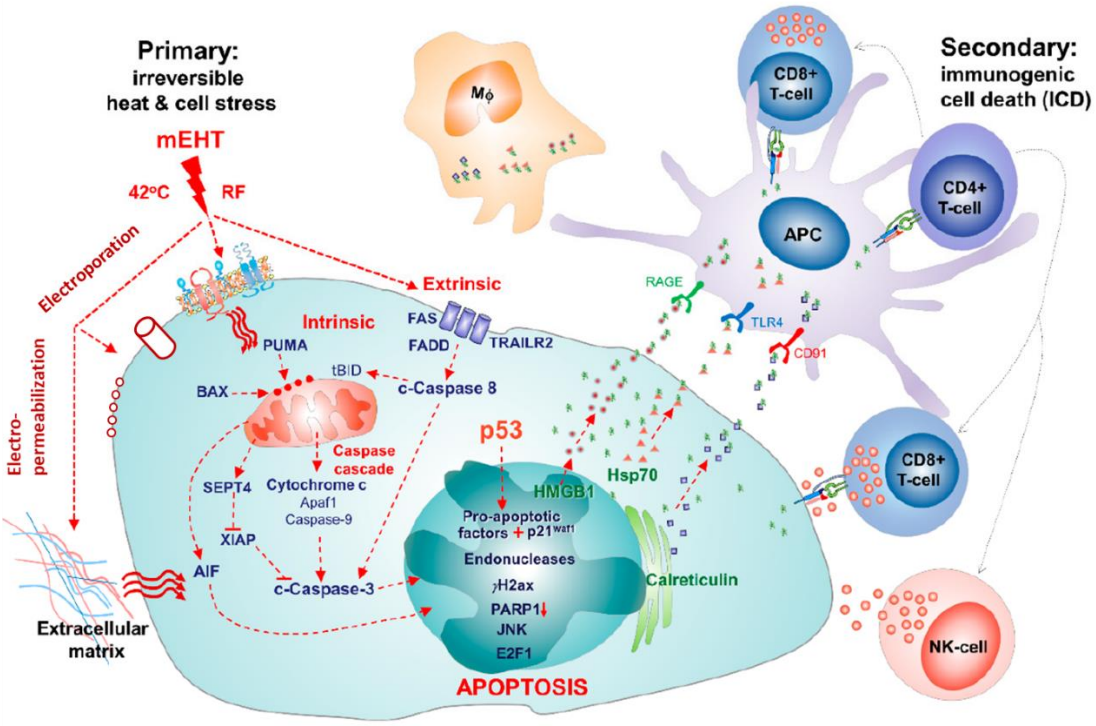

Figure 3. Summary of the most important cellular-level anti-cancer mechanisms of mEHT. The energy of the EMF is absorbed in the extracellular space, generating heat, fluid and ion flows towards intracellular space, which hurts the membranes. Energy is also absorbed by the membrane dipoles, like death receptors and other lipid rafts. mEHT-induced stress activates caspase-dependent and – independent apoptotic pathways and the release of DAMPs. With the assistance of antigen-presenting cells, DAMP signals initiate T cell-mediated and NK cell-mediated immunogenic cell death consequentially. Beside the thermal effects, the EMF has its own cell-damaging effects, like electroporation and electropermeabilization of the cancer cells' membrane. Modified from the original image, published by Krenács et al. (13).

1.1.6. Clinical applications of oncological hyperthermia

Oncological hyperthermia is used in the clinics mostly as a complementary therapy. It improves the therapeutic effects of radio-and chemotherapy (1.1.1/Table 1). Furthermore, the combination of hyperthermia with chemo-or radiotherapy can reduce the therapeutic dose and consequently, the adverse effects' severity can be attenuated.

Phase III randomized controlled trial of head and neck cancer patients, treated with radiotherapy or thermoradiotherapy, demonstrated a remarkable improvement of complete response (CR). In 451 cases, radiotherapy alone reached 39.6% CR, while the combinational treatment (thermoradiotherapy) reached CR in 62.5% (53). A meta-analysis demonstrated, that the risk difference to achieve CR was 22% greater ($p < 0.001$) and to achieve loco-regional control (LRC) was 23% greater ($p < 0.001$) with thermoradiotherapy compared to radiotherapy alone in cervical cancer (54). In a review summarizing 38 trials on different tumor types (breast, cervix, head and neck, rectum, urinary bladder, esophagus, lung, skin melanoma, choroidal melanoma, anal canal) the overall complete response rate (RR) was 54.9% from 1761 patients treated with hyperthermia and radiotherapy, while CR was 39.8% from 1717 participants treated with radiotherapy alone. A breast cancer study demonstrated, that the efficacy of hyperthermia treatment depends on the tumor size. In terms of local response (LR), capacitive coupled thermoradiotherapy was 13.7% more effective, when tumors were smaller than 100 cm^3, compared to mono-radiotherapy, while 22.6% more efficacy was gained, when the tumors were bigger, than 100 cm^3 (55).

Phase I and II studies, evaluated in a small number of intracranial metastatic patients, treated with interstitial hyperthermia in monotherapy showed 53.8% decrease in volume, measured by CT or stabilization of the disease and no serious complications, like bleeding, meningitis, abscesses, occurred (56).

A study from 2017, involving 38 patients with cervix carcinoma, compared the effectiveness of platinum-based chemotherapy alone or in combination with mEHT. Combinational therapy was significantly more effective: CR: 50%, partial response (PRe): 11.1% and stable disease (SD): 11.1%, while these results were 20%, 15% and 5% in the chemotherapy-alone group. Progression of the disease happened in 27.8% of patients in the combination group and 60% in the chemotherapy alone group (57). The most recent randomized controlled Phase III trial with high number (210) of cervical cancer patients demonstrated that combination of chemoradiotherapy with mEHT is beneficial: mEHT improved both Disease Free Survival (DFS) rates (control group: 13.7%, mEHT group: 36.4%, $p < 0.0001$) and the quality of patients' life (58). Local chemoembolization technique's efficacy in hepatocellular carcinoma (HCC) was synergistically improved with hyperthermia: remission rate (RR) increased by more than

12% by adding hyperthermia to the treatment, (59). Hyperthermia, applied together with liposomal doxorubicin was reported to elongate the 4-year survival almost four times, than liposomal doxorubicin alone in recurrent breast cancer phase I and II study (60). A retrospective analysis in 2020 in metastatic colorectal cancer patients demonstrated that Bevacizumab plus FOLFOX-4 regimen combined with electro-hyperthermia reached a 95% disease control rate (DCR) - counted as the percentage of patients who had the best response rating – 90 days after treatment and 89.5% 180 days after the treatment. The median overall survival was 21.4 months (61). The median progression-free survival (PFS) was 12.1 (61) months. Furthermore, a recent study demonstrated, that the median PFS of the first three lines of Folfox–avastin treatment were 8.5, 5 and 3 months, respectively (62).

Taken together, mEHT can be considered as an efficient anti-cancer method, which is capable of selective, local treatment of solid tumors in monotherapy and can bountifully potentiate and complete the effect of traditional oncological therapies.

1.2. Breast cancer

1.2.1. Types, staging, prognosis

1.2.1.1. Histological types

The GLOBOCAN study has demonstrated, that breast cancer (BC) had the highest incidence in 2020 and was responsible for most tumor-related deaths among women worldwide (63). Breast cancer represents a very heterogenous group of cancer. The vast majority of breast cancers are carcinomas (epithelial origin). By the histological/morphological appearance, the two most common types are ductal and lobular breast carcinomas. Ductal carcinomas are derived from milk ducts, lobular carcinomas originate from the milk-producing glands of the breast. Those, which don't break through the basal membrane of the affected tissue and stay at the place of development (non-invasive) are called carcinoma in situ (ductal carcinoma in situ (DCIS); lobular carcinoma in situ (LCIS)). However, most BCs are invasive, with the ductal origin being more common than the lobular origin. More than 50% of all breast cancers are invasive ductal carcinomas and less than 10% are invasive lobular carcinoma (64).

1.2.1.2. Molecular types

According to the presence or absence of molecular markers, hormone-receptor positive and negative breast cancers can be distinguished. In the hormone receptor-positive group, two subgroups, Luminal A (estrogen receptor (ER)+, progesteron receptor (PR)+/-, Human epidermal growth factor receptor 2 (Her2)-, Ki67↓) and Luminal B (ER+, PR+/-, HER2+/-, Ki67↑) are discerned. The hormone receptor-negative group contains HER2+ (ER-, PR-, HER2+, Ki67↑) and Triple Negative (ER-, PR-, HER2-, Ki67↑) subgroups. Cancer cells' receptor-expressing properties greatly affect whether targeted therapy is applicable or not and therefore the prognosis of BC.

1.2.1.3. Staging

Nottingham grading system is used to assess the aggressiveness of breast cancer cells and the prognosis of the disease. The Nottingham system enrolls breast cancers into Grade 1 (well-differentiated, best prognosis), Grade 2 (moderately differentiated, medium prognosis) and Grade 3 (poorly differentiated, worst prognosis), considering attributes like tubule formation, nuclear pleomorphism and mitotic count (65). Tumor size (T), lymph node involvement (N) and the presence of metastasis (M) are the basics of the TNM classification and the enrollment of breast cancer into stages. Early stage breast cancer cases can be cured, primarily with surgical removement and with additional, chemo-, immuno-, targeted or radiotherapy. However, in advanced-stage breast cancer the 5-year survival is < 28% (66).

1.2.2. Triple Negative Breast Cancer (TNBC)

12% of BC cases are triple negative BC (TNBC) (Figure 4), where the neoplastic cells lack the intracellular ER, PR and surface HER2 expression. TNBC tumors have particularly aggressive behaviour with a high recurrence rate after diagnosis, high pathological grade, and greatly reduced 5-year survival compared to non-TNBC patients (67).

The lack of hormone- and HER2 expression hamstrings the anti-hormone and targeted therapies. The primary treatment regime for TNBC is anthracycline (Doxorubicin) and taxane (Paclitaxel)-based chemotherapy. These cytotoxic agents have

serious side effects such as cardiotoxicity (cardiomyopathy), enterocolitis, neutropenia, fever, diarrhoea and vomiting.

Based on recent genomic profiling, TNBC can be classified into 7 major classes of molecular subtypes: Basal Like 1 (BL1), Basal Like 2 (BL2), Immunomodulatory (IM), Mesenchymal (M), Mesenchymal stem-like (MSL), Luminal androgen receptor (LAR) and Unstable (UNS). According to their expression profile, these seven major subtypes have unique ontologies and different characteristics: in BL1 tumors, the main upregulated cellular mechanisms are the cell cycle, cell division, and DNA replication. BL2 are susceptible to growth factors and metabolic signaling is essential. In M and MSL types, the Epithelial-Mesenchymal Transition (EMT) is a pivotal process, while in LAR, the androgene-hormone mediated and in IM type the immune-mediated signaling are articular (68, 69).

Despite recent years' diagnostic and therapeutical efforts, TNBC treatment is still challenging and remains one of the breast cancer types with the worst prognosis. Prevalence and prognosis in breast cancer and TNBC subtypes are presented in Figure 4.

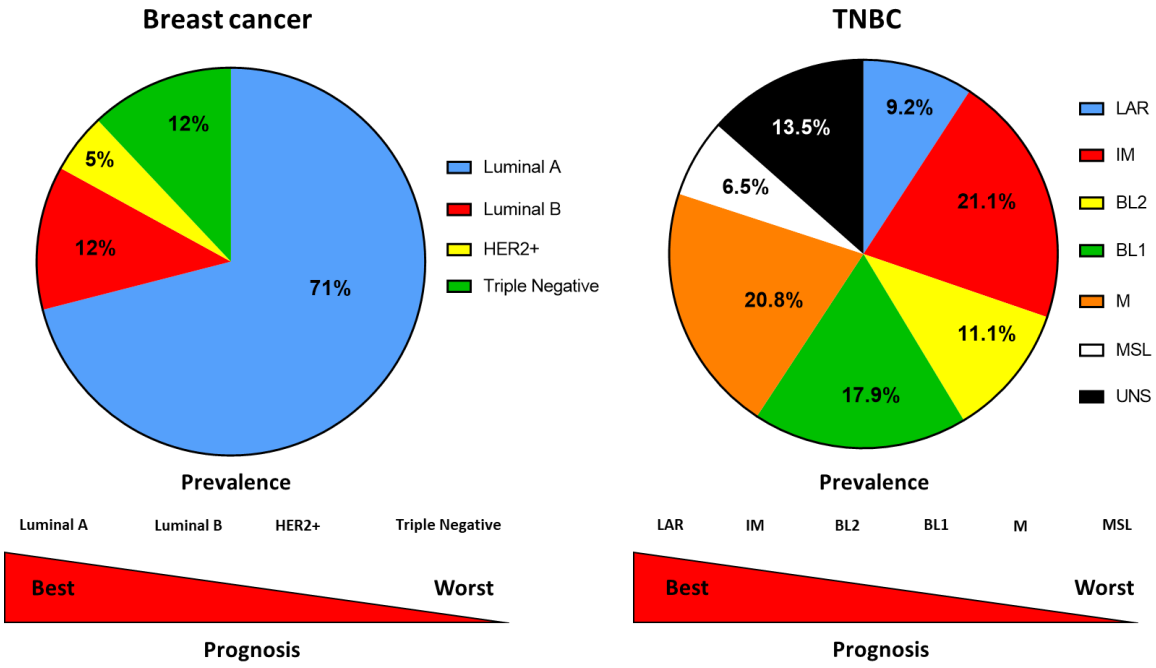

Figure 4. Prevalence and prognosis of breast cancer and TNBC subtypes. Prevalence, breast cancer: (70), TNBC: TNBC prevalence: (69) Prognosis, breast cancer and TNBC: (71)

1.2.3. TNBC mouse model

Several laboratory animal models were established to model and study the human TNBC disease in preclinical conditions (72). 410.4-derived mammary carcinoma cell lines, 4T1 and 4T07 are the most commonly used TNBC cell lines to create syngeneic (non-immunogenic) isografts in BALB/c mice. 410.4 was isolated from a single spontaneous tumor raised in BALB/c mouse. 4 subclones originates from 410.4 cell line: 168FARN, 67NR 4T07 and 4T1 in the order of agressiveness and metastatic ability, respectively (73). Subcutaneous implantation of these cells into immunocompetent BALB/c mice creates syngeneic isograft, which is feasible for modelling human TNBC. In the present study, the most agressive 4T1 cell line was used for in vitro and short and medium-term in vivo experiments. The less aggressive 4T07 was used for long-term experiments in vivo. 4T1 tumors are capable of performing the whole process of Epithelial-Mesenchymal Transition (EMT) and by the reverse Mesenchymal-Epithelial Transition (MET) process, they can form macrometastases in the lungs of the host. 4T07 tumors are capable of EMT but not MET, therefore they can leave the primary tumor but can only form micrometastases (74) (Figure 5A). 4T1 cell line-derived tumors are described as an immune desert phenotype in the literature (75), while 4T07 tumors are characterized by higher immunogenicity, making them a promising model for studying immunotherapy, such as checkpoint inhibitor (CPI) therapy. Our data supports these characteristics, as both CD3 and PD-1 were less expressed and the CD3+ T cell infiltration was also lower in 4T1 than 4T07 tumors (Figure 5B). In the TNBC classification, 4T1 cells correspond mostly to the basal-like subtype and can be referred to as “Basal-like and immune suppressed (BLIS)” type (76). Characteristics of 410.4-derived subclones are presented in Figure 5.

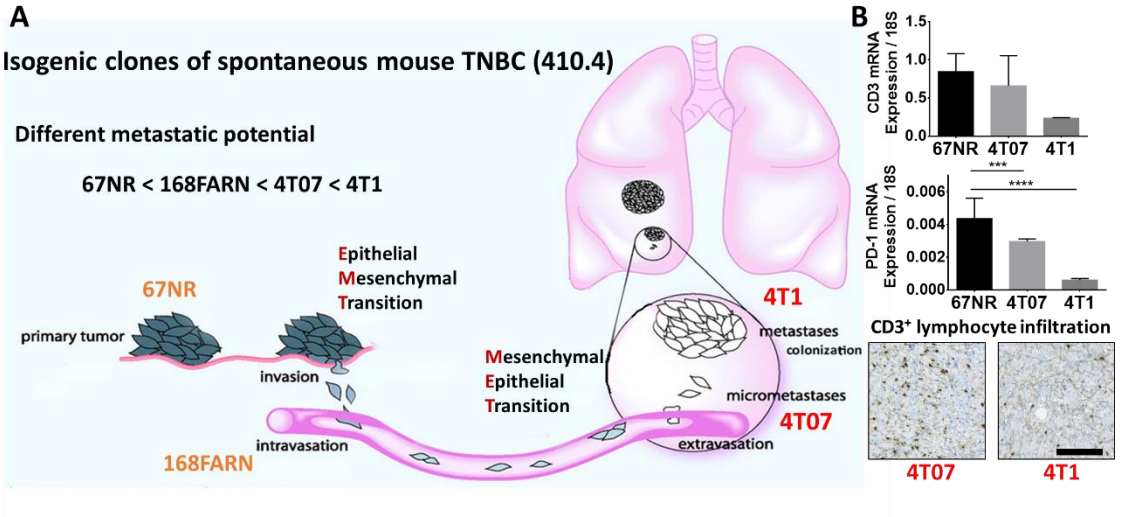

Figure 5. Characteristics of 410.4 derived subclones. Four isogenic subclones, derived from the spontaneous 410.4 mouse breast cancer. 67NR cells cannot leave the primary tumors, 168FARN cells can enter vessels but not leave it, therefore cannot form metastases. 4T07 are capable of leaving the vessels and form only micrometastases and the most aggressive phenotype, 4T1 cells can form macrometastases in the lungs. Based on the data published by D. M. Dykxhoorn, J. Lieberman et al., 2009 (77) and Korpal et al., 2011 (78) (A). 4T1-developed tumors are poorly immunogenic, as their CD3 and PD-1 expression is low and their CD3+ T cell infiltration is low (lower, immunohistochemistry panel, DAB staining of CD3, magnification: 12x, scale: 100 μm), while 4T07-derived tumors show more immunogenic features. (B) our workgroup's data, unpublished.

1.3. Cellular stress response and acute-phase proteins (APPs)

The stress theory was established by János Selye, who described stress as 'the non-specific response of the body to any demand' (79). Cellular stress response serves the adaptive purpose of protecting prokaryotic and eukaryotic cells against contrarious environmental impacts. Cellular stressors can be positioned on a wide spectrum like mechanical (shear stress (80)), physical (heat, ionizing radiation, EMF (47)), chemical (oxidative stress, heavy metals) or biological (toxins) stressors. Living organisms develop different mechanisms to adapt to stress. One of the most widely known molecules serving as protectors against cellular stress is heat shock proteins (Hsps). In response to different cellular stressors, Heat shock factor-1 (Hsf-1), the key regulator of Heat Shock Response (HSR) is activated and translocated into the nucleus to initiate the transcription of Hsps. Their intracellular expression can be induced not just by heat but by almost any other aforementioned stressors (81). Hsps function as inducible chaperones, as part of the cellular adaptational mechanism to prevent or correct damage caused by misfolding of

proteins as a result of heat (81). Therefore Hsps are important participants of the cancer cells to avoid programmed cell death. Hsps are responsible for thermotolerance during hyperthermia treatment as heat shock proteins prevent or parry the cell-killing effects at the cellular level (8, 82). Induction of Hsps are presented in Figure 6.

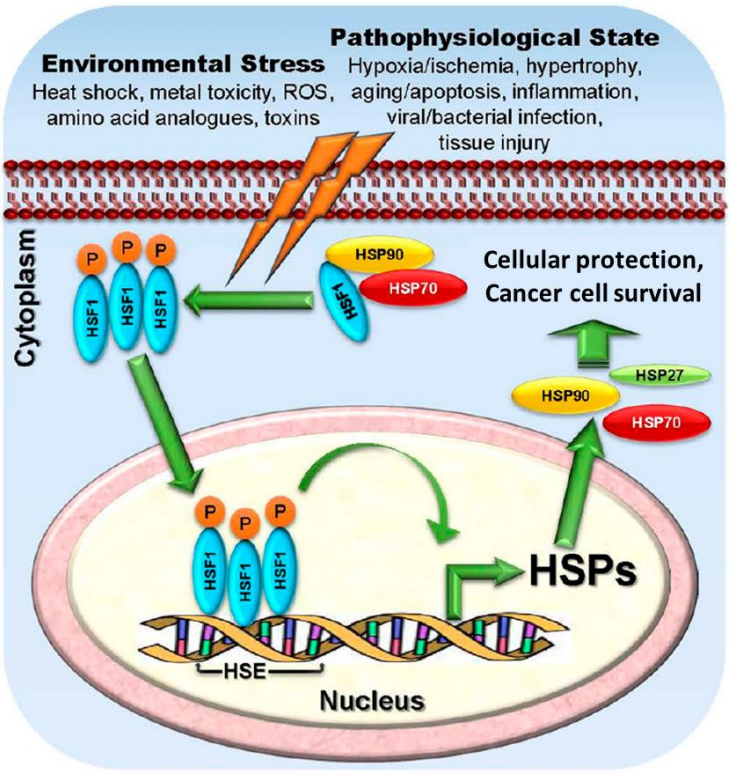

Figure 6. Induction of Heat Shock Proteins. In response to stress, HSPs-HSF1 complex dissociates and HSF1 is translocated into the nucleus. HSF1 binds to specific Heat Shock Element (HSE) sequences that are present upstream of heat shock gene promoters. Therefore, the transcription of HSPs are activated in order to promote cellular protection for the survival. Modified from the original image, published by Chatterjee and Burns (83).

Stress can also induce the activation of the Acute-Phase Response (APR) with increased production of acute-phase proteins (APPs) by the liver (84). APR is classically interpreted as a nonspecific, systemic response of vertebrate organisms to different types of harming stimuli/stress, e.g. infection, tissue injury or different chronic diseases. It is also described, that heat stress (85), sepsis (86) or ischemia (87) can induce the APR. Factors that increase during the APR are called positive APPs and those that decrease are negative APPs. APR is part of the innate immune system acting as a humoral defense mechanism to restore the homeostatic state and tissue repairment. APPs are ancient evolutionarily conserved types of proteins, found throughout most species. In vertebrates,

APPs are traditionally considered to be produced by the liver (88). However, the local, non-hepatic production of APPs has been studied in a vary of extra-hepatic cells, including immune (89), epithelial (90), kidney (86) and other healthy cell types (91) and cancer cells (92) as well.

1.3.1. Complement factors

Complement is the humoral arm of the innate immune system and acts as a first line of defence against pathogens and stressed host cells to maintain homeostasis (93, 94). The complement system is composed of more than 50 plasma proteins, released into the circulation by the liver and activated on the membrane surface of target cells (95). Canonically, complement works as a cascade system of the blood, activated by pathogens. There are three pathways, via the complement system can be activated: classical, alternative and lectin pathways (96). The classical pathway can be activated by pathogen antigen-antibody complex, the alternative pathway is continously acitvated on a low level and the lectin pathway can be activated by binding mannose-binding lectin (MBL) on the pathogen surface. Classical and lectin pathways can also be initiated by pentraxins, such as Ptx3 (97). The result of the activation of all pathways is the terminal pathway and the assembly of the Membrane Attack Complex (MAC). The three main functions of complement cascade are opsonization, anaphylatoxic effects, and MAC formation. Anaphylatoxins (C3a, C4a, C5a) induce the degranulation of endothelial cells, mast cells or phagocytes, contributing to local inflammatory processes. Opsonization promotes the phagocytosis of targeted cells, while the MAC transmembrane pore, formed at the end of the complement cascade enables the osmotic flux through cell membrane, causing the lysis of the cell (98). The complement system provides a substantial connection between the innate and adaptive immune systems. Besides the classical, pathogen-mediated activation of complement, it can be activated by different types of cellular stress like oxidative stress (99), mechanical (shear) stress (80) or ischemia-reperfusion (87).

1.3.1.1. Extrahepatic production of complement factors

Beyond their canonical roles, complement factors comprise other, non-canonial functions locally, that are independent from the activation of complement cascade. Moreover, the source of complement factors is not exclusively the liver and some of the complement factors, like C1q have non-hepatic origin decisively. C1q has an

important role during pregnancy in remodeling of the decidua and during embryonic development. In addition, C1q acts in coagulation processes and neurological synapse functions (100). Several complement factors are reported to be produced by immune cells (89). Locally produced and activated complements act in the initiation of the immune response. Complement activation increases vessel permeability and a subsequent systemic plasma protein (APP) leakage contributing to the initial local immune response. Complement factors can exert non-canonical, local effects via complement receptors, which are abundantly expressed on immune cells, therefore complement factors can perform paracrine or autocrine functions. Complements participate such way in the T cell – DC synapse, promoting T cell differentiation, expansion and survival (101). Another non-canonical role of complement factors is based on their intracellular effects. It has been reported, that intracellular cleavage and activation of C3 and C5 can contribute to the activation of T cells (102, 103). Complement factors (C3, C5), interacting with their corresponding receptors can also regulate physiological and pathological angiogenesis processes like wound healing or retinal regeneration either as anti-or proangiogenic actors (104). Ptx3 is a member of the pentraxin superfamily, a highly evolutionary conserved protein group. The blood level of Ptx3 elevates in response to external, harming stimuli therefore it is considered as a positive acute-phase protein. Ptx3 also participates in the activation of complement system and acts in several crosstalk mechanisms in humoral, innate immune responses. Extrahepatic production of Ptx3 was reported in macrophages and dendritic cells (97, 105).

Complement expression by different immune cells are summarized in Table 3. Complement production is reported by several tumor cell types, which is presented in details in chapter 1.3.5. APPs role in cancer.

Table 3. Complement factor and receptor production/secretion/expression by immune cells. Modified from the original table by Lubbers et al. (2017) (89).

Immune cell type	Secreted Complement factor	Complement factor receptor
Polymorphonuclear leukocytes	C3, Cfp, Cfb, C6, C7, ficolin	CR3, CR4, C3aR, C5aR
Macrophages	C1q, C1s, C2, C4, C3, Cfb, Cfd, C5, C2, C3, Cfb, Ptx3	C3aR, C5aR1, C5aR2, CR1, CR3, CR4
Dendritic cells	C1q, C1s, C1r, C2, C3, C4, C4bp, C5,C7, C8, C9, Cfb, Cfd, Cfi, Cfh Cfp , Ptx3	CR1, CR3, CR4, CRIg, C3aR, C5aR1
Natural killer cells	-	C3aR, C5aR, C5aR2, CR3, CR4
B lymphocytes	C5, Cfh, Cfi	CR1, CR2, CR4
T lymphocytes	C3, C5, Cfb, Cfd, Cfp, CD46	CR1

Besides immune cells, other non-hepatic cells are able to produce complement factors: production of several complement factors by renal cells has been described, especially in pathological states. C4 can be expressed in healthy tubular epithelial cells (106). In systemic lupus erythematosus (SLE) patients' kidneys tubular epithelial cells produced C3 and Cfb only in affected kidneys. It has been also demonstrated, that C3 takes part in the local APP response of the kidneys in sepsis-induced acute kidney injury (86). Local complement production on protein (C1r, C4b, Cfp, CRP) and mRNA (Cfi, Cfb, C7) level were demonstrated in focal segmental glomerulosclerosis (107). Complement factor synthesis was also reported by adipocytes (C3, Cfb, Cfd) (108) and by brain cells, like astrocytes (C1q, C1r/s, C2, C4, C1-INH) and microglia (C1q, C4) (91). Ptx3 is expressed by a wide spectrum of cells, including epithelial cells, adipocytes, mesangial cells and different glial cells (105).

1.3.2. Protease inhibitors

Protease inhibitors (serpins and Itihs) have been described as ancient markers of cell stress (109). Protease inhibitors participate in different processes like coagulation, fibrinolysis, inflammation, tumor-suppression etc. The main function of protease inhibitors is to maintain a fine-tuned balance of proteolysis. Protease inhibitors exert an auto-protective function, preventing auto-lysis by granule proteinases. Protease inhibitors

are often found in proteinase-secreting cells, either produced by the cell itself, or may get into the cell by uptake (endocytosis) (110).

Serpins are the largest superfamily of protease inhibitors in nature, with more than 1500 members identified to date. They are homologous proteins with a size of around 350-500 amino-acids and sorted into 16 clades, marked with letters (A-P). Serpins are found in all kingdoms of life (110). Genomic analysis demonstrated, that all eukaryotic multicellular organisms from fungi to humans and procaryotes, moreover, even viruses use serpins for protection (111). The name 'serpin' comes from 'Serine protease inhibitor', as serine proteases are the enzymes, serpins inhibit the most, however, serpins have other activities as well. Serpins are mostly extracellular molecules and have a unique mechanism: they perform an irreversible conformational change to inhibit their target protease, therefore they are often referred to as suicide or single-use inhibitors (112, 113). They function like a mouse-trap, with a protruding reactive center loop (114). The first described human serpins interestingly share a common tertiary structure with chicken ovalbumin, implementing that they could have been derived from a common ancestor, corroborating the ancient origin of these molecules (115). Serpins regulate homeostasis by keeping balance with serine proteases.

Serpins are participants of the humoral immune response. Serpins are released from the liver as part of the Acute-Phase Response. They can effectively fight against pathogens by directly neutralizing pathogen proteases, interfering with pathogen binding, and enhancing the host immune cell's functions (116).

Inter-alpha trypsin inhibitors (IαIs) are another ancient type of serine-protease inhibitors. They form approximately a 225 kDa complex and are made of two heavy (Inter-alpha-trypsin inhibitor heavy chain = ITIH) and one light chain called bikunin. Heavy chains have four isoforms: ITIH1, ITIH2, ITIH3, ITIH4 (117). The serine protease inhibitor activity of ITIHs is linked to the bikunin component (118). ITIHs have a vital role in extracellular matrix (ECM) stabilization via crosslinking hyaluroniac acid molecules and thus, the inhibition of cell migration. ITIHs have an inhibitory effect on the complement cascade, blocking all (the classical, alternative and lectin) pathways (119). ITIHs - especially ITIH4 - have been also reported as APPs (93).

1.3.2.1. Extrahepatic production of protease inhibitors

SerpinA1 (AAT) production by macrophages

SerpinA1 also known as Alpha-1 antitrypsin (AAT), encoded by the SERPINA1 gene in humans is one of the most abundant serpins. Besides the hepatic production, monocytes and macrophages also express AAT locally (120, 121), even in greater orders of magnitude, than hepatocytes (122). AAT expression can be induced by lipopolysaccharides (LPS) and by different cytokines in human monocytes (123). AAT has also been demonstrated in human alveolar macrophages in lung tissue, which express large quantities of proteases. AAT exerts a prominent protective function in alveolar macrophages against enzyme (cathepsin) overactivation, autolysis and consecutive emphysema (124).

Serpin production by other cells

Human neutrophil polymorphonuclear granulocytes (PMN) can also produce AAT (125). Moreover, different subfractions of T lymphocytes can express AAT (126, 127). Both SerpinA1 and SerpinA3 are expressed by hemopoietic progenitor cell populations in the bone marrow (114). Macrophages can express SerpinA3 in the hypothalamus under pathological conditions (128).

Expression of AAT was described in the kidney in tubular epithelial cells in the proximal tubule and in the loop of Henle (129). The upregulation of protease inhibitors was also documented in the kidneys in focal segmental glomerulosclerosis (FSGS) at protein (SerpinA1, SerpinA3, Itih1) and mRNA (SerpinA1) level (107).

AAT production was also described in human bowel's enterocytes, namely in the Paneth cells of the jejunum and ileum. Under physiologic conditions, protease inhibitors may exert a protective function against self-digestion. Protease inhibitor expression is further increased in inflammatory states, like Crohn-disease (130). AAT in human intestinal epithelial cells is regulated by inflammatory cytokines (IL-1, IL-6, TNFα) (90).

Moreover, the presence of AAT in pancreatic islet cells was also demonstrated (131). Overexpression of SerpinA3 was detected in JEG-3 trophoblast cells, and contributed to decreased cell adhesion to adjacent cells and ECM and shielded cells from apoptosis (132). Astrocytes express low-level antichymotrypsin, coded by SerpinA3 (133). Monocyte-derived macrophages express SerpinC1 during HIV-1 infection

following estrogen pre-treatment (134). ITIHs are also predominantly synthesized in the liver, however they are also reported to be produced by extrahepatic cells:

ITIH production by non-hepatic cells

- proximal tubular epithelial cells (bikunin and Itih3) - stimulated by IL-1β (135).
- Epithelial and stromal cells of human amniotic membrane constitutively express Itih1, 2 and 3 besides bikunin (136).
- Lung fibroblasts express Itih5 and it is related to the transformation from fibroblast to myofibroblast (137).
- Bikunin, itih1 and 2 production by chondrocytes in cartilages of osteoarthritis patients were abundantly increased, while absent in normal donors' cartilages (138).
- ITIH components were expressed in the human cerebral cortex from early phase of development through the neonatal period as well as in adults (139).

1.3.3. Haptoglobin

The primary role of haptoglobin (Hp) is binding free hemoglobin (Hb), released by erythrocytes upon hemolysis and expedite their removal from the circulation by the reticuloendothelial system (primarily the spleen and macrophages) (140). As cell-free hemoglobin is an oxidant, Hp can be considered as a protective factor, as it reduces the oxidative stress induced by hemolysis (141) and has anti-inflammatory effects. Hp is also regarded as a bacteriostatic agent through anti-inflammatory and antioxidant activities via facilitating free Hb clearance (142).

1.3.3.1. Extrahepatic production of haptoglobin

Immune cells:

Haptoglobin is expressed in granulocytes during their maturation and differentiation and is stored in specific granules (142). Mature neutrophil granulocytes also have been described as a source of Hp (143). Furthermore, T-, B-, and dendritic (D)- cells are capable of producing Hp, also in a form that is different from the hepatic Hp (144, 145). Macrophages are able to produce fucosylated Hp and prohaptoglobin (ProHp) (146).

Non-immune cells:

There is evidence for Hp expression, followed by septic injury in kidneys (86). The local expression of Hp has been described in the lungs of pigs, after influenza virus infection (147). Several components of the skin, namely epidermal keratinocytes, epithelial cells of hair follicles, sebaceous glands and eccrine glands may produce Hp mRNA. In addition, the Hp expression increase in different dermatopathies, like psoriasis, lichen planus, erythroderma, seborrhoea keratosis and verruca vulgaris (148). Hp production was also detected in human keratinocytes and in Langerhans cells of the skin (149, 150).

1.3.4. Fibrinogens

The coagulation factor fibrinogen (Fg) is classically interpreted as a liver-derived plasma-protein. Fibrin (Fb) is the precipitated form of fibrinogen. Precipitation may be a consequence of cleavage of fibrinogen side chains by thrombin or the consequence of direct contact of fibrinogen with the extracellular matrix (ECM). Fb is the final effector of blood coagulation: as the last step, Fb molecules polymerize to form an extensive interconnected fibrin network (fibrin clot) (151).

However, Fb/Fg participates in the fight against pathogens by forming a fibrin matrix. As a rapidly assembled matrix protein, fibrin(ogen) functions as one of the earliest lines of host protection by limiting bacterial growth, suppressing the dissemination of microbes, and mediating host bacterial killing (152).

1.3.4.1. Extrahepatic production of fibrinogens

Fibrinogen production is reported in human lung epithelial cells (A549) in vitro, after glucocorticoid (dexamethasone) and IL-6 induction (153), while IL-1β inhibits the expression of fibrinogen (154). Granulosa cells of the ovarium are also capable of generating fibrinogen and after stimulation by FSH, the fibrinogen production could be elevated by 2-3 times (155). Human intestinal epithelial cells have been also reported to produce fibrinogen in response to inflammatory cytokine exposure (90). Local production of all fibrinogen chains (Fga, Fgb, Fgg) among other APPs as a major proteomic response to septic injury of the kidney has been also reported (86). Moreover, fibrinogen (Fga, Fgb, Fgg) were locally produced in the kidneys during focal segmental glomerulosclerosis (107).

1.3.5. APPs' role in cancer

The association of APPs with cancer is complex and the source of the factors/proteins greatly influence, whether a factor performs a tumor-promoting or tumor-suppressing role (94). Most of these factors act extracellularly.

Besides pro- and antitumoral cellular components of the immune system, like dendritic cells, macrophages, $CD4^+$ helper and $CD8^+$ cytotoxic T cells, T_{reg} cells, the tumor microenvironment (TME) is enriched with humoral factors, including **complement components** (94). For a long time, it was thought, that complement acts as an effector arm of the immune system in TME and contributes to the destruction of tumor cells. Recent studies demonstrated, that complement also can articulate pro-tumoral effects in TME and even cancer cells can express complement factors. Complement factors produced by cancer cells are intensively examined in many remarkable publications from recent years and they are described to exert mostly non-canonical functions, different from the plasmatic cascade (156). Several complement factors have been reported to promote tumor growth via modulating the antitumoral immune processes. Summary of the pro-tumoral roles of complement factors in general in the TME is presented in Figure 7.

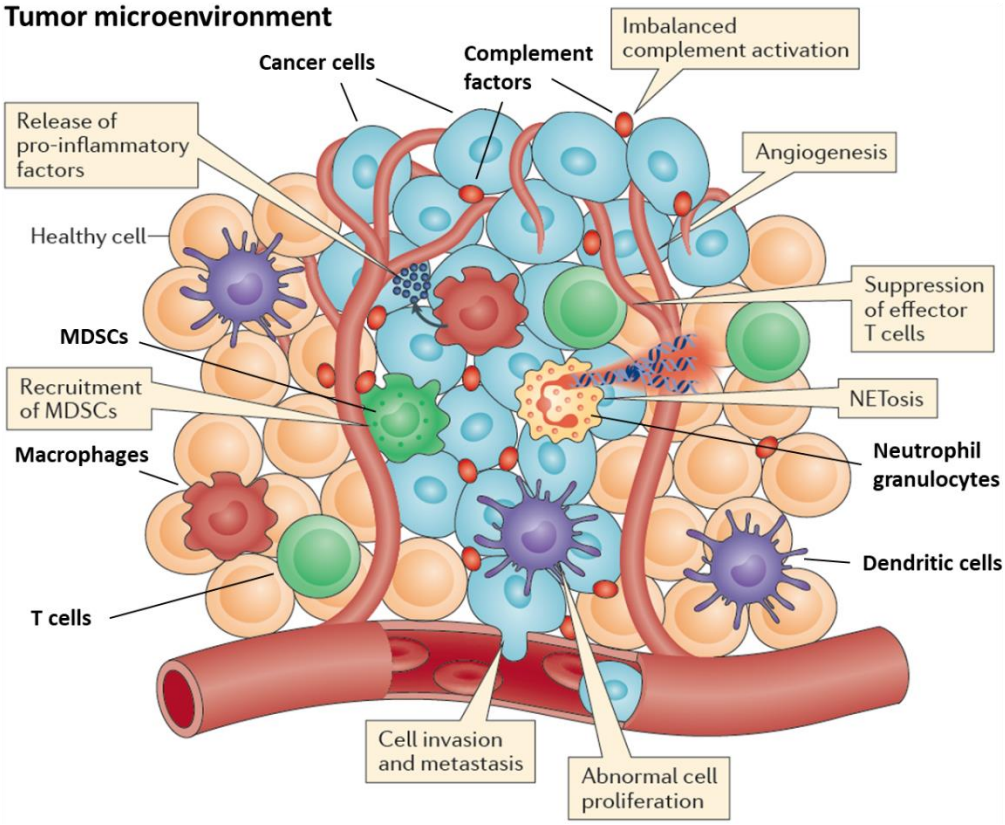

Figure 7. Pro-tumoral roles of complements in tumor microenvironment. Cancer cells and tumor-infiltrating immune cells can secrete complements in TME. Local pro-tumoral activities of complements include the release of pro-inflammatory factors, recruitment of Myeloid Derived Suppressor Cells (MDSCs), oppression of T cell response, facilitation of angiogenesis, metastasis formation, invasion and proliferation. Modified from the original image, published by Reis et al. (157)

C5a depressed $CD8^+$ T cell-mediated antitumor response in primary lung epithelial cell line-derived tumors (TC-1) in vivo. The effect was related to the C5a-mediated recruitment and promotion of RNA and ROS production of myeloid-derived suppressor cells (MDSC) (158).

C1q was expressed in the vascular endothelium and fibroblasts of several human malignant tumors in mouse models. C1q was an important actor in tumor progression via the promotion of tumor growth, metastasis-formation and angiogenesis. Moreover, C1q-deficiency was related to prolonged survival (159).

C5 receptor (C5aR1) was recently reported to be important in metastasis formation via increasing motility and metalloprotease activity in lung xenograft model (A549M1, H460M5) (160).

4T1 cells express C3 (161) and C5a receptors on their membrane (161, 162) and the blockage of this receptor with antagonist (PMX205) significantly decreased tumor growth and viability in vitro (162).

Complement factor 4 (C4), encoded by C4a and C4b genes is a participant of the classical and lectin pathway of the complement cascade. The cleavage products of C4 were found to be associated with poor response to chemoradiotherapy in esophageal cancer (C4a) (163) and decreased survival in lung cancer patients (C4d) (164).

Ptx3 has a dual role in tumors, which is highly dependent on the cancer type. Via the regulation of complement processes, Ptx3 can contribute to carcinogenic inflammatory processes in colon cancer. However, Ptx3 was found to be an antitumoral factor, as it exerts anti-angiogenic effects in fibrosarcoma, melanoma and prostate cancer (165). Ptx3 was pro-tumoral by promoting cell migration, invasion and proliferation in different cancer types (165). In basal-like breast cancer Ptx3 contributes to the stem cell-like properties via the PI3K pathway and can be a potential target aiming this pathway (166). Ptx3 expression was also found to be an unfavorable prognostic marker in basal breast cancer (166) and ovarian epithelial cancer patients (167).

Theoretically, the MAC, dedicated to destroy pathogen cells by cell-lysis, is capable of damaging tumor cells as well. However tumors express a broad spectrum of negative regulators of the complement system (CFH, CFI, CD46, CD55), especially of the terminal pathway (94). The gene encoding the terminal pathway negative regulator, CD59 is among the most highly expressed of all complement genes in the analysed tumour types. High expression and active secretion of negative complement regulator factor H (Cfh) was found in non-small cell lung cancer cell lines. The blockage of Cfh activity increased the susceptibility of these cells to complement-mediated cytotoxicity (168). Complement regulators, CD46, CD55 and CD59 were highly expressed in head and neck squamous cell- (HNSC), ovarian-, and renal- carcinomas, implicating a widespread protective role of these factors (94). The complement regulator expression was much lower or absent in non-neoplastic squamous epithelia or in the submucosa of both normal and tumor tissues. Moreover, the expression of C8A, C8B, C9 genes, participants of the terminal pathway's MAC were expressed at a particularly low level by cancer cells, contributing to the avoidance of complement-mediated cell lysis (94).

Haptoglobin protect cells from oxidative stress (141). While, the tissue expression of Hp in hepatocellular carcinoma (HCC) is a favorable marker, (169). Elevated plasma Hp is a poor prognostic biomarker in TNBC (170). Hp contributes to tumor-promotion in BC. Hp knockdown inhibited proliferation, cell cycle and increased apoptosis in breast cancer cell lines (MDA-MB-231, MDA-MB-468) (171). Hp knockdown decreased glycolysis-related key enzyme expression. Hp and glucose-6-phosphate isomerase (GPI) - a downstream effector of Hp - knockdowns significantly decreased tumor growth in breast cancer (MDA-MB-231) xenografts, in vivo (171).

SerpinA1 was anti-apoptotic factor in non-small cell lung cancer (NSCLC) and had an elevated serum level in several cancer types (NSCLC, pancreas, prostate, cervix, ovary, breast, larynx) (92). SerpinA3 expression was upregulated in tissue samples of colon cancer patients (172). In vitro experiments had demonstrated, that the SerpinA3 expresson correlated with the metastatic potential. SerpinA3 silencing impaired the migration and invasion ability of NSCLC cells. In addition, SerpinA3 inhibition reduced liver metastasis formation (172). Elevated SerpinA3 expression with consecutive cell growth-promotion was also reported in endometrial cancer cells and the knockdown of SerpinA3 inhibited cell viability and induced apoptosis (173). Moreover, the increased SerpinA3 expression correlated with high mortality in melanoma patients (174). However, proper operation of serpins prevents steps of cancer development, like invasion and metastasis, thus inhibiting tumor progression (175).

The association of **coagulation factors** and cancer was first described in 1865 (176). **Fibrin**(ogen) has an essential role in ECM formation. The tumor stroma may be considered “wound healing gone awry” and tumors themselves can be considered “wounds that do not heal” (177). Deposition of fibrin(ogen) into the ECM, and also other adhesive glycoproteins, function as a scaffold, binding growth factors, like vascular endothelial growth factor (VEGF) and fibroblast growth factor (FGF). Thus, Fibrinogen (Fg) can serve as a reservoir of growth factors, increasing their bioavailability for tumor-promoting processes like adhesion, proliferation, migration and tumor cell growth (177, 178). Moreover, fibrinogen was reported to be a key actor in tumor angiogenesis and consecutive metastasis formation via regulating endothelial cell migration, proliferation, and other direct and indirect vessel development processes (179).

Fg (especially Fibrinogen G (Fgg)) production by breast cancer cells has been demonstrated in patients without coagulation activation (180) and in MCF-7 breast cancer cell line in vitro without fibrin formation (181). The cleavage product of fibrinogen (fibrin) surrounding tumor cells can also be protective by acting as a barrier against tumor-targeting immune cells (177). Thus, inhibition of mEHT-induced Fg upregulation may have anti-tumor effects via diminishing the tumor-supportive microenvironment and may synergize with mEHT. Fgg was reported to contribute to therapy (anthracycline)-resistance, and the inhibition of Fgg expression reversed chemoresistance in breast cancer (MCF-7) xenografts (182). Moreover, loss of fibrinogen was protective against pulmonary metastases formation in a mouse model of melanoma (183).

1.3.6. Heat shock inhibitor, KRIBB11

KRIBB11 (N2-(1H-indazole-5-yl)-N6-methyl-3-nitropyridine-2,6-diamine) is a direct inhibitor of heat shock factor-1 (Hsf-1), which is a key regulator of the heat shock response. It's a synthetic low molecular weight compound that acts by inhibiting HSF1-dependent recruitment of positive transcription elongation factor b (p-TEFb) to the promoter region of hsp70 gene (184). KRIBB11 has been reported as a selective and potent inhibitor of HSR and also to induce cell cycle arrest and apoptosis in vitro and tumor growth inhibition in vivo (184, 185).

2. Objectives

We aimed to investigate the tumor growth-inhibiting effects of mEHT in TNBC mouse model. We aimed to reveal the most relevant molecular effects and pathways induced by mEHT in treated tumors with a comprehensive, multiplex analysis at mRNA and protein level.

- To investigate the short, medium and long-term effects of mEHT treatment protocols with 1 ×, 3 × and 5 × repeated treatments were applied.
- For the assessment of time-kinetic changes of the most important molecular markers, experiment with different sampling times (4, 12, 24, 48, 72 hours after last treatment) was performed.
- To evaluate the most important gene- and protein changes in response to mEHT, multiplex-level measurements (NGS, Nanostring, MS) were performed.
- To assess the most important networks, that are affected by mEHT, pathway analysis was performed using the Gene Ontology database.
- To confirm the cellular source of the most promising targets, cell culture measurements were performed with in vitro mEHT applicator.

3. Materials and Methods

3.1. Tumor model

Female BALB/c mice (Six- to eight-week-old) were kept with ad libitum access to food and water under 12 h dark/light cycles in the Basic Medical Science Center animal facility, Semmelweis University Budapest. Triple negative murine breast cancer cells, derived from 410.4 cell-line (4T1/4T07) were cultured and prepared for inoculation to generate orthotopic isografts, described previously by Ostrand-Rosenberg et al. (186). The last passage was performed freshly on the day of inoculation. Cells were inoculated in standard concentration, 1×10^6 cells/50 μL PBS (Phosphate Buffered Saline without Calcium and Magnesium #17-516F, Lonza A. G., Basel, Switzerland) subcutaneously by Hamilton syringe (Hamilton Company, Reno, NV, USA) into the 4th mammary gland's fat pad of each mice. Mice were shaved in the inguinal area on the day before inoculation. Tumor progression was investigated in experiments with different repeats: experiments with once or three-times repeated treatments (short-term) were performed on the most aggressive, 4T1 cell line, however, to minimalize the deteriorative effects, long-term experiment with five treatments was performed on the more immunogenic, less aggressive 4T07 cell-derived tumors. The multiplex, gene-level and proteomic response analyses were performed on the more commonly used and more aggressive 4T1 cell line to obtain results that are more generally applicable to the treatment of human TNBC.

Euthanasia was performed on mice by cervical dislocation. Tumors were resected, cleaned from fat and connective tissue and precisely cut into two equal pieces along the longest diameter. One part was fixed for histological evaluation in 10% formaldehyde solution (Molar Chemicals Ltd., Halásztelek, Hungary) and transferred for histological processing, detailed later. The other part was fixed in liquid nitrogen for molecular analysis (RNA isolation).

For tumor-cell inoculation, animals were anesthetized with isoflurane (Baxter International Inc., Deerfield, IL, USA), 4–5% for induction, 1.5–2% to maintain anesthesia, with compressed air (0.4–0.6 L/min).

Laboratory animals were kept and interventions were performed following the Hungarian Laws No. XXVIII/1998 and LXVII/2002 about the protection and welfare of animals, and the directives of the European Union. The study was approved by the

Governmental Ethical Committee under the No. PE/EA/50-2/2019, date of approval: 01/11/2019.

3.2. Experimental design

After the inoculation, size of tumors (Figure 8.) and body weight (BW) of mice (Figure 13) were monitored during the experiment. Tumor size was measured by digital caliper (Fine Science Tools lnc., Foster City, CA, USA) and ultrasound (Phillips Sonos 5500, Philips, Amsterdam, Netherlands). Tumors were measured in two perpendicular planes, diameters (a, b) and depth of the tumor (c) was determined. Assuming an ellipsoid form, the volume (V) of tumors was calculated based on both the ultrasound and the caliper data by the following formula: $V = (a \times b \times c \times \pi)/6$. Mice were randomized into mEHT- and sham-treated groups based on the size of the tumors, measured by US and their BW. Mice were randomized on day 3 in the short-term experiments and on day 6 in the medium- and long-term experiments. Luciferase transfected 4T1 cells were used to assess tumor growth in vivo in the short-term experiment. A rapid, immun-mediated reduction of transfected 4T1 cells was observed in tumor bearing mice from day 10. Therefore we used non-labeled cells in medium- and long-term experiments (data not shown). Randomization US data on day 6 from the medium-term experiment are presented in Figure 8. US and caliper measurements were made at the third and fifth day after inoculation (day 3 and day 5) and at the day of termination (day 7) in the short-term (1 × mEHT), day 6 and day 12 in the medium-term experiment (3 × mEHT), while in the long-term experiment (5 × mEHT) tumor size was measured on every other day beginning on day 6 after inoculation until the termination of the experiment. mEHT 24 hours was spent after the last treatment until tumor sampling (harvest). To assess time-kinetic changes after treatment, medium-term experiment after 3 × mEHT was repeated with multiple harvest times at 4, 12, 24, 48 and 72 hours after last treatment.

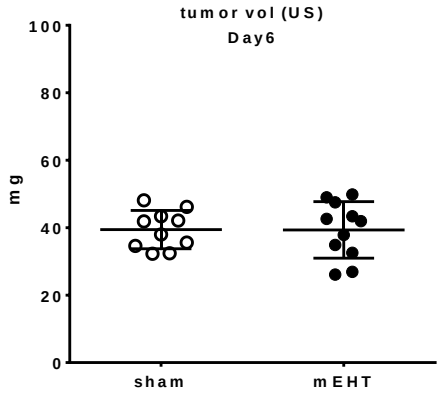

Figure 8. Randomization of mice into sham and mEHT groups according to tumor volume as measured by US at day 6. 3 × mEHT $n_{sham} = 10$, $n_{mEHT} = 11$. Mean ± SEM, Mann-Whitney test. Cell line: 4T1. (187)

Tumor progression and tissue-level analysis were performed on short (1 × mEHT), medium-long (3 × mEHT) and long-term (5 × mEHT) experiment samples. As demonstrated in the histological sections, five treatments had such a strong effect on the tumors that RNA or protein isolation in plausible quantity and quality was not feasible. Thus, mRNA and proteomic studies were performed after three mEHT treatments, when the mEHT tumor size reductive effect was already significant, but RNA and protein isolations were still possible. Numbers of animals were $n_{sham} = 7$ and $n_{mEHT} = 6$ in the short-time experiment, $n_{sham} = 7$, $n_{mEHT} = 18$ in the medium-term experiment in vivo part, $n_{sham} = 10$ and $n_{mEHT} = 11$ in the histological analysis, $n_{sham} = 9$ and $n_{mEHT} = 7$ in the long-term experiment. The schematic schedule of the experiments are presented in Figure 9.

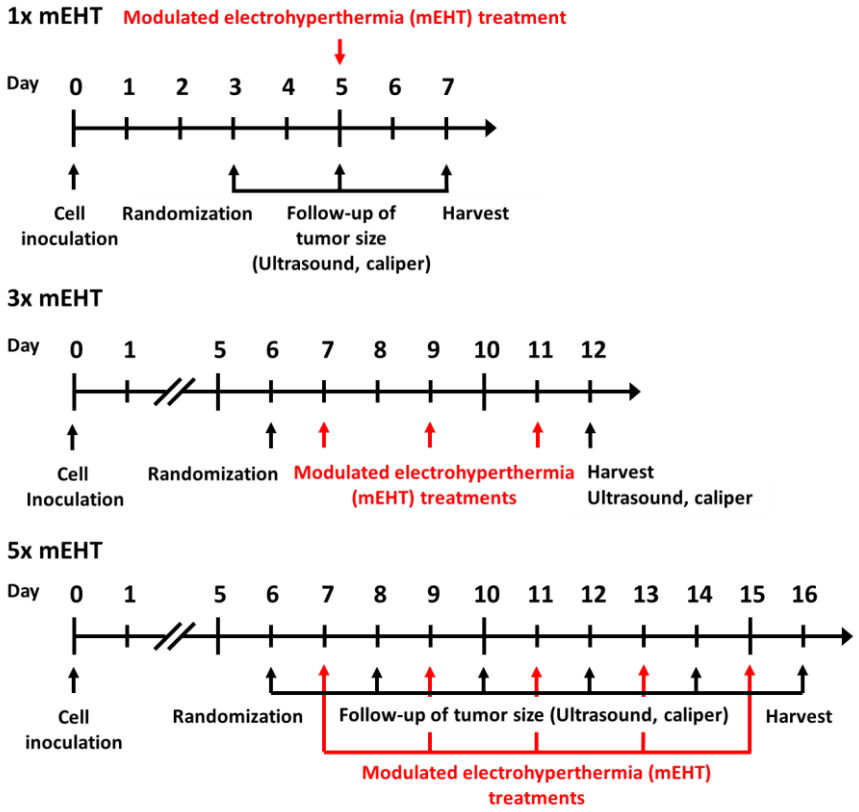

Figure 9. Design of experiments with differently repeated treatments. Cell inoculation was performed at day zero, randomization at day 3 in short- and at day 6 in both medium- and long-term experiments. Modulated electro-hyperthermia treatments were performed at day 5 in short-, day 7, 9, 11 in the medium- and on day 7, 9, 11, 13, 15 in the long-term experiment. Ultrasound, and caliper measurements were performed at day 3, 5 and 7 in the short-term, day 6 and 12 in the medium-term, and at day 6, 8, 10, 12, 14, 16 in the long-term experiment. Harvests were performed in the short-, medium- and long-term experiments at day 7, 12 and 16, respectively. (187)

3.3. In vivo treatments

Tumors were treated with the LabEHY200 modulated electro-hyperthermia device (Oncotherm Ltd., Budaörs, Hungary), dedicated for laboratory usage of rodents as described in detail in our earlier work (188). A capacitively coupled, amplitude-modulated, 13.56 MHz electromagnetic field was established between two (upper and lower) electrodes around the tumor in the inguinal region of the mice. The upper electrode, placed on a mobile pivot arm was a column-shaped plastic case with 2 mm diameter, filled with stainless steel rods, enveloped with a 3.1 cm^2 silver-plated textile, positioned on the tumor. Animals were placed on an in vivo applicator, which was functioning as the lower electrode and as a heating pad, connected to the LabEHY200

device with a heating and radiofrequency (RF) cable. The mice were shaved on the day before the first treatment in the inguinal and abdominal region, where the mobile pole electrode was positioned. No active cooling of the area under the electrode was applied. Constant temperature was assured by the new, highly adaptable electrode, ensuring a closed microenvironment between the electrode and tumor surface with low chance of temperature fluctuation. We have estabilished this method and its reproducibility in pilot experiments (188). For optimal electric coupling the back of the mice was shaved before the treatments. Treatments were performed for 30 minutes after a 5-minute long warmup. The forwarded power was 0.7 ± 0.3 watts on average. Treatments were executed in a temperature-controlled way. The four-channel TM-200 thermometer (Oncotherm Ltd., Budaörs, Hungary) was used for temperature monitoring. Temperature sensors were placed on the skin above tumor (1), in the rectum for core temperature monitoring (2), on the heating pad (3) and nearby the treatment setup for room temperature monitoring (4). For the most optimal mEHT effects, tumors should be heated up to 42 °C. Our workgroup reported that there's a 2.5 °C higher temperature inside of the tumor than on the skin during mEHT treatment (188). Therefore skin temperature was kept at 40 ± 0.5 °C throughout the treatments, as it assured the required 42 °C inside of the tumor. The applicator's temperature was set between 37.0-38.0 °C and the rectal temperature was maintained in the physiologic range (37.5 ± 0.5 °C). Room temperature was at 25 ± 1 °C. Sham treatments equaled the mEHT treatment (anesthesia, treatment length, heat pad temperature, upper electrode position), except the electromagnetic field was not turned on. Schematic visualization of the treatment is presented in Figure 10.

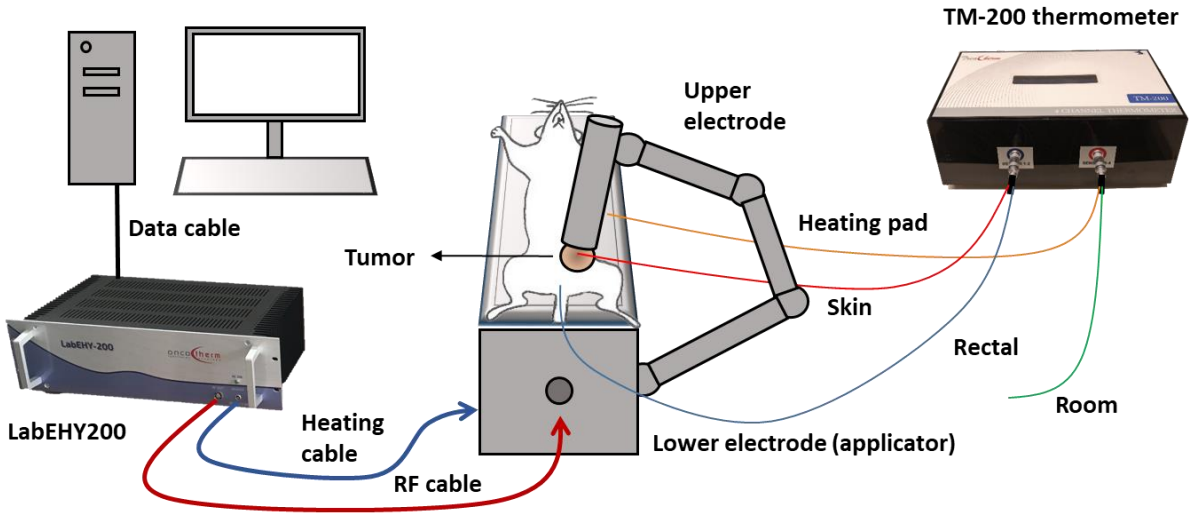

Figure 10. Schematic illustration of in vivo mEHT treatment setup. Mice were placed on the lower electrode (applicator) under isoflurane anesthesia. The upper electrode was positioned on the tumor in the inguinal region. The LabEHY200 was connected with the lower electrode with a radiofrequency (RF) and a heating cable. Temperature monitoring of tumor surface (red: skin temp. sensor), rectum (blue), heating pad (yellow) and room temperature (green) was performed by a TM-200 thermometer and the data were registered with Labehy Controller software on a computer during the treatment. (187)

3.4. In vitro treatments

4T1 cells in suspension with 1×10^6 concentration were treated with the LabEHY200 and in vitro applicator in a plastic bag. The cells were pretreated with 5 μM KRIBB11 (#385570, Sigma-Aldrich Co., St. Louis, MO, USA) or 0.01% DMSO (#D2438, Sigma-Aldrich Co., St. Louis, MO, USA) as a control for 1h before mEHT in cell culture. Thermal sensor TM-200 (Oncotherm Ltd., Budaörs, Hungary) was placed into the bag for monitoring temperature during treatment. The plastic bag was placed into a glass cuvette, filled with distilled water, and the electromagnetic field was established around it by the two electrodes of the applicator surrounding the cuvette (Oncotherm Ltd., Budaörs, Hungary). 4 ± 1 Watt was applied on average with the same amplitude-modulation (AM) as it was used during in vivo treatments. 2.3 ± 0.8 °C/min of temperature rise was established at the beginning of treatment. After attainment of 42 °C, treatment was continued for 30 minutes in a temperature-driven way. 2 h after mEHT treatment, cells were collected and lysed with Tri-Reagent (#TR118/200, Molecular Research Center, lnc., Cincinnati, OH, USA) for RNA isolation.

3.5. Histopathology and Immunohistochemistry

Formalin-fixed tumor samples were dehydrated, embedded in paraffin (FFPE), and cut 2.5 μm wide serial sections. Sections were mounted on silanized glass slides and kept in a thermostat at 65 °C for 1 h. The sections were dewaxed and rehydrated for hematoxylin-eosin (H&E) staining and immunohistochemistry (IHC). For antigen retrieval, Avair electric pressure cooker (ELLA 6 LUX (D6K2A), Bitalon Kft, Pécs, Hungary) was used. The samples were heated for 20 min in Tris-EDTA (TE) buffer pH 9.0 (0.1 M Tris base and 0.01 M EDTA), followed by a 20-min cooling with an open lid. Endogenous peroxidase blocking was performed for 15 min using 3% H_2O_2 in methanol. Non-specific proteins were blocked for 15 min in 3% bovine serum albumin (BSA, #82-100-6, Millipore, Kankakee, Illinois, USA) diluted in 0.1 M Tris-buffered saline (TBS, pH7.4) containing 0.01% sodium azide. Primary antibodies diluted in 1% BSA/TBS + TWEEN (TBST, pH 7.4) were incubated on the sections overnight in a humidity chamber. To visualize the reaction, peroxidase-conjugated anti-rabbit & anti-mouse IgGs (HISTOLS-MR-T, micropolymer -30011.500T, Histopathology Ltd., Pécs, Hungary) were used for 40 min incubations and the enzyme activity was revealed with 3, 3'-diaminobenzidine (DAB) chromogen/hydrogen peroxide kit (DAB Quanto-TA-060-QHDX-Thermo Fischer Scientific, Waltham, MA, USA) under microscopic control. The incubations were performed at room temperature with washing the samples between the steps in TBST buffer for 3 × 5 min.

Digitally scanned slides (Pannoramic Digital Slide Scanner, 3DHISTECH Ltd., Budapest, Hungary) were used for evaluation with the CaseViewer image-analysis software (3DHISTECH Ltd., Budapest, Hungary).

To assess the strength of the reactions on IHC slides, the area with positive immunoreaction was masked by setting the intensity, color, and saturation in the QuantCenter module of CaseViewer. The masked area was evaluated in the digitally annotated area, which was the intact, living area of the tumor in the case of hsp70 and the whole tumor area in the case of cC3. The ratio of the masked area to the annotated area was used to quantify the staining of the target protein, expressed in percentage (masked area/annotation area*100), as relative mask area (rMA). Hsp70 was evaluated regardless of cellular location (HistoQuant module). TDR (%) was calculated on H&E-stained slides as dividing the pale, damaged area with the whole tumor area, annotated digitally.

Antibodies used for IHC were purchased from Cell Signaling (Danvers, MA, USA): cC3 (#9664), Hsp70 (#4872). All antibodies were rabbit, polyclonal antibodies used in dilution 1:300 (cC3) and 1:200 (Hsp70).

3.6. RNA isolation and real-time PCR

RNA was isolated, using TRI reagent (Molecular Research Center Inc., Cincinatti, OH, USA) according to the manufacturer's protocol. Reverse transcription of isolated RNA was performed using High-Capacity cDNA Reverse Transcription Kit (Applied Biosystems, Carlsbad, CA, USA) and after amplification, cDNA was used as a template for RT-PCR. SYBER Green based RT-PCR with SsoAd-vanced™ Universal SYBER® Green Supermix and the CFX96 Touch Real-Time PCR Detection System (Bio Rad, Hercules, CA, USA) was used to detect messenger RNAs in the samples. Expressions were normalized to 18S. Primers used were as follows: 18S [Mus musculus] forward: CTCAACACGGGAAACCTCAC, reverse: CGCTCCACCAACTAAGAACG; C4b [Mus musculus] forward: AACCCCTCGACATGAGCAAG, reverse: TGGAACACCTGAAGGGCATC; Hp [Mus musculus] forward: GTGGAGCACTTGGTTCGCTA, reverse: CCATAGAGCCACCGATGATGC; AIF [Mus musculus] forward: CTGGTTCATCAGGGGGCAAA, reverse: CCTCTGTAGCGGAGGCAATG.

3.7. Next-Generation Sequencing (RNA Seq) and Bioinformatical Analysis

Based on the quality and quantity of the isolated RNA and the relative Hsp70 expression (used as a marker of effective treatment), measured by immunohistochemistry, five-five 3 × treated tumor samples from sham and mEHT group were chosen. RNA HS Assay Kit with the Qubit 3.0 Fluorometer (Thermo Fisher Scientific, Waltham, MA, USA) and the RNA ScreenTape system with the 2200 Tapestation (Agilent Technologies, Santa Clara, CA, USA) were used for RNA integrity and concentration measurement. The Ribo-Zero rRNA removal (Illumina, San Diego, CA, USA), the KAPA Stranded RNA-Seq libraries (Roche Diagnostics, Indianapolis, IN, USA) and the DNaseI treatment (Thermo Fisher Scientific, Waltham, MA, USA) were prepared, following manufacturer's instructions. The High Sensitivity DNA1000 ScreenTape system with the 2200 Tapestation (Agilent Technologies, Santa Clara, CA, USA) and dsDNA HS Assay

Kits with Qubit 3.0 Fluorometer (Thermo Fisher Scientific, Waltham, MA, USA) were used to determine the quality and quantity of libraries. Pooled libraries were diluted to 1.6 pM for 2 × 80 bp paired-end sequencing with 150-cycles of the High Output v2 Kit on the NextSeq 550 Sequencing System (Illumina, San Diego, CA, USA) following the manufacturer's instructions. Raw sequenced reads >50 M per sample were demultiplexed and adapter-trimmed with NextSeq Control Software, and for trimming bases at the 3′- and the 5′-ends with a quality score < 30, the FastQ Toolkit (Illumina, San Diego, CA, USA) was used. Reads shorter than 32 bp and with a mean quality score < 30 were filtered out.

Reads were aligned with reference genome of the adequate species (Mus musculus, GRCm38 Ensembl release, STAR v2.6.1c) and associated with known protein-coding genes. The number of reads aligned within a given gene was quantified by the HTSeq tool v0.6.1p1. The trimmed mean of M values (TMM) normalization method of the edgeR R/Bioconductor package (v3.28, R v3.6.0, Bioconductor v3.9) was used for the normalization of gene count data. For statistical testing, data were further log transformed using the voom approach in the limma package and TMM normalized counts were displayed as transcripts per million (TPM) values. Fold-change (FC) values were calculated by comparing the sham and mEHT treated groups, using a linear modeling process and modified t-test p-values, produced by the limma package. FC > 2 and p-value < 0.05 thresholds were used for filtering out differentially expressed (DE) genes. As a result of comprehensive literature search on PubMed, UniProt, Protein Atlas, nonprotein-coding genes, previously unidentified genes or genes with insufficient literature data (lack of information on expression, function, and regulation) were excluded from further analysis. Remaining DE genes were grouped into categories according to the main role of gene product. Functional analysis was performed using the gene ontology (GO) database to consider the functional annotations of given genes. Detection of functional enrichment was performed in the DE gene list (DE list enrichment) and towards the top when all genes were ranked according to the evidence for being differentially expressed (ranked list enrichment) applying the topGO v2.37.0 packages. Results of the significantly upregulated genes (DEListEnrichment_upR) from the GO analysis are presented. Kendall tau's method was used to create heat map from the normalized NGS RNA Seq data with heatmapper.ca (Wishart Research Group, University of Alberta,

Canada). Raw RNA-Seq data sets generated as part of this study are publicly available at the European Nucleotide Archive (https://www.ebi.ac.uk/ena, accessed on 19/03/2021), under study accession number PRJEB43813.

3.8. Mass Spectrometry Analysis

From the same samples used for NGS RNA Seq, liquid chromatography with tandem mass spectrometry (LC-MS/MS) analysis was performed using the EASY-nanoLC II HPLC unit (Thermo Fisher Scientific, Waltham, MA, USA) coupled with the Orbitrap LTQ Velos mass spectrometer (Thermo Fisher Scientific, Waltham, MA, USA). C18 trap column (Proxeon Easy-column, Thermo Fischer Scientific, West Palm Beach, FL, USA) was used for samples containing 0.1% FA and separated on a C18 PicoFrit Aquasil analytical column (New Objective, Inc., Woburn, MA, USA). Peptides were eluted using a 5–40% (v/v) for 90 min linear gradient of acetonitrile at a constant flow rate of 300 nL/min in a 0.1% formic acid solution. The Orbitrap mass analyzer was used for obtaining the full MS mass spectra in the mass range of 300 to 2000 m/z at a resolution of 30,000. The MS/MS spectra were acquired by higher-energy collisional dissociation (HCD) fragmentation of the nine most intense MS precursor ions and recorded at a resolution of 7500. Only those precursor ions that possessed charge states (>1) were selected for the MS/MS fragmentation. The dynamic exclusion was adjusted to a repeat count of 1, exclusion duration of 20 s and repeat duration of 30 s. MaxQuant proteomics software (version 1.6.0.13; Max-Planck Institute for Biochemistry, Martinsried, Germany) was used for data analysis, database search and quantification by spectral counting. The database search was performed against the adequate species (Mus musculus, Uniprot database, database date 15.10.2017, 16,923 entries). Methionine oxidation (+15995 Da) and protein N-terminal acetylation (+45011 Da) were conceded as variable modifications in the database search and carbamidomethylation of cysteines (+57021 Da) as a fixed modification. For enzyme specificity trypsin cleavage at arginine and lysine residues was used. One missed cleavage was allowed in the database search. Besides, precursor ion and fragment ion mass tolerances were adjusted to 20 ppm and 0.5 Da, respectively. A peptide and protein identification was performed with reversed database search and the false discovery rate was adjusted to 1%. Raw data and database search files are available

at ProteomeXchange (identifier PXD024150). The quantification of identified proteins was performed by the relative label-free quantification (LFQ) algorithm in MaxQuant.

3.9. Nanostring Analysis

RNA samples from the same tumors used for sequencing (NGS) and one additional sample per group were chosen for gene expression validation by Nanostring. The RNA concentration of samples was examined by Qubit 4 Fluorometer (Thermo Fisher Scientific, USA). The samples compassing adequate RNA concentrations were hybridized to the customized nCounter® gene panel (NanoString, Redwood, CA, USA). The custom gene panel we applied, contained 134, differentially expressed genes, identified by NGS RNA Seq. The chosen genes had the highest FC and lowest p values and fulfilled the criteria to be relevant in breast cancer and/or heat shock response according to literature. Those genes, that resulted no or deficient information according to the literature search were excluded from subsequent analysis. Samples were transferred to the nCounter Prep Station for further processing. The nCounter Digital Analyzer was used to digitalize the samples' gene expression profiles, and the nSolver 4.0 Analysis Software (NanoString, Redwood, CA, USA) was used to quantify the results. Background was determined as the level of maximum negative control count number, which were defined by synthetic negative probes provided by the Nanostring company.

3.10. Statistical Analysis

GraphPad Prism software (v.6.01; GraphPad Software, Inc., La Jolla, CA, USA) was used for statistical analysis. For comparing sham and mEHT treated groups, parametric unpaired t tests or nonparametric unpaired Mann-Whitney tests were performed. One-way ANOVA was used for comparing more than two groups in the time-kinetic experiment. Follow-up experiments were statistically evaluated by Two-way ANOVA with Bonferroni or without correction. Differences were declared as statistically significant at * $p < 0.05$, ** $p < 0.01$, *** $p < 0.001$, **** $p < 0.0001$. Data are presented as mean ± SEM.

4. Results

4.1. Tumor growth inhibition by mEHT

Single treatment didn't result detectable difference between the mEHT treated and sham group in tumor growth. The growth curve of tumors in mEHT group showed a smaller slope followed by traditional methods, like ultrasound and caliper (Figure 11A), however, the reliability of both modalities are low, in measuring tumors at this small size. The final volume of tumors didn't show any difference measured by caliper (sham: 48.59 ± 3.797 mm^3 vs mEHT: 53.35 ± 12.05 mm^3; Figure 11D) and US (sham: 69.07 ± 8.932 mm^3 vs. mEHT: 73.84 ± 12.86 mm^3; Figure 11E).

Three treatments were enough to eventuate significant reduction in tumor growth rate (Figure 11B) and the size of tumors was also significantly smaller 24 hours after the last treatment, measured by both modalities (caliper: sham: 193.8 ± 26.62 vs mEHT: 129.1 ± 13.50 mm^3; Figure 11D; US: sham: 265.4 ± 47.61 vs. mEHT: 133.5 ± 13.83; Figure 11E).

Elevating the number of treatments to five had resulted an even greater effectiveness. The growing tendency of the tumors in the mEHT group turned into a reduction tendency (Figure 11C) and the difference in final volume after the last treatment became even greater (caliper: sham: 223.9 ± 38.30 mm^3 vs. mEHT: 106.0 ± 25.21 mm^3; Figure 11D; US: sham: 282.1 ± 54.45 mm^3 vs. mEHT: 102.0 ± 25.48 mm3; Figure 11E). Ultrasound images of representative tumors from sham and mEHT groups, measured by longest diameter are presented in Figure 11F.

To assess tumor size the most possible objective way, weight of the tumors were measured on the day of harvest after euthanasia. Three (sham: 245.5 ± 46.17 mg vs mEHT: 127.7 ± 12.72 mg; Figure 12A) and five (sham: 288.3 ± 58.05 mg vs mEHT: 97.51 ± 20.10 mg; Figure 12B) mEHT treatments both resulted in significantly lower tumor weight. Tumor weights were not measured after one treatment. Proportionally scaled pictures of tumors after 3 and 5 treatments are presented in Figure 12A and B, respectively.

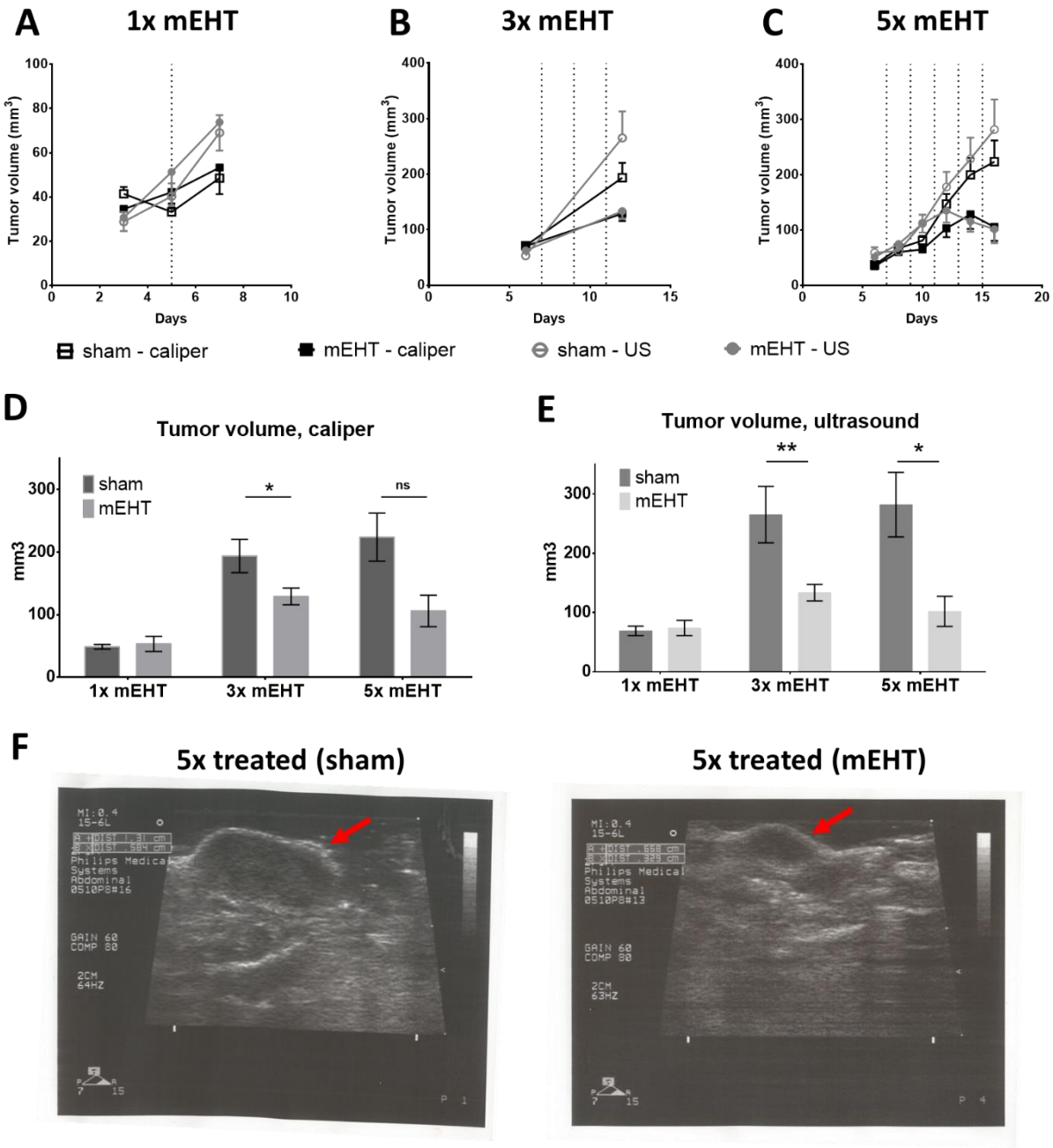

Figure 11. Effect of repeated modulated electro-hyperthermia (mEHT) treatments on tumor growth and final tumor volume. Tumor growth curves measured by digital caliper and ultrasound after 1 (A), 3 (B) and 5 (C) treatments (dotted lines, A,B,C). Final tumor volumes after 1, 3 and 5 treatments, measured by caliper (D) and ultrasound (E). Ultrasound images of representative sham and mEHT tumors after 5 treatments, red arrow shows the tumor (F). 1 × mEHT n_{sham} = 7, n_{mEHT} = 6, 3 × mEHT n_{sham} = 7, n_{mEHT} = 18, 5 × mEHT n_{sham} = 9, n_{mEHT} = 7. Mean ± SEM, Two-way ANOVA (A, B, C), Mann-Whitney test (D, E), ns: $p = 0.059$, *: $p < 0.05$, **: $p < 0.01$. Cell line: 4T1 (1 ×, 3 × treated), 4T07 (5 × treated). (187, 188)

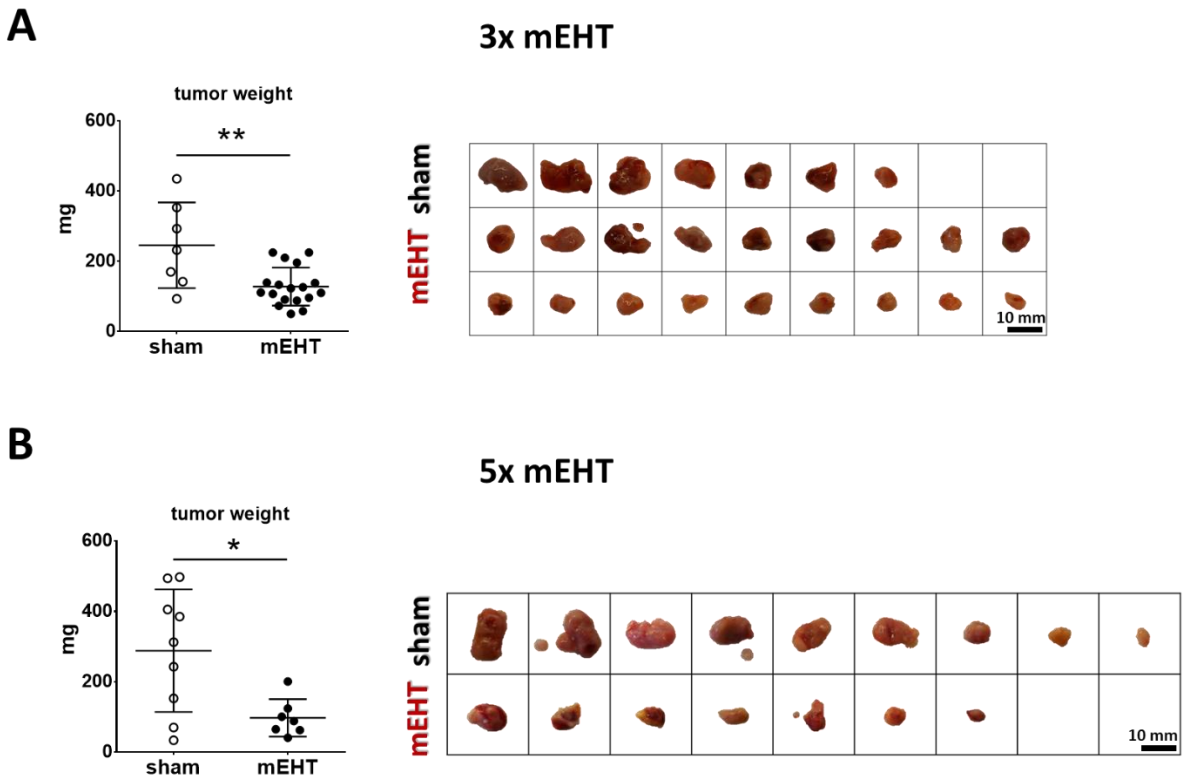

Figure 12. Effect of repeated modulated electro-hyperthermia (mEHT) treatments on tumor weight. Tumor weight and scaled images of the excised tumors after 3 mEHT treatments (A). Tumor weight and scaled images of the excised tumors after 5 mEHT treatments (B). 3 × mEHT n_{sham} = 7, n_{mEHT} = 18, 5 × mEHT n_{sham} = 9, n_{mEHT} = 7. Mean ± SEM, Mann-Whitney test. *: $p < 0.05$, **: $p < 0.01$. Cell line: 4T1 (3 × treated), 4T07 (5 × treated). (187)

4.2. mEHT had no toxic effect on mice

Measurement of the body weight (BW) of animals is a widely approved indicator of the well-being of laboratory animals. From the BW changes the general status of the animals and the tolerability of the treatment or intervention can be concluded. BW was taken into consideration during the mice's randomization, creating similar BW distribution in mEHT and sham treated groups. One treatment didn't affect the body BW of mice. The mEHT treated group's BW was reduced with 3.1% (mEHT: Mean $BW_{day\ 4}$: 23.01 ± 0.3424 g vs Mean $BW_{day\ 7}$: 22.30 ± 0.3921 g), while the sham-treated group's BW was reduced with 0.7% (sham: $BW_{day\ 4}$: 23.28 ± 0.5078 g vs $BW_{day\ 7}$: 23.12 ± 0.6253 g). Three treatments also didn't seem to be toxic to the animals at all, the average weight loss of mEHT treated mice was 3.8% (mEHT: Mean $BW_{day\ 6}$: 20.68 ± 0.3985 g vs Mean $BW_{day\ 12}$: 19.90 ± 0.3610 g). The BW of sham-treated mice increased by 2.2% on average

(sham: Mean $BW_{day\ 6}$: 20.49 ± 0.6900 g vs Mean $BW_{day\ 12}$: 20.95 ± 0.6508 g). Even five consecutive treatments were tolerated well by the mice: the mean BW loss was 5.4% in the mEHT group (mEHT: Mean $BW_{day\ 6}$: 20.75 ± 0.9327 g vs Mean $BW_{day\ 16}$: 19.63 ± 0.7461 g) and a 2.7% higher average BW was observed in the sham group (sham: Mean $BW_{day\ 6}$: 20.74 ± 0.7485 g vs Mean $BW_{day\ 12}$: 21.30 ± 0.7167 g). There was no significant difference between the groups during the whole experiment, analysed with Two-way ANOVA (Figure 13).

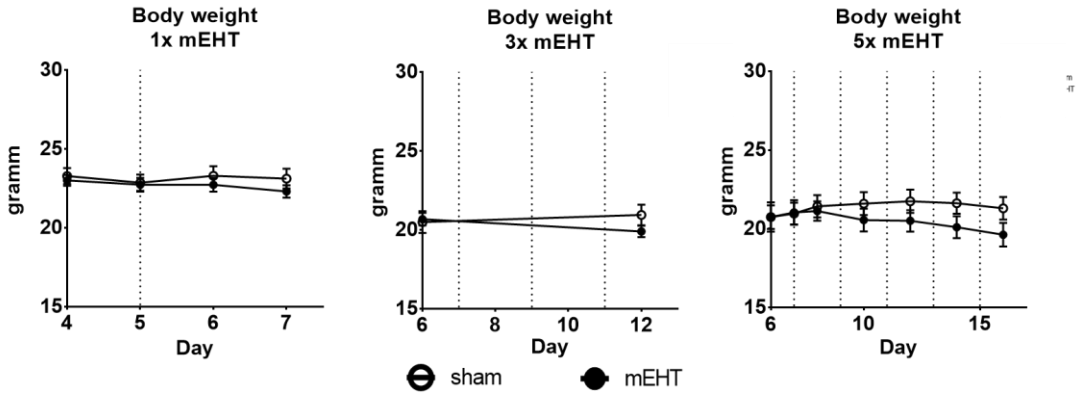

Figure 13. Body weight changes after repeated mEHT treatment. Follow-up measurement of the mice body weight during 1 × (A), 3 × (B), 5 × (C) repeated mEHT treatments. 1 × mEHT n_{sham} = 7, n_{mEHT} = 6, 3 × mEHT n_{sham} = 7, n_{mEHT} = 18, 5 × mEHT n_{sham} = 9, n_{mEHT} = 7. Mean ± SEM. Cell line: 4T1 (1 ×, 3 × treated), 4T07 (5 × treated). Our workgroup's unpublished data.

4.3. Tumor tissue destruction induced by mEHT

To investigate the tissue-level destructive effects of mEHT, H&E stained slides were digitally assessed. The area of the eosinophil, damaged part of the tumor demonstrated the region that was harmed by mEHT. These damaged parts appeared mostly in the central area of the tumors. Tissue Destruction Ratio (TDR), expressed in percentage (%), was assessed on the H&E stained slides to quantify the damage. Elevated TDR ratio was observed in some of the tumors already after a single mEHT treatment, however, this tissue-level damage didn't emerge in all of the tumors, therefore no significant difference was seen between sham and mEHT groups (TDR: sham: 1.376 ± 1.282 % vs mEHT: 16.43 ± 8.294 %; Figure 14A). Three mEHT treatments were enough to reach considerable damaging effects: TDR ratio was significantly higher in the mEHT group tumors (72.23 ± 7.143 %), than in the sham-treated ones (34.88 ± 6.080 %; Figure 14B). Increasing the number of treatments to five, TDR became even greater in the mEHT-

treated tumors (78.86 ± 5.140 %). However, TDR was also high in some of the sham-treated tumors (52.84 ± 10.27 %) and no statistically significant difference was seen between sham and mEHT groups (Figure 14C). The sham-treated tumors, presenting elevated tumor-tissue destruction were the heaviest ones in this group and there was a strong correlation between TDR and tumor size (Figure 14D). Comparing the TDR values in the tumors of the two groups with comparable tumor weight (Figure 14E), mEHT-treated tumors represented significantly elevated TDR values, implementing that in the sham group TDR elevation was size-dependent, whereas in the mEHT group it was size-independent but treatment-related (Figure 14F). Representative H&E stained samples from sham and mEHT-treated groups with low (0.9 ×) and high (40 ×) magnification is presented in Figure 14G.

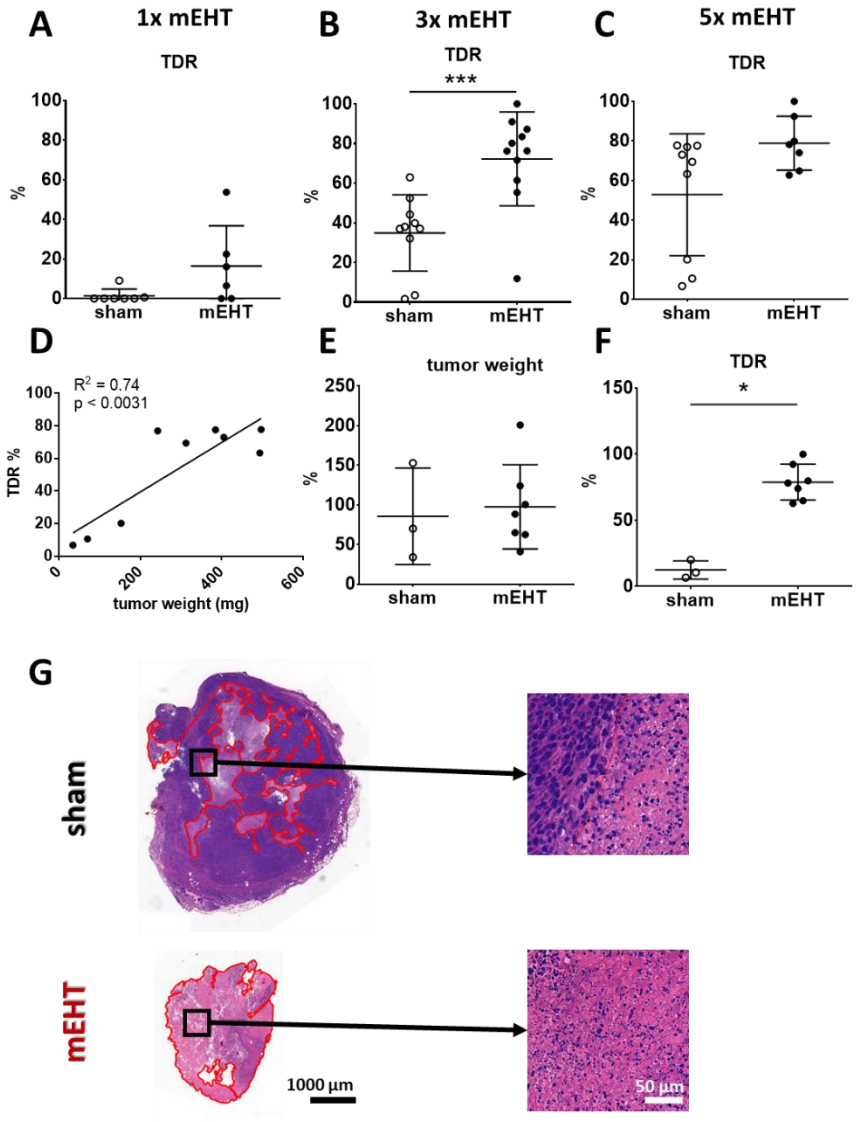

Figure 14. Tissue-level destructive effect of mEHT. TDR% quantified in hematoxylin-eosin-(H&E)-stained sections, 24 h after 1 × (A), 3 × (B) and 5 × (C) mEHT treatment. Correlation between tumor weight and TDR (%) in sham animals (D). Three smallest sham tumors' weights comparable to those of mEHT tumors (E). Comparison of TDR (%) of sham and mEHT tumors of comparable weight (F). Representative H&E-stained tumors from sham and mEHT-treated groups with 0.9 × and 40 × magnification (G). 1 × mEHT $n_{sham} = 7$, $n_{mEHT} = 6$, 3 × mEHT $n_{sham} = 7$, $n_{mEHT} = 18$, 5 × mEHT $n_{sham} = 9$, $n_{mEHT} = 7$. Mean ± SEM, Mann-Whitney test. *: $p < 0.05$, ***: $p < 0.001$. Cell line: 4T1 (1 ×, 3 × treated), 4T07 (5 × treated). (187, 188)

4.4. mEHT induced caspase-related apoptosis

Examining the mechanism of the tumor tissue damage, caused by mEHT, cleaved-caspase-3 (cC3) IHC staining was performed on FFPE tumor samples. The area of cC3+ was compared to the whole tumor area and expressed in %. The mEHT treatment resulted considerable-size cC3-positive areas in half of the tumors, even after one treatment. However, the other half of the tumors were lack of these cC3+ areas (14.45 ± 7.916 %) and no significant difference was observable compared to sham tumors (0.9632 ± 0.7733 %, Figure 15A). After three treatments, almost all of the mEHT treated tumors displayed higher than 50% cC3+ area relative to total area, and the difference compared to sham-treated tumors was significant (sham: 29.84 ± 5.065 % vs mEHT: 67.71 ± 7.448 %, Figure 15B). Five treatments were enough to cause an elevation of cC3+ areas more than 60% in all tumors. However, the significant difference between the groups disappeared since 6 out of 9 sham treated tumors displayed elevated cC3+ area too (sham: 54.73 ± 9.991 % vs mEHT: 72.23 ± 6.808 %, Figure 15C).

Comparing the H&E and cC3+ areas, a highly overlapping arrangement pattern was observed in the tumors, implementing, that the main tissue destructive effect of mEHT was caspase-related cell death. Representative cC3-stained samples from sham and mEHT-treated groups with low (0.9 ×) and high (40 ×) magnification are presented in Figure 15D. To investigate, if mEHT induced apoptosis via caspase-independent pathway, Apoptosis Inducing Factor (AIF) expression was measured with qPCR. Samples from five different time points (4,12,24,48,72 hour) were investigated from tumors that were treated three-times. No significant difference was detected in AIF expression, at the five different time-points compared to sham tumors (Figure 15E).

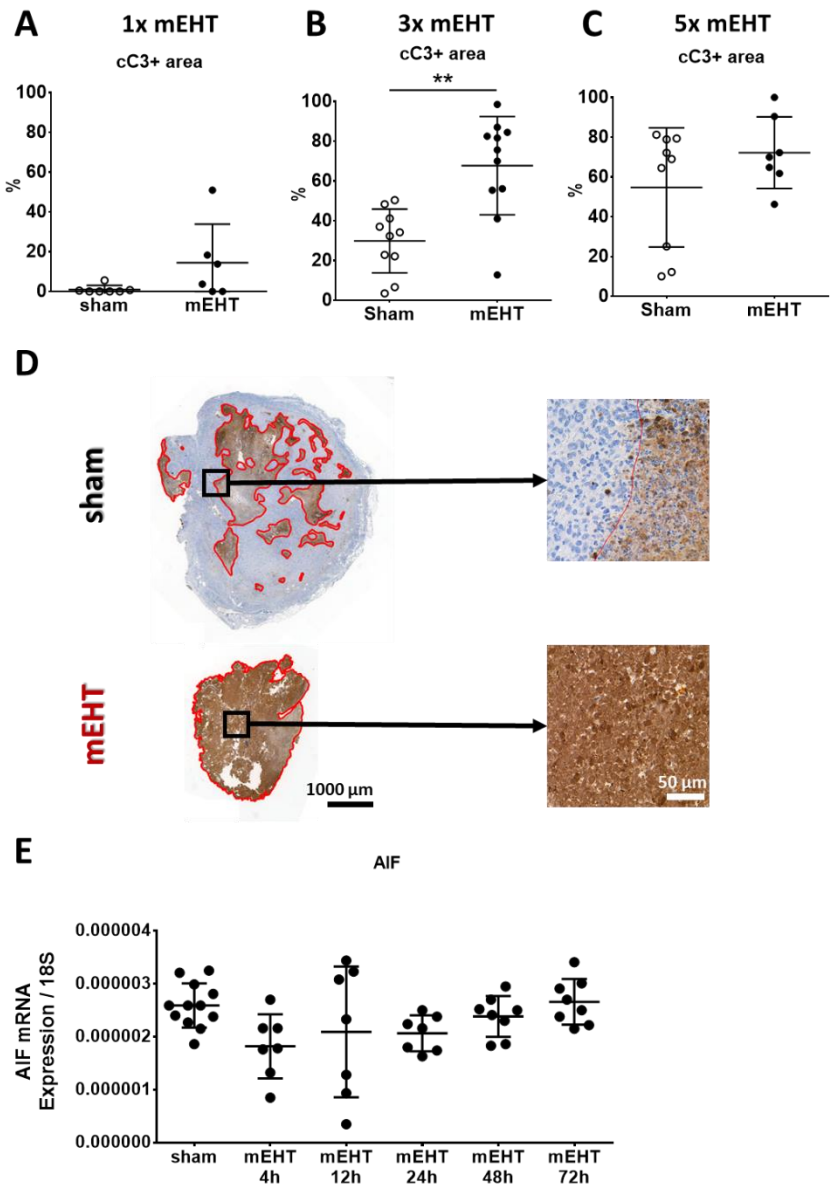

Figure 15. Caspase-dependent tissue destruction, caused by mEHT. Quantification of cC3+ area in the ratio of total area in cC3-stained immunohistochemical sections, 24 h after 1 × (A), 3 × (B) and 5 × (C) mEHT treatment. Representative cC3-stained tumors from sham and mEHT-treated groups with 0.9 × and 40 × magnification (D). 1 × mEHT n_{sham} = 7, n_{mEHT} = 6, 3 × mEHT n_{sham} = 7, n_{mEHT} = 18, 5 × mEHT n_{sham} = 9, n_{mEHT} = 7. Mean ± SEM, Mann-Whitney test. **: $p < 0.01$. Cell line: 4T1 (1 ×, 3 × treated), 4T07 (5 × treated). (187, 188). AIF mRNA relative expression of tumors at different time-points after 3 × mEHT (E). n_{sham} = 12, n_{4hour} = 7, n_{12hour} = 7, n_{24hour} = 7, n_{48hour} = 8, n_{72hour} = 8). Mean ± SEM, One-way ANOVA. Cell line: 4T1. Our workgroup's unpublished data.

4.5. mEHT induced heat shock protein 70 (Hsp70) accumulation

Hsp70 expression was assessed as the ratio of specific staining area/living tumor area (relative mask area: rMA%). Strong, specific Hsp70 expression was detected in the mEHT treated tumors (1.11 ± 0.715 %, Figure 16A), especially in a ring-shaped form around the central damaged area, demonstrated by the still viable cells (Figure 16B, C). This expression elevation was absent inside the damaged area and also, no specific hsp70 expression elevation was detectable in the sham-treated tumors (0.18 ± 0.2 %, Figure 16A). This Hsp70 expression elevation may considered as a defensive reaction of the harmed but still viable tumor cells.

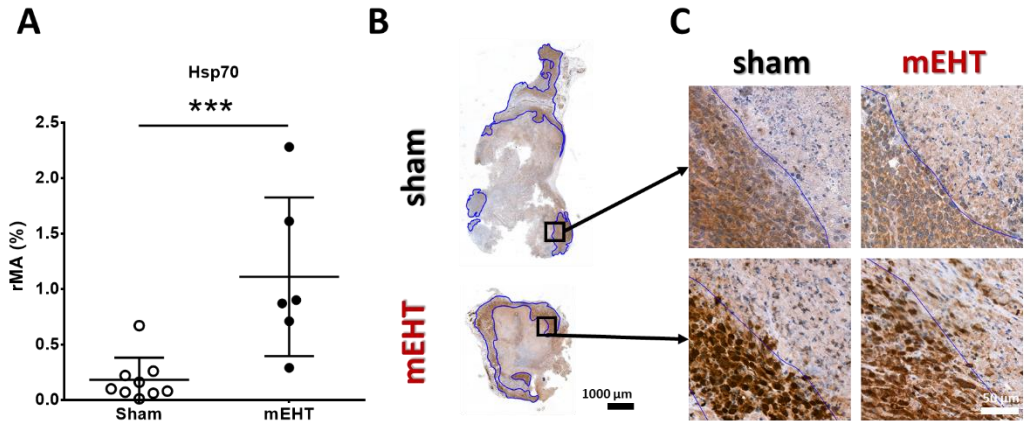

Figure 16. Heat shock response induced in tumors after 5 × mEHT. Quantification of hsp70 protein expression as rMA% in the ratio of total tumor area on immunohistological sections, 24 h after treatment (A). Representative tumors from sham and mEHT-treated mice with Hsp70 staining (0.9 × magnification), black rectangles magnified at 'C' (B). Representative sections of Hsp70 expression near the damaged tumor area (blue annotation), 40 × magnification (C). $n_{sham} = 9$, $n_{mEHT} = 7$. Mean ± SEM, Mann-Whitney test. ***: $p < 0.001$. Cell line: 4T07. (187)

4.6. Multiplex analysis revealed mEHT-induced activation of a local acute-phase response

4.6.1. Next-generation sequencing (RNA-Seq) and pathway analysis demonstrated locally elevated expression of APPs, induced by mEHT in vivo

Three-times treated samples, examined 24 hours after the last treatment, were analysed with NGS RNA Seq for a more comprehensive investigation of mEHT effects.

Comparing sham and mEHT, NGS measurement resulted 290 differentially expressed (DE) genes, which fulfilled the following criteria: $p < 0.05$ ($\log10(p) < 1.30103$); Fold Change (FC) > 2 (logFC > 1). DE genes, clustered into a heat map with Kendall's Tau distance measurement demonstrated that 63.8% (185/290) of the DE genes got upregulated due to the treatment and 36.2% (105/290) genes got downregulated (Figure 17A). Since the vast majority of DE genes, recognized with NGS analysis, demonstrated upregulated expression by mEHT, these genes were further investigated with pathway analysis. Based on the literature search, we established 19 categories from the genes (not presented). The Gene Ontology (GO) database was used for further functional enrichment (DEListEnrichment_upR) of the genes. 200 pathways was found, 'Response to stimulus' pathway (GO:0050896 pathway, p value: 0.00012) contained the most, 38 genes after ranked list enrichment. 15 upregulated pathways with the most genes and lowest p values are presented at Table 4.

Table 4. Significant Gene Ontology pathways, according to NGS (RNA-Seq) data after 3 × mEHT treatment. Our workgroup's unpublished data.

GO pathway	GO ID	Nr. of sign. genes	p value
Response to stimulus	GO:0050896	38	0.00012
Response to chemical	GO:0042221	31	2.7E-09
Regulation of biological quality	GO:0065008	24	0.000052
Response to organic substance	GO:0010033	20	0.000048
Cell surface receptor signaling pathway	GO:0007166	17	0.00062
Nervous system development	GO:0007399	16	0.0012
Response to external stimulus	GO:0009605	16	0.00032
Positive regulation of cell communication	GO:0010647	13	0.00179
Positive regulation of signaling	GO:0023056	13	0.00184
Response to endogenous stimulus	GO:0009719	13	0.000039
Cell-cell signaling	GO:0007267	12	0.00043
Ion transport	GO:0006811	11	0.00121
Response to drug	GO:0042493	11	4.9E-06
Response to oxygen-containing compound	GO:1901700	11	0.00091
cellular response to endogenous stimulus	GO:0071495	10	0.00088

38 genes, organized into the 'Response to stimulus' pathway, according to their FC values are presented in Figure 17B. 7 stress-related genes (coagulation factors – Fgb,

Fgg, protease inhibitors – Itih4, Serpina3n, Serpina3m, complement factors – Cfd, Hp) out of total 38 genes were part of the 'Response to stimulus' pathway. These factors – marked with red names in Figure 17B - are traditionally interpreted as Acute-Phase Proteins (APPs), however, they fulfill different, non-canonical effects, produced locally by certain cells, when exposed to different types of cellular stress (e.g. ischemia reperfusion, heat, etc.). Investigating further these factors, 13 stress-related genes were observed to be significantly upregulated in total from the entire NGS database, including complement cascade-related genes: pentraxin-related protein 3 gene (Ptx3), classical pathway (C1s1, C4b), alternative pathway (Cfd) and terminal pathway (Hc) complement components, protease inhibitors (Itih2, Itih4, Serpina3n, Serpina3c, Serpina3c), coagulation factors (Fbg, Fgg) and the free hemoglobin-binding haptoglobin (Hp). 4 heat shock factors (Hspb1, Hspa1a, Hspa1b, Hsph1) were found to be upregulated by mEHT according to NGS data, however, the level of upregulation didn't reach level of significance. A Volcano plot visualization of gene logFC and –log10(p) values of NGS data is presented in Figure 17C, where APPs are highlighted as red dots and numbered 1-13. APPs are identified in Table 8. Individual NGS RNA Seq expression data of further analysed APPs and heat shock factors are presented in Table 5.

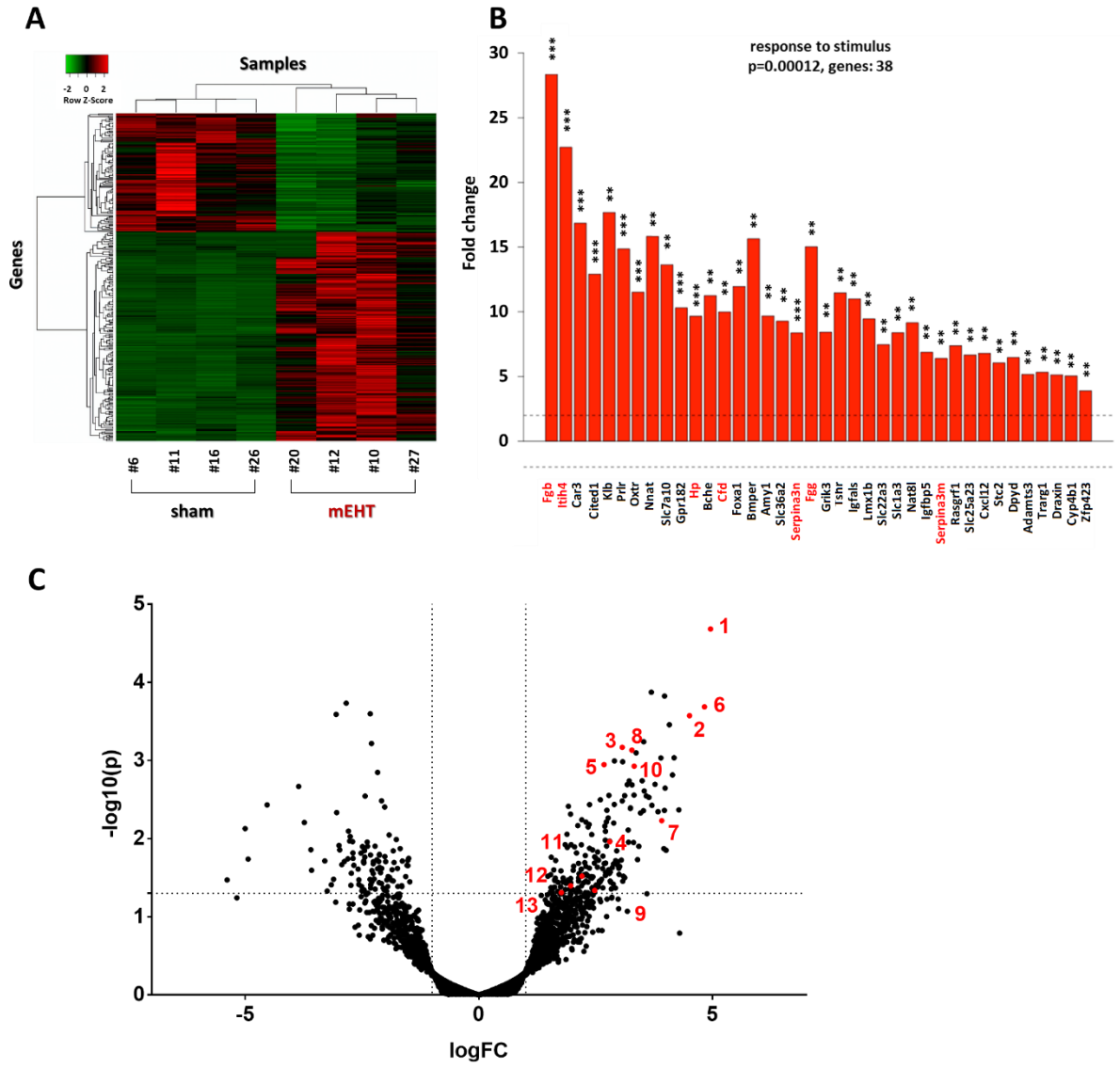

Figure 17. NGS and pathway analysis of 3 × mEHT treated tumor samples, 24 h after treatment. Heat map clusterization with dendograms (Kendall tau's method) of differentially expressed (DE) genes according to next-generation sequencing (NGS) RNA Seq data. Columns represent samples, rows represent genes. Red = upregulation, green = downregulation (A). Pathway with most upregulated genes (Response to stimulus pathway, GO:0050896) based on the gene ontology (GO) analysis of the NGS data. Dotted line: FC = 2. Red: further analysed genes (B). Volcano plot visualization of all genes according to NGS RNA Seq data. −log10(p) values plotted against fold changes (logFC). Vertical dotted line: logFC = 1, horizontal dotted line: −log10(p) =1.30103. Red dots marked with numbers (1-13) represent APPs, further analysed and presented in Table 8. (C). n_{sham} = 4, n_{mEHT} = 4. Mean ± SEM. Statistical analysis described in chapter 3.7. *: $p < 0.05$, **: $p < 0.01$, ***:$p < 0.001$, ****: $p < 0.0001$. Cell line: 4T1. (187)

Table 5. Expression data of APPs, measured by NGS RNA Seq after 3 × mEHT treatment (sham vs. mEHT). $n_{sham} = 4$, $n_{mEHT} = 4$. Mean ± SEM. Statistical analysis described in chapter 3.7. *: $p < 0.05$, **: $p < 0.01$, ***:$p < 0.001$, ****: $p < 0.0001$. Cell line: 4T1. Our workgroup's unpublished data.

Gene Expression	sham				Mean sham	mEHT				Mean mEHT	p value
Itih2	0.0071	0.0023	0.0000	0.0000	0.0023	0.2491	0.2031	0.0388	0.1567	0.1619	****
Itih4	0.0000	0.0000	0.0000	0.0046	0.0012	0.0746	0.1277	0.1160	0.0717	0.0975	***
Serpina 3n	1.3335	2.2827	0.6600	1.5898	1.4665	20.3675	15.3504	19.1424	9.1429	16.0008	***
Serpina 3c	0.0953	0.1327	0.0319	0.0104	0.0676	0.9129	0.6584	0.6087	0.2929	0.6182	*
Serpina 3m	0.0527	0.0677	0.0529	0.0172	0.0476	0.5866	0.4476	0.3603	0.4127	0.4518	**
Fgb	0.0000	0.0034	0.0000	0.0000	0.0009	0.3017	0.0797	0.0147	0.0791	0.1188	***
Fgg	0.0000	0.0514	0.0000	0.0000	0.0128	0.3541	0.3963	0.0000	0.4585	0.3022	**
Hp	0.1574	0.3822	0.1453	0.2966	8.7733	1.4097	1.3107	0.5856	0.3307	103.2392	***
Ptx3	0.0325	0.2398	0.0434	0.1062	0.1055	1.0274	1.1953	1.3912	0.2992	0.9783	*
Cfd	6.6680	14.9655	3.3919	2.9289	6.9886	109.9876	65.6001	122.9642	48.5822	86.7835	**
C4b	0.6526	0.5658	0.1686	0.9452	0.5830	4.3547	2.9110	3.1118	1.5990	2.9941	*
Hc	0.0119	0.0255	0.0139	0.0454	0.0242	0.2301	0.1116	0.0217	0.1188	0.1206	*
C1s1	0.5484	0.8426	0.2792	0.5357	0.5515	4.9577	2.6261	1.4571	1.4873	2.6320	*
Hspb1	1.6838	3.5277	5.2901	1.4372	2.9847	16.0510	9.7997	49.0756	9.9873	21.2284	ns
Hspa1a	0.0442	0.2982	0.1686	0.0983	0.1523	0.3006	0.6198	8.6106	0.1304	2.4153	ns
Hspa1b	1.8818	3.1755	3.2405	1.2898	2.3969	2.9264	6.6712	32.1136	5.0305	11.6854	ns
Hsph1	0.2712	0.2931	0.3328	0.1804	0.2694	0.8451	0.5277	0.6856	0.4728	0.6328	ns

4.6.2. Nanostring analysis demonstrated upregulated absolute RNA count of locally produced APPs

After a comprehensive literature search, 134 DE target genes, found with NGS were selected for further analysis and validation with Nanostring method, creating a customized gene panel. Nanostring nCounter® Technology (Nanostring Technologies, Seattle, WA, USA) counts individual RNA molecules without reverse transcription and amplification, enabling a direct quantification of mRNA molecules of the genes of interest. 77,6% of the genes (104/134) were identified and all of the genes' changing direction (up- or downregulation), found by NGS was confirmed by Nanostring measurement. 3 genes confirmed with Nanostring didn't fulfill the DE criteria ($p < 0.05$ and Fold Change (FC) > 2). Nanostring results of the genes, logFC values (x) plotted against –log10(p) (y) are portrayed as a volcano plot in Figure 18. Genes numbered 3, 4,

5, 7, 8, 9, 10, 11, 12, 13 are the APP genes that have been detected with Nanostring. Stress-related APPs' individual RNA count data are presented in Table 6.

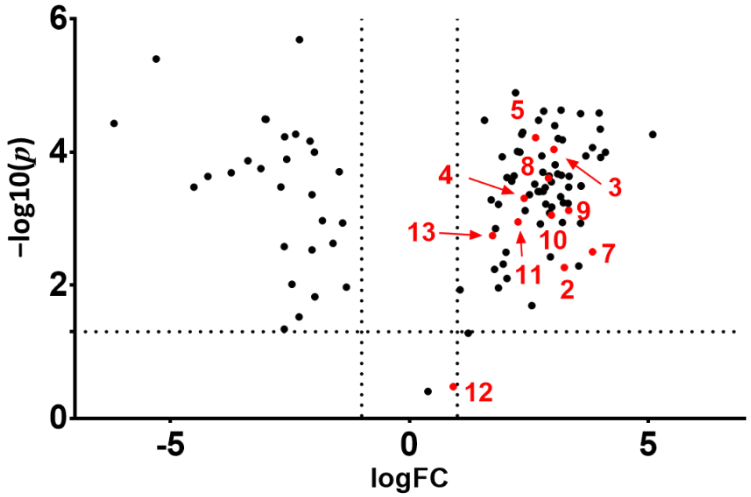

Figure 18. Nanostring analysis of 3 × mEHT treated tumor samples, 24 h after treatment. Volcano plot visualization of all genes according to Nanostring data. −log10(p) values plotted against fold changes (logFC). Vertical dotted line: logFC = 1, horizontal dotted line: −log10(p) =1.30103. Red dots marked with numbers (3, 4, 5, 7, 8, 9, 10, 11, 12, 13) represent APPs, further analysed and presented in Table 8. n_{sham} = 6, n_{mEHT} = 6. Mean ± SEM. Cell line: 4T1. (187)

Table 6. Absolute RNA count of APPs measured by Nanostring after 3 × mEHT treatment (sham vs. mEHT). n_{sham} = 6, n_{mEHT} = 6. Mean ± SEM. **: p < 0.01, ***:p < 0.001, ****: p < 0.0001. Cell line: 4T1. (187)

RNA Count	sham						Mean sham	mEHT						Mean mEHT	p value
Itih4	48	9	9	13	2	4	14.2	196	42	60	20	158	40	86	**
Serpina 3n	109	62	186	110	25	96	98	1265	614	565	444	1016	352	709.3	****
Serpina 3c	69	37	78	47	12	18	43.5	284	191	216	64	251	111	186.2	***
Serpina 3m	17	13	16	15	7	8	12.7	85	49	30	19	75	34	48.7	****
Fgg	7	16	9	19	4	5	10	4	103	121	18	19	170	72.5	**
Hp	7782	3082	4825	7449	1505	1632	4379.2	48983	25954	16208	11680	56174	16738	29289.5	***
Ptx3	244	87	180	100	15	107	122.2	2024	568	983	566	2202	185	1088	***
Cfd	3224	975	1846	2293	260	402	1500	22431	7571	7408	2341	16311	4961	10170.5	***
C4b	1242	1081	997	1244	166	1443	1028.8	9234	4573	3806	2930	5258	1794	4599.2	**
Hc	17	28	16	32	6	33	22	2	77	47	6	6	49	31.2	ns
C1s1	493	479	744	233	141	345	405.8	2036	1638	1390	841	979	672	1259.3	**

4.6.3. Local APP and heat shock factor protein production were induced by mEHT in TNBC isografts

Mass spectrometry analysis was performed from the tumor samples to study the target genes identified by NGS on protein level. 69.2% (9/13) of the APPs were identified with mass spectrometry as well. All of these APPs showed same direction in their changed expression (upregulation) as seen from NGS data and 88.9% (8/9) of these upregulated proteins reached significance level. Moreover, 4 heat shock proteins (Hspb1, Hspa1a, Hspa1b, Hsph1) were identified as significantly upregulated by MS, which has not been found as DE by NGS. LFQ data of different APPs and heat shock factors, detected by MS are presented in Table 7.

Table 7. LFQ values of APPs and Hsps, measured by mass spectrometry after 3 × mEHT treatment (sham vs. mEHT). $n_{sham} = 5$, $n_{mEHT} = 5$. Mean ± SEM. *: $p < 0.05$, **: $p < 0.01$, ***:$p < 0.001$, ****: $p < 0.0001$, *****:$p < 0.00001$. Cell line: 4T1. Our workgroup's unpublished data.

LFQ intensity	**sham**					**Mean sham**	**mEHT**					**Mean mEHT**	**p value**
Itih2	23.05	24.26	23.34	22.19	22.59	23.08	25.55	26.38	25.73	25.91	26.42	26.00	****
Itih4	25.46	25.24	24.86	24.69	24.33	24.92	26.82	26.84	28.16	27.77	27.58	27.44	****
Serpina3n	24.14	22.95	21.84	23.26	21.30	22.70	25.06	26.46	26.60	26.21	25.33	25.93	***
Serpina3m	21.87	21.30	20.81	22.14	20.80	21.38	20.29	19.44	21.72	22.63	22.34	21.29	ns
Fgb	27.12	27.97	27.01	27.47	26.77	27.27	29.67	29.39	29.77	29.97	29.77	29.72	*****
Fgg	26.42	26.64	26.16	26.57	26.42	26.44	27.89	28.04	28.71	29.01	29.06	28.54	****
Hp	23.26	24.52	21.09	24.22	21.64	22.95	27.44	25.41	28.48	28.35	28.44	27.62	***
Cfd	24.43	25.59	24.18	23.70	23.62	24.30	26.68	26.44	26.00	25.73	26.66	26.30	**
C4b	23.06	23.08	21.22	21.40	21.75	22.10	24.51	24.68	25.19	25.36	26.24	25.20	***
Hspb1	26.20	25.67	26.61	26.44	25.83	26.15	29.20	28.33	28.85	29.37	28.37	28.82	****
Hspa1a Hspa1b	25.78	25.17	26.07	25.49	25.88	25.68	27.96	27.44	28.20	27.77	27.40	27.75	****
Hsph1	22.51	23.20	24.65	23.00	24.27	23.52	25.37	24.36	24.68	24.39	25.23	24.81	*

Summarizing all three multiplex methods, fold-changes and p values of the aforementioned upregulated APP genes with ID numbers, detected with NGS RNA Seq, Nanostring and MS data are presented in Table 8.

Table 8. Cellular stress response upregulated by 3 × mEHT treatment. Genes (official name abbreviations as used in all multiplex platforms and descriptions of the coded proteins) detected as upregulated with all three multiplex methods (NGS RNA Seq, Nanostring, MS) are designated with bold letters. Nanostring validated all NGS hits with a similar FC value. Hspa1a and Hspa1b are the most common isoforms of Hsp70. Cell line: 4T1. # uniquely expressed in mEHT-treated samples but not in the sham-treated tumors, no FC applies by the Nanostring evaluation. (187)

Nr	Gene Name	Description	NGS		Nanostring		MS	
			FC	*p*	FC	*p*	LFQ Intensity Difference	*p*
Protease inhibitors								
1	Itih2	inter-alpha trypsin inhibitor. heavy chain 2	31.1	2.1E-05	#		2.9	7.7E-05
2	**Itih4**	**inter alpha-trypsin inhibitor. heavy chain 4**	**22.7**	**2.7E-04**	**9.5**	**0.005**	**2.5**	**6.1E-05**
3	**Serpina3n**	**serine (or cysteine) peptidase inhibitor. clade A. member 3N**	**8.4**	**6.8E-04**	**8.1**	**9.11E-05**	**3.2**	**6.1E-04**
4	Serpina3c	serine (or cysteine) peptidase inhibitor. clade A. member 3C	7.0	0.011	5.3	5.0E-04	Not detected	Not detected
5	Serpina3m	serine (or cysteine) peptidase inhibitor. clade A. member 3M	6.4	0.001	6.2	6.1E-05	0.1	0.891
Fibrinogens and haptoglobin								
6	**Fgb**	**fibrinogen beta chain**	**28.4**	**2.1E-04**	**#**		**2.4**	**5.2E-06**
7	**Fgg**	**fibrinogen gamma chain**	**15.0**	**0.006**	**14.2**	**0.003**	**2.1**	**3.8E-05**
8	**Hp**	**haptoglobin**	**9.7**	**7.4E-04**	**7.5**	**2.5E-04**	**4.7**	**8.3E-04**
Complement factors								
9	Ptx3	pentraxin related gene	5.6	0.046	10.1	7.5E-04	Not detected	Not detected
10	**Cfd**	**complement factor D (adipsin)**	**10.0**	**0.001**	**7.8**	**8.8E-04**	**2.0**	**0.001**
11	**C4b**	**complement component 4B (Chido blood group)**	**4.6**	**0.03**	**4.8**	**0.001**	**3.1**	**2.9E-04**
12	Hc	hemolytic complement	3.9	0.04	1.9	0.335	1.2	1.7E-04
13	C1s1	complement component 1. s subcomponent 1	3.4	0.049	3.3	0.002	Not detected	Not detected
Heat shock factors								
	Hspb1	Heat shock protein beta-1	3.8	0.075	not investigated		2.7	1.1E-05
	Hspa1a	Heat shock 70 kDa protein 1A	2.0	0.551	not investigated		2.1	1.3E-05
	Hspa1b	Heat shock 70 kDa protein 1B	2.4	0.362				
	Hsph1	Heat shock protein 105 kDa	1.8	0.761	not investigated		1.3	0.023

4.7. Local APP production is induced by mEHT in a time-dependent manner in vivo

To further analyse the procession of local APP activation of tumor cells, a time-kinetic experiment was performed. According to Nanostring analysis, two APPs, C4b and Hp, have been identified as differentially expressed with all three multiplex methods (Table 8) and had the highest absolute RNA count (Table 6). Measurement with qPCR in

different time-points (4,12,24,48,72 hour) after last mEHT corroborated the significant upregulation of both APPs on mRNA level, compared to sham (Hp: 3.220e-005 ± 5.184e-006, Figure19A; C4b: 5.394e-006 ± 6.805e-007, Figure19B). None of the APPs had significantly increased level at 4 or 12 hour, but reached at 24 hour (Hp: 9.640e-005 ± 3.572e-005; C4b: 9.246e-006 ± 2.025e-006). Expression of Hp showed a decrease at 48 hours (4.255e-005 ± 1.394e-005) and returned to almost sham level at 72 hours (3.593e-005 ± 1.005e-005) after treatment. However, expression of C4b remained high at 48h (8.309e-006 ± 1.317e-006) and was significantly increased even 72 hours (8.961e-006 ± 1.508e-006) after treatment (Figure 19).

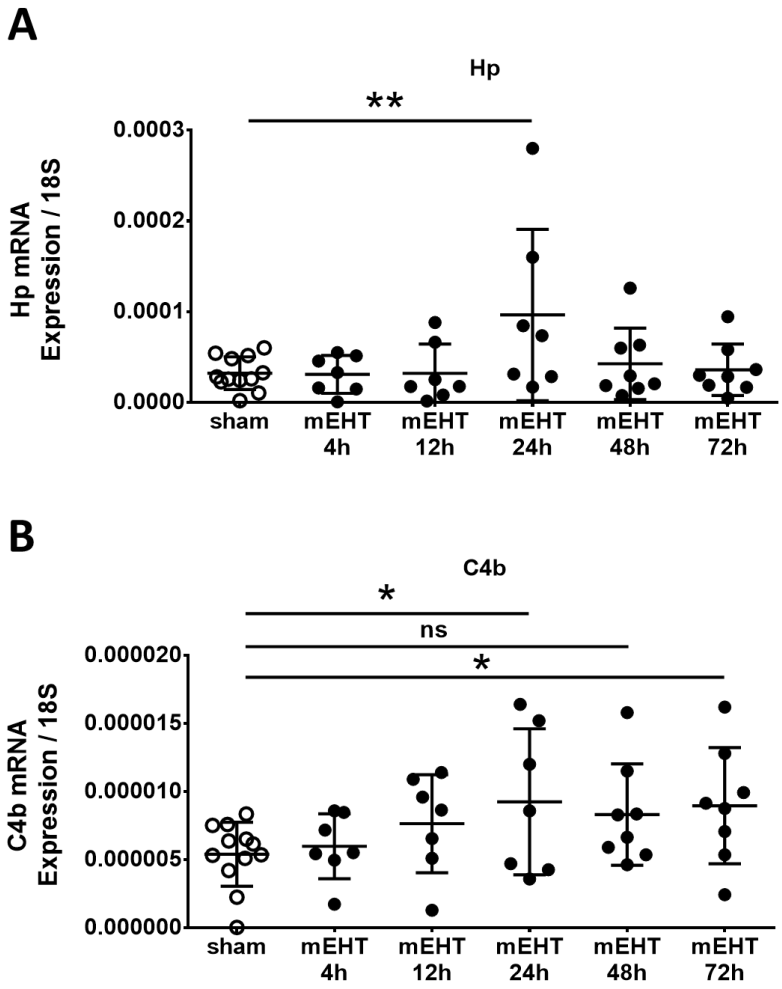

Figure 19. Time kinetic changes of APP (Hp, C4b) expression after three mEHT treatments. Hp mRNA relative expression of tumors at different time-points (4,12,24,48,72 hour) after last treatment (A). C4b mRNA relative expression of tumors at different time-points (4,12,24,48,72 hour) after last treatment (B). n_{sham} = 12, n_{mEHT} = 7-8. Mean ± SEM, One-way ANOVA (Fisher's LSD test). ns: $p = 0.0864$, *: $p < 0.05$, *: $p < 0.01$. Cell line: 4T1. Our workgroup's unpublished data.

4.8. Local APP production by 4T1 can be partially inhibited by KRIBB11 in vitro

To determine the source of the APPs, found by multiplex methods, in vitro experiment was performed, culturing the 4T1 cell line and C4b and Hp expression was measured with qPCR. Both factors were measured in a detectable amount in 4T1 monoculture, confirming that they are produced by the cancer cells. KRIBB11 is a heat shock response inhibitor, by selectively inhibiting the heat-shock factor-1 (Hsf-1) function (184). In our in vitro treatment, KRIBB11 reduced the C4b baseline expression of the 37 ^{o}C-treated control 4T1 cells, compared to DMSO treated cells ($p = 0.0256$). However, similar effect was not observable in Hp expression. Single mEHT treatment induced significant upregulation of C4b, 2 hours after treatment ($p < 0.0001$), whereas in the Hp expression, this upregulation didn't reach significance levels, but an increasing tendency was perceptible. Combination of mEHT + KRIBB11 treatment resulted in a significant reduction of C4b expression, compared to mEHT + DMSO treatment ($p < 0.0001$; Figure 20A), while this effect was not observable in Hp expression (Figure 20B). Moreover, a strong correlation was detected between the expression of C4b and hsp70 ($R^2 = 0.75$, $p < 0.0001$; Figure 20C), and a similar correlation was also apparent between Hp and hsp70 ($R^2 = 0.48$, $p < 0.0001$; Figure 20D).

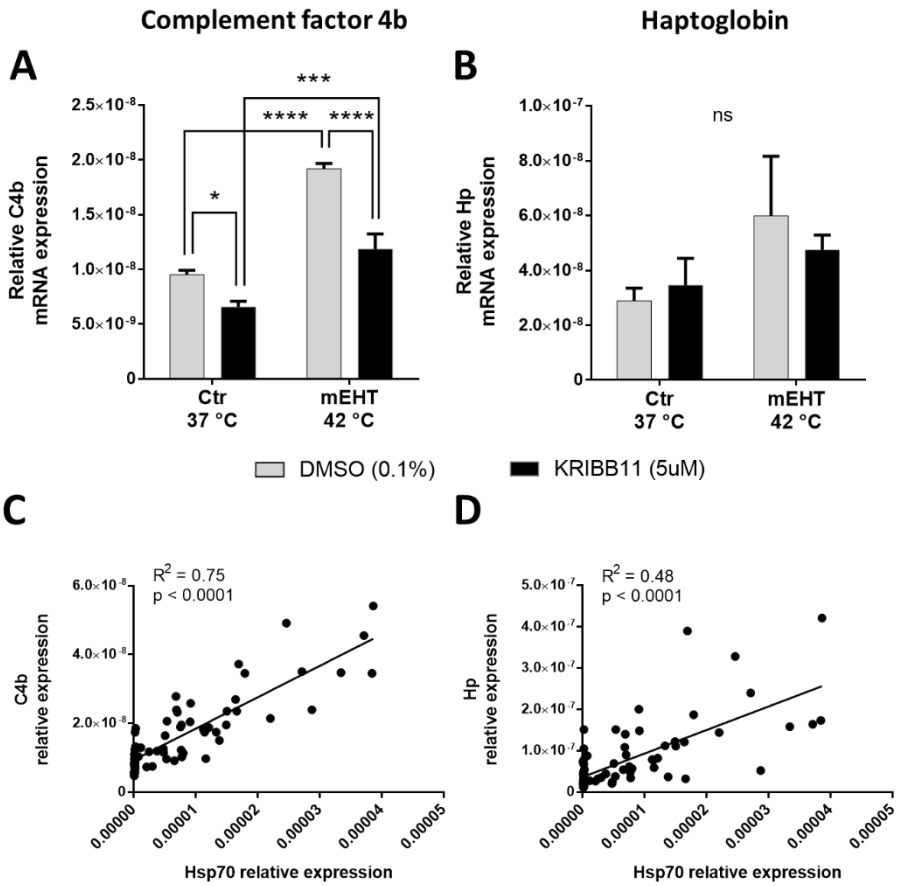

Figure 20. mEHT-induced and KRIBB11-affected production of APPs in 4T1 in vitro. C4b mRNA relative expression, 2 h post-mEHT, normalized to 18S, with KRIBB11 treatment, vs. DMSO (A). Hp mRNA relative expression, 2 h post-mEHT, normalized to 18S, with KRIBB11 treatment, vs. DMSO (B). Correlation between C4b and Hsp70 expression (C). Correlation between Hp and Hsp70 expression (D). , n = 5–15/group. Mean ± SEM, Two-way ANOVA. *: $p < 0.05$, ***: $p < 0.001$, ****$p < 0.0001$. Cell line: 4T1. (187) and our workgroup's unpublished data.

5. Discussion

Modulated electro-hyperthermia (mEHT) is a complementary therapeutical method used as a locoregional hyperthermia treatment in solid tumors (189, 190). Previously, our workgroup presented significant tumor inhibitory effect of mEHT monotherapy, demonstrated by impaired cell viability after two mEHT treatments in vivo and enhanced efficacy via simultaneous inhibition of the heat shock response by KRIBB11 in vitro (188). Several mEHT-induced antitumoral mechanisms have been identified before (13), however, a comprehensive, integrative analysis of mEHT-induced molecular pathways with multiplex methods in an in vivo tumor model was not performed before.

We investigated the impact of mEHT on tumor growth in monotherapy. Our data suggests that 1 × mEHT treatment was insufficient to impair tumor size, although in our previous study, viable tumor-cell count was already reduced by 2 × mEHT treatment (188). Increasing the number of treatments to 3 × with 48 intervals was enough to significantly slow down tumor growth and 5 × treatment was enough to reach decline in the growth tendency, achieving tumor shrinkage in both tumor volume and weight. Five treatments resulted repetitively (in 2 separate experiments) in RNA degradation (not presented in current study), so we were unable to isolate adequate RNA from the tumor samples. Therefore 3 × repeated samples seemed to be optimal for all further investigations.

mEHT treatment is a complementary therapy in the clinics, but it's effectiveness in monotherapy has been demonstrated already in both preclinical and clinical settings (190-192). Single treatment with mEHT in monotherapy was enough to compass tumor growth arrest in melanoma (A2058) model. However, that study used a xenograft model, which affects the immune-related anti- and protumoral aspects of the TME, therefore it is not completely comparable to our isograft model. In a different, BALB/c isograft model (colon carcinoma, CT26 cell line), similarly to our findings, single mEHT treatment reached no significant (193) or moderate tumor growth inhibitory effect (194) in monotherapy. However, three treatments resulted significant decrease in tumor growth in syngeneic squamous cell carcinoma model (195). Five mEHT treatments induced traceable growth decline and tumor shrinkage in hepatic cancer xenografts (HepG2) (196) and rat glioma xenografts (U87-MG) (197).

Toxicity is a critical problem of every anti-cancer modality. In small animal experiments, body weight (BW) reduction is a widely-used marker of treatment-associated toxicity.

There was no significant BW decrease in our study after one-, three- or five-times repeated mEHT treatments. In vivo pancreatic adenocarcinoma xenograft study reported, that even a total dose of ten mEHT treatments didn't affect the mouse BW significantly (8). mEHT treatment was also reported to be well tolerable without severe side effects in a Phase II study of hepatocellular carcinoma patients (198). Moreover, a recent clinical study with 210 cervical cancer patients demonstrated, that mEHT has no additive toxicity to chemoradiotherapy (199).

In our present study, cancer tissue destruction, as interpreted by elevated TDR was demonstrated in all three-times treated samples, but just in some tumors after a single mEHT treatment. TDR evaluation is a frequently used method to assess treatment-related tumor tissue destruction and it is a reliable marker for measuring the effectiveness of mEHT treatment (13, 200, 201). Five × mEHT treatments induced an even greater tumor tissue destructive effect, however, TDR was present in large sham tumors as well and the difference was not significant between mEHT-treated and sham-treated tumors. TDR in even untreated large tumors is often a consequence of fast tumor growth with inadequate concomitant neoangiogenesis. Thus, the blood supply becomes insufficient leading to necrosis in the central core of these tumors. This phenomenon is described articularly in 410.4-derived tumors (202). In contrast, mEHT-treated tumors with high TDR were much smaller, implementing, that the increase of tumor tissue destruction was only size-related in the sham group, but treatment-related in the mEHT group.

Histological analysis showed, that cleaved caspase-3 (cC3) expression was upregulated already after three mEHT treatments, but not after one treatment. Further analysis revealed a highly overlapping pattern of the destructed area on H&E stained sections and the cC3+ areas on the IHC sections, implementing that the tumor tissue-destruction was primarily caspase-mediated apoptosis in our model.

Our previous studies demonstrated that tissue destruction and cC3-mediated apoptosis peaks 24 hours after mEHT treatment in 4T1 isografts (188). Our workgroup described, that this cC3 upregulation-related apoptosis peak is connected to the exhaustion of defensive mechanisms in the 4T1 model (188). mEHT induced caspase-

dependent apoptosis was described in other preclinical, in vivo tumor models: after single and repeated mEHT treatments in colorectal cancer C26/CT26 (200, 203, 204) and melanoma (205) models.

Contrarily, caspase-independent apoptosis didn't play significant role in the mEHT-induced cell damaging process, AIF didn't show significant change at any time point after treatment in our model.

Caspase-independent apoptosis, induced by single mEHT treatment was demonstrated in colorectal cancer (HT29) model (201), however, in this case, not the expression, but the nuclear translocation of AIF was demonstrated. Upregulated expression of AIF induced by mEHT was described, but only at protein level, in a different, melanoma (A2058) model (205). Moreover, hsp70 is able to inhibit the action of AIF by forming a complex with it (206). Overall, we can say, that caspase-mediated apoptosis seemed to be more relevant, mEHT-induced cell death form in our TNBC model.

In our study, Hsp70 expression at protein level was elevated 24 hours after the last mEHT treatment in surviving cells around the destructed tumor area, implementing their upregulation as a defense mechanism against heat stress. This data was corroborated by the MS results, which demonstrated the significant upregulation of two paralogs of Hsp70 (Hspa1a, Hspa1b) and two other hsps (Hspb1, Hsph1) 24 hours after last treatment. NGS data showed a non-significant upregulation of these Hsps. One possible explanation is, that the heat shock response on mRNA level decreased earlier than the sampling time in our experiment (24 hours).

Heat shock proteins (Hsps) are among the most highly conserved and abundant intracellular proteins in nature. Hsps were originally described as chaperones, whose expression is induced by heat as a part of the intracellular defense mechanism, Heat Shock Response (11, 81). However, further studies revealed, that their expression can be initiated by several different cell stressor types, such as oxygen radicals, ethanol, heavy metals, ischemia-reperfusion or haemorrhagic shock (81), so their upregulation can be considered as an ancient, general stress response. Our previous report documented that the RNA-level, mEHT-induced Hsp70 expression peaks 4 hours, stays high until 12 hours, and decreases back to sham level 24 hours after treatment (188). Moreover, we described that the exhaustion of the Hsp-related defense mechanism contributes

significantly to tumor tissue destruction (188). Furthermore, the inhibition of the Heat Shock Response by KRIBB11 could synergistically improve the effectiveness of mEHT treatment in vitro (188). Therefore, heat shock proteins are a promising target for inhibition to improve the efficacy of mEHT. However, Hsps can act as a double-edged sword: beside the intracellular, chaperone function, Hsps can act extracellularly (207), e.g. as Damage-associated Molecular Patterns (DAMPs). Deployment of these DAMPs on the cancer cell's surface facilitate the T cell mediated immunogenic cell death (200). Inhibition of this and other antitumor functions of Hsps can act contrary to the medical intentions. Therefore the aiming of heat shock response in cancer therapy should be highly specific to intracellular Hsps and targetting other, protective factors may also be essential.

Although the most relevant heat shock protein, Hsp70 was upregulated at the mRNA level within 12 hours and at the protein level up to 24 hours, several other heat shock proteins (Hspb1, Hspa1a, Hspa1b, Hsph1) were not differentially expressed according to our multiplex screens, detecting mRNA (NGS). On the other hand, another group of stress-related molecules, classically interpreted as acute-phase proteins (APPs: complement factors: C1s1, C4b, Hc, Cfd, Ptx3; protease inhibitors: Serpina3n, Serpina3m, Serpina3c, Itih2, Itih4; coagulation factors: Fgb, Fgg; and haptoglobin) were massively upregulated after mEHT treatment on the mRNA level as demonstrated by RNA Seq NGS. These RNA results, measured by NGS were corroborated by Nanostring and qPCR measurements. Moreover, the mEHT-induced upregulation of these APPs were also confirmed at the protein level by MS. It is important to emphasize, that the data, demonstrating APP upregulation comes from RNA and protein isolated directly from the tumor tissue, implementing the local production of these factors by cancer cells.

The generally held concept is, that APPs are produced mainly by the liver upon cytokine stimulation of hepatocytes as part of a general inflammatory response to cell-stress in any part of the body (84). Contrary to this concept, our data strongly support a local APP production by non-hepatic cells. These locally produced APPs may fulfill non-canonical functions and the APP genes we found massively upregulated by mEHT, related to cellular stress response appear to have a tumor-protective or tumor-promoting role in different types of cancer (92, 94, 171, 175, 177).

Several complement factors were upregulated by mEHT according to the NGS and MS data. The 4T1 isograft model is considered as an immune-desert phenotype, confirmed by our data (see in 1.2.2.). Therefore we assumed, that the major source of APPs were more likely the cancer cells themselves and not the infiltrating immune cells, which are another relevant source of complement factors in the TME (94). The tumor cell origin of complement factors was corroborated in vitro when detectable complement expression and mEHT-induced upregulation was demonstrated in 4T1 cell monoculture.

In our studies one of the complement factors, identified with all multiplex methods (NGS, Nanostring, MS) and demonstrated one of the highest absolute RNA counts (Nanostring) was C4b (Chido blood group). C4b is the basic isotype of C4 in mice and humans as well, whereas the acidic form is C4a (Rodgers blood group). C4b production by 4T1 cells and upregulated expression after mEHT was confirmed in vitro in monoculture, a phenomenon never described before, according to our current knowledge. Furthermore, we demonstrated in vitro, that mEHT-induced expression of C4b can be inhibited by KRIBB11 treatment.

Growing evidence suggests, that besides the cellular arm of immunity, humoral immune response has a vital role in the antitumor immune response. Thus, modulation of complement factors/local complement expression may prove beneficial in the fight against cancer (208). The inhibition of local complement production in tumors has great potential and may be another tool to utilize in immune-modulation based techniques in cancer therapy (208). C4 has been reported to be fundamental in cervical tumor (TC-1) growth (158). Moreover, the co-inhibition of C4 and VEGFA repressed tumor progression significantly in colorectal cancer (161).

In our study, protease-inhibitors demonstrated remarkable upregulation, detected by NGS (RNA-Seq). Itih2 showed the highest (31.1x) upregulation.

Protease-inhibitors play essential roles by neutralizing proteases, which are derived from injurious cells and threatening host cells. Serpina3n was another highly upregulated gene, according to the RNA-Seq data. Serpina3n inhibition by RNA silencing decreased matrix metalloprotease (MMP-2, MMP-9) expression and inhibited the migration and invasion of colon cancer cells (172). In addition, silencing Serpina3n reduced the abilities of colon cancer to form liver metastasis (172). Serpina3 was also an

important gene in endometrial cancer. Serpina3 knockdown reduced cell viability, inhibited proliferation and induced apoptosis in vitro (HEC-1A; KLE) (173).

Haptoglobin (Hp) was upregulated with the highest absolute mRNA count by our Nanostring analysis. qPCR measurements from in vitro 4T1 monoculture corroborated that Hp was produced by the cancer cells.

Hp's major known canonical role is to scavenge extracellular, free hemoglobin (Hb) and thus, Hp has an important protective role against oxidative stress (140). Hp production by a TNBC cell line (171) as well as serum Hp's role as a progression marker of 4T1-tumor in mice has been demonstrated before (209). In our studies, Hp induction was time-dependent with a peak at 24 hours after treatment. The serum level of Hp was elevated in TNBC patients' serum (170). Furthermore, Hp may be oncogenic in breast cancer: Hp knockdown leads to increased apoptosis and cell cycle arrest in TNBC cells (MDA-MB-231, MDA-MB-468) in vitro. Furthermore, Hp knockdown reduced tumor growth and proliferation in MDA-MB-231xenografts (171). Therefore, the Hp inhibition may be beneficial via dampening the unfavorable metabolic reprogramming of cancer cells.

We reported the upregulation of two fibrinogen-coding genes, Fbb and Fbg, 24 hours after mEHT treatment.

The local production and deposition of fibrin(ogen) into the extracellular matrix (ECM) of 4T1 tumors can be tumor-promoting by serving as a scaffold to bind growth factors and also by promoting cellular processes of adhesion, proliferation, and migration during angiogenesis and tumor cell growth (177). Ligustrazine, a phytogenic agent was able to decrease Fgg expression. Fgg inhibition was accompanied by chemotherapy-sensitization and cancer stem-cells elimination in breast cancer cells (MCF-7) in vitro. Furthermore, in vivo Fgg inhibition by Ligustrazine was accompanied by apoptosis promotion and reduced proliferative activity of MCF-7 xenografts (182).

The observed local production of fibrinogen and protease-inhibitors may contribute to the reprogramming of TME towards a tumor-promoting state, and the inhibition of these factors may enhance the efficacy of mEHT. From the studied factors C4b inhibition may be the most promising as we observed a long-lasting elevation after treatment, implementing it's importance in the cancer cells' stress response and indicating a good targetability of this molecule for inhibitors.

Our data suggest, that modulated electro hyperthermia (mEHT) has effective antitumor effects and capable to inhibit tumor growth even in monotherapy in the highly aggressive TNBC. Significant portion of cancer cells commit to apoptosis, the surviving cells initiate cellular stress response (Heat Shock Response). Besides the intracellular protective response, the most substantial response to the mEHT treatment is the development of an extracellular defensive mechanism in the form of local production of APPs (complement factors, protease inhibitors, fibrinogens, haptoglobin). The two processes may complement each other's function and cooperate to protect the cancer cells from therapy-induced damage. As the local APP production is the most abundant response to the mEHT treatment, those factors, that show the most robust upregulation can serve as therapeutic targets. Inhibition of these intra- and extracellular protective factors and mechanisms may enhance the therapeutic effect of mEHT and probably other heat shock or local APP production inducing treatment modalities (such as chemo- or radiotherapy). The main findings of this thesis is summarized in Figure 21.

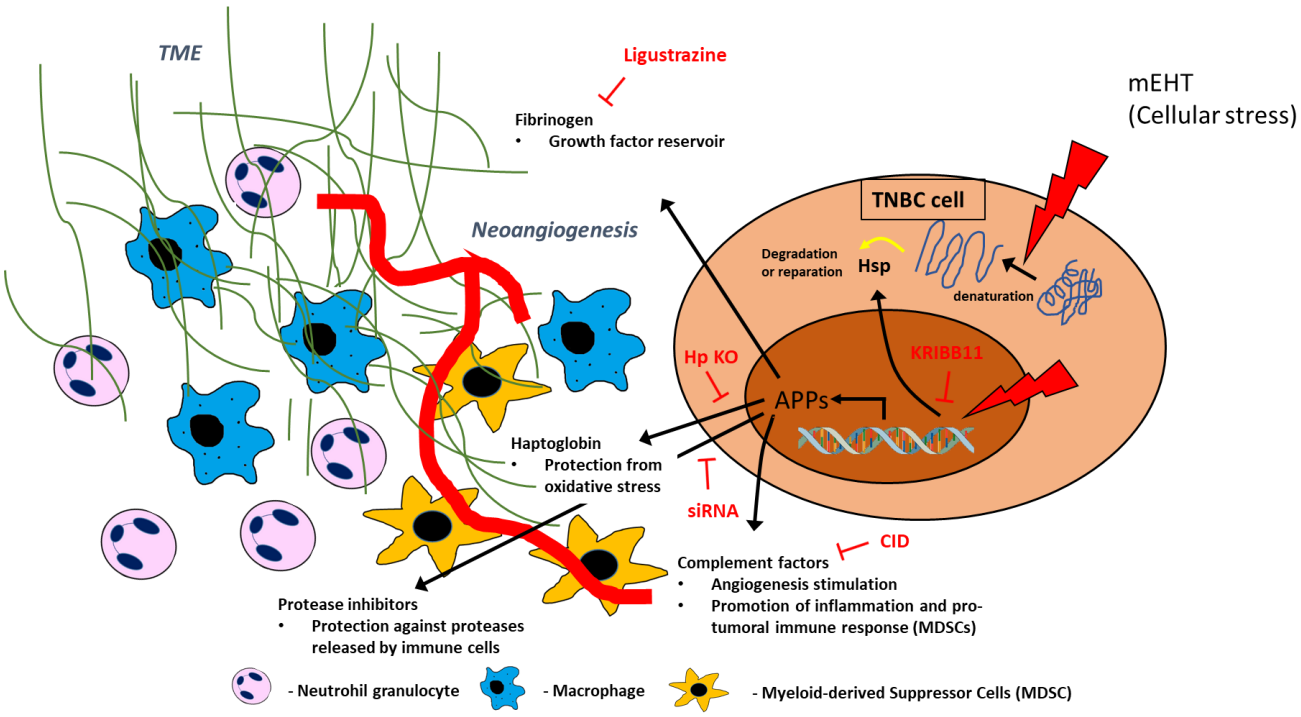

Figure 21. Local APP production, induced by mEHT. In response to mEHT treatment, those TNBC cancer cells that did not receive lethal dose of mEHT and did not commit to cell death react with a local stress-response. Intracellular part of this reaction is the heat shock response and extracellularly, a local upregulation of Acute Phase Proteins (APPs) is induced. These APPs act mostly in the extracellular space via the modulation of the tumor-microenvironment serving as a protective mechanism for the cancer cells

against the harming stimuli. These APPs fulfill a non-canonical function: fibrinogens without fibrin-formation contribute to the formation of extracellular matrix of the TME and serve as a scaffold for growth factors, promoting tumor progression. Complement factors without activation of the complement cascade process promote angiogenesis, improving the blood supply, thus the nutrient and O2 supply of the tumors. Moreover, they can participate in the pro-tumoral immune-editing of tumor microenvironment. Haptoglobin protects cancer cells from oxidative stress, and helps the metabolic shift of the cancer cells. Serine-protease inhibitors and inter-alpha trypsin inhibitors protect the host cells from the protease enzymes, released by effector immune cells. The arranged expression of multiple, different Acute Phase Proteins in response to a cellular stressor stimulus by cancer cells was never described before. Inhibition of these factors by phytogenic agents, like Ligustrazine, by fusion proteins, like CR1-Fc fusion protein (CID) or by silencing RNA or by gene knockout have antitumoral effects, according to literature. Combination of mEHT or other, cellular stress-inducing anticancer treatments with these aforementioned APP inhibition may beneficially improve the theraputic efficiency.

6. Conclusions

This study synthesizes the tumor-growth inhibitory effects and multiplex analysis data about the pathways activated by modulated electro-hyperthermia in mouse TNBC model.

Novel observations of the thesis:

- Repeated modulated electro hyperthermia (mEHT) inhibited tumor growth in the 4T1/4T07 TNBC mouse isografts. Tumor size reduction become manifest after > 3 treatments in our model.
- mEHT treatment induced a local acute phase protein (APP) production in the still-living cancer cells.
- Protease inhibitors, haptogobin, complement and coagulation factors demonstrated the most significant response which are all considered acute phase proteins. This local APP production may serve as a mechanism to protect cancer cells, that received a non-lethal dose of mEHT and did not commit to cell death.
- 4T1 cancer cells express C4b and Hp as a response to mEHT treatment at the mRNA level in 4T1 monoculture in vitro.
- Local Hp and C4b, induced by mEHT was most significant 24 hours after last treatment. Hp production returned to baseline, while C4b production stayed high even 72 hours after the last mEHT treatment.
- The inhibition of the heat shock response by KRIBB11 was accompanied by inhibition of mEHT-induced C4b upregulation in vitro.
- Hsp70 expression correlated with C4b and Hp expression 2 hours after treatment, in vitro.

7. Summary

Oncological hyperthermia is a complementary therapeutic option in cancer patients. In the clinical setting, several hyperthermia forms (whole body, regional or local) and application methods (microwave, ultrasound, radio waves) are applied. In local hyperthermia, treatment effectiveness is related to the dose-absorbing capability of the targeted tissue, which is affected by the tissue itself and the heat-communicating method. Modulated electro-hyperthermia using an EMF with a well-chosen frequency (13.56 MHz) enables a selective heat-and energy transmission into the malignant tissue. The reprogrammed metabolism of cancer cells and the consequently altered bioelectrical properties (elevated electric conductivity) of the tumor are the basis of the selective energy absorbtion.

We implanted syngeneic TNBC (4T1/4T07) cells in BALB/c mice to form orthotopic isografts. Repeated mEHT treatment slowed down tumor growth without toxic side effects. Tumor growth inhibition was related to elevated caspase (cC3)-mediated apoptosis. mEHT induced a Heat Shock Response (HSR) of the surviving cancer cells. RNA sequencing analysis revealed a significant upregulation of 2/3 part of the differentially expressed genes. The pathway analysis of these genes revealed a prominent, local upregulation of acute-phase proteins (APPs: protease inhibitors: Itih2, 4; Serpina3n,m,c; complement components: C1s1, Ptx3, C4b, Hc, Cfd; coagulation factors: Fgb, Fgg; haptoglobin). Absolute RNA count analysis (by Nanostring) corroborated the local production of APPs and the majority of these factors were upregulated on the protein level as well, detected by Mass Spectrometry (MS). This local upregulation of APPs can be interpreted as a protective mechanism of the tumor, complementing the intracellular HSR with an extracellular mechanism of the injured but surviving cells. The production of two of the most significant factors (C4b, Hp) showed a time-dependently elevated expression after mEHT. The heat shock response inhibition by KRIBB11 concomitantly inhibited the mEHT induced C4b upregulation. Interfering with this newly described, coordinated, local acute-phase protein production of tumor cells may be applied in the future to synergistically enhance the antitumor effects of modulated electro-hyperthermia or other antitumor therapies in the hard-to-treat Triple Negative Breast Cancer setting.

8. Összefoglaló

Az onkológiai hipertermia kiegészítő terápiás lehetőség rákos betegek számára. A klinikumban különböző hipertermia típusokat (teljes test, regionális, lokális) és módszereket (mikrohullám, ultrahang, rádióhullám) használnak. Lokális hipertermia esetén a kezelés hatékonysága a célzott szövetrész dózis-elnyelő kapacításától függ, amelyet maga a szövet és a hőközlés módja is befolyásol. Modulált elektro-hipertermia (mEHT) során 13.56 MHz-es elektromágneses tér (EMT) használata teszi lehetővé a szelektív energia- és hőátadást a daganatnak. A rákos sejtek módosult anyagcseréje és a tumor következményesen megnövekedett elektromos vezetőképessége biztosítják a szelektív energiaelnyelést.

Szingeneikus háromszorosan negatív emlőrák (Triple Negative Breast Cancer: TNBC) sejteket (4T1/4T07) ültettünk ortotopikusan BALB/c egerekbe, izograft tumorokat létrehozva. Ismételt mEHT kezelés lelassította a tumorok növekedését toxikus mellékhatások nélkül. A tumornövekedés gátlása a sejtek megnövekedett kaszpáz (cleaved caspase-3: cC3)-függő apoptózisának volt köszönhető. A mEHT kezelés hősokkválaszt (Heat Shock Response: HSR) indított be a túlélő rákos sejtekben. RNS szekvenálási vizsgálattal az eltérően expresszált gének 2/3-ában szignifikáns felülregulálódás volt megfigyelhető. Útvonal elemzéssel a rákos sejtek jelentős akutfázis fehérje (APP: Acute Phase Protein: proteáz inhibitorok: Itih2, 4; Serpina3n,m,c; komplement komponensek: C1s1, Ptx3, C4b, Hc, Cfd; véralvadási faktorok: Fgb, Fgg; haptoglobin) termelése volt kimutatható. Abszolút RNS szám meghatározás (Nanostring) megerősítette az APP-k lokális termelődését, ezen faktorok fehérje szintű felülregulálódását a tömegspektrometriai vizsgálat (Mass Spectrometry: MS) is alátámasztotta. Az APP-k lokális termelődése a tumorsejtek védekezési mechanizmusként értelmezhető, mely extracelluláris komponensként kiegészíti a hősokkfehérjék intracelluláris funkcióját a károsodott, de még életképes tumorsejtekben. A két, legjelentősebben felülregulálódott faktor (C4b, Hp) idő-függő expressziót mutatott a mEHT kezelést követően. A hősokkválasz KRIBB11-el történő gátlása megakadályozta a mEHT indukálta C4b expressziót is. Több APP ezen újonnan leírt, ráksejtek által történő, összerendezett termelődése egy új terápiás beavatkozási pontot jelenthet és ennek a védekezési mechanizmusnak a gátlása szinergikusan növelheti a mEHT és egyéb tumorellenes terápiák hatékonyságát a nehezen kezelhető TNBC-s betegek esetében.

9. Bibliography

1. Gas P. Essential Facts on the History of Hyperthermia and their Connections with Electromedicine. In: Przeglad Elektrotechniczny Vol. 87(12b), 2011: 37-40.
2. Behrouzkia Z, Joveini Z, Keshavarzi B, Eyvazzadeh N, Aghdam RZ. (2016) Hyperthermia: How Can It Be Used? *Oman Med J,* 31(2): 89-97.
3. Berry SL, Walker K, Hoskins C, Telling ND, Price HP. (2019) Nanoparticle-mediated magnetic hyperthermia is an effective method for killing the human-infective protozoan parasite Leishmania mexicana in vitro. *Scientific reports,* 9(1): 1059-1059.
4. Jeziorski K. (2018) Hyperthermia in rheumatic diseases. A promising approach? *Reumatologia,* 56(5): 316-320.
5. Boreham DR, Gasmann HC, Mitchel RE. (1995) Water bath hyperthermia is a simple therapy for psoriasis and also stimulates skin tanning in response to sunlight. *Int J Hyperthermia,* 11(6): 745-754.
6. Perugia G, Liberti M, Vicini P, Colistro F, Gentile V. (2005) Role of hyperthermia in the treatment of Peyronie's disease: a preliminary study. *Int J Hyperthermia,* 21(4): 367-374.
7. Adam Chicheł JS, Magda Kubaszewska, Marek Kanikowski. (2007) Hyperthermia – description of a method and a review of clinical applications. *Rep Pract Oncol Radiother,* 12(5): 267-275.
8. A. Szasz NS, O. Szasz. Oncothermia: Principles and Practices. Springer2011.
9. Szász András SO, Szász Nóra. (2002) Onkotermia Fizika a rák ellen. *Fizikai szemle,* 52(2): 45-52.
10. Hildebrandt B, Wust P, Ahlers O, Dieing A, Sreenivasa G, Kerner T, Felix R, Riess H. (2002) The cellular and molecular basis of hyperthermia. *Crit Rev Oncol Hematol,* 43(1): 33-56.
11. Sharp FR, Massa SM, Swanson RA. (1999) Heat-shock protein protection. *Trends Neurosci,* 22(3): 97-99.
12. Jentsch M, Snyder P, Sheng C, Cristiano E, Loewer A. (2020) p53 dynamics in single cells are temperature-sensitive. *Sci Rep,* 10(1): 1481.

13. Krenacs T, Meggyeshazi N, Forika G, Kiss E, Hamar P, Szekely T, Vancsik T. (2020) Modulated Electro-Hyperthermia-Induced Tumor Damage Mechanisms Revealed in Cancer Models. *Int J Mol Sci,* 21(17).
14. Ohno S, Siddik ZH, Kido Y, Zwelling LA, Bull JM. (1994) Thermal enhancement of drug uptake and DNA adducts as a possible mechanism for the effect of sequencing hyperthermia on cisplatin-induced cytotoxicity in L1210 cells. *Cancer Chemother Pharmacol,* 34(4): 302-306.
15. Kaur P, Hurwitz MD, Krishnan S, Asea A. (2011) Combined hyperthermia and radiotherapy for the treatment of cancer. *Cancers (Basel),* 3(4): 3799-3823.
16. Ranieri G, Ferrari C, Di Palo A, Marech I, Porcelli M, Falagario G, Ritrovato F, Ramunni L, Fanelli M, Rubini G, Gadaleta CD. (2017) Bevacizumab-Based Chemotherapy Combined with Regional Deep Capacitive Hyperthermia in Metastatic Cancer Patients: A Pilot Study. *Int J Mol Sci,* 18(7).
17. Hurwitz MD. (2019) Hyperthermia and immunotherapy: clinical opportunities. *Int J Hyperthermia,* 36(sup1): 4-9.
18. Lee S-Y, Fiorentini G, Szasz AM, Szigeti G, Szasz A, Minnaar CA. (2020) Quo Vadis Oncological Hyperthermia (2020)? *Frontiers in oncology,* 10: 1690-1690.
19. Sun X, Xing L, Ling CC, Li GC. (2010) The effect of mild temperature hyperthermia on tumour hypoxia and blood perfusion: relevance for radiotherapy, vascular targeting and imaging. *Int J Hyperthermia,* 26(3): 224-231.
20. Szasz A, Vincze G, Szasz O, Szasz N. (2003) An Energy Analysis of Extracellular Hyperthermia. *Electromagnetic Biology and Medicine,* 22(2-3): 103-115.
21. Horsman MR, Overgaard J. (2007) Hyperthermia: a potent enhancer of radiotherapy. *Clin Oncol (R Coll Radiol),* 19(6): 418-426.
22. Repasky E, Issels R. (2002) Physiological consequences of hyperthermia: heat, heat shock proteins and the immune response. *Int J Hyperthermia,* 18(6): 486-489.
23. Gian Franco Baronzio RDS, Mario D'Amico, Attilio Baronzio, Isabel Freitas, Giorgio Forzenigo, Alberto Gramaglia, E. Dieter Hage. Effects of Local and Whole Body Hyperthermia on Immunity. Landes Bioscience, Austin (TX), 2000-2013.

24. Chatterjee DK, Diagaradjane P, Krishnan S. (2011) Nanoparticle-mediated hyperthermia in cancer therapy. *Ther Deliv,* 2(8): 1001-1014.
25. Valdagni R, Amichetti M, Dell'Orsola G. (1982) Local microwave hyperthermia in cancer therapy. Preliminary report. *Tumori,* 68(3): 247-251.
26. Hitchcock RT. Radio-frequency and Microwave Radiation. American Industrial Hygiene Assn2004: 1.
27. Yang WH, Xie J, Lai ZY, Yang MD, Zhang GH, Li Y, Mu JB, Xu J. (2019) Radiofrequency deep hyperthermia combined with chemotherapy in the treatment of advanced non-small cell lung cancer. *Chin Med J (Engl),* 132(8): 922-927.
28. Napoli A, Alfieri G, Scipione R, Leonardi A, Fierro D, Panebianco V, De Nunzio C, Leonardo C, Catalano C. (2020) High-intensity focused ultrasound for prostate cancer. *Expert Rev Med Devices,* 17(5): 427-433.
29. Faubert B, Solmonson A, DeBerardinis RJ. (2020) Metabolic reprogramming and cancer progression. *Science,* 368(6487).
30. Liberti MV, Locasale JW. (2016) The Warburg Effect: How Does it Benefit Cancer Cells? *Trends in biochemical sciences,* 41(3): 211-218.
31. Devic S. (2016) Warburg Effect - a Consequence or the Cause of Carcinogenesis? *J Cancer,* 7(7): 817-822.
32. Vander Heiden MG, Cantley LC, Thompson CB. (2009) Understanding the Warburg effect: the metabolic requirements of cell proliferation. *Science,* 324(5930): 1029-1033.
33. de la Cruz-López KG, Castro-Muñoz LJ, Reyes-Hernández DO, García-Carrancá A, Manzo-Merino J. (2019) Lactate in the Regulation of Tumor Microenvironment and Therapeutic Approaches. *Frontiers in oncology,* 9: 1143-1143.
34. O'Rourke AP, Lazebnik M, Bertram JM, Converse MC, Hagness SC, Webster JG, Mahvi DM. (2007) Dielectric properties of human normal, malignant and cirrhotic liver tissue: in vivo and ex vivo measurements from 0.5 to 20 GHz using a precision open-ended coaxial probe. *Phys Med Biol,* 52(15): 4707-4719.
35. G. Mátay LZ. A rádiófrekvenciás sugárzás élettani hatásai és orvosbiológiai alkalmazásai. Műegyetemi Kiadó.2000.

36. B. Scholz RA. (2000) On electrical impedance scanning-principles and simulations. *Electromedica,* 68: 35-44.
37. Assenheimer M, Laver-Moskovitz O, Malonek D, Manor D, Nahaliel U, Nitzan R, Saad A. (2001) The T-SCAN technology: electrical impedance as a diagnostic tool for breast cancer detection. *Physiol Meas,* 22(1): 1-8.
38. Sarac E, Meiwes A, Eigentler T, Forchhammer S, Kofler L, Häfner HM, Garbe C. (2020) Diagnostic Accuracy of Electrical Impedance Spectroscopy in Non-melanoma Skin Cancer. *Acta Derm Venereol,* 100(18): adv00328.
39. Das L, Das S, Chatterjee J. (2015) Electrical Bioimpedance Analysis: A New Method in Cervical Cancer Screening. *J Med Eng,* 2015: 636075.
40. Smith SR, Foster KR, Wolf GL. (1986) Dielectric Properties of VX-2 Carcinoma Versus Normal Liver Tissue. *IEEE Transactions on Biomedical Engineering,* BME-33(5): 522-524.
41. Zou Y, Guo Z. (2003) A review of electrical impedance techniques for breast cancer detection. *Med Eng Phys,* 25(2): 79-90.
42. Hahn GM. Blood-flow. In: Field SB, Franconi, C. (szerk.), Physics and Technology of hyperthermia Vol. 127. Martinus Nijhoff Publishers, 1987: 441-446.
43. Cho MR, Thatte HS, Silvia MT, Golan DE. (1999) Transmembrane calcium influx induced by ac electric fields. *FASEB J,* 13(6): 677-683.
44. Papp E, Vancsik, T. , Kiss, E. and Szasz, O. (2017) Energy Absorption by the Membrane Rafts in the Modulated Electro-Hyperthermia (mEHT). *Open Journal of Biophysics,* 7: 216-229.
45. Robertson B, Astumian RD. (1990) Michaelis-Menten equation for an enzyme in an oscillating electric field. *Biophysical journal,* 58(4): 969-974.
46. Blank M, Goodman R. (2011) DNA is a fractal antenna in electromagnetic fields. *Int J Radiat Biol,* 87(4): 409-415.
47. Blank M, Goodman R. (2009) Electromagnetic fields stress living cells. *Pathophysiology,* 16(2-3): 71-78.
48. Pohl HA. (1951) The Motion and Precipitation of Suspensoids in Divergent Electric Fields. *Journal of Applied Physics,* 22(7): 869-871.

49. Teixeira-Pinto AA, Nejelski LL, Cutler JL, Heller JH. (1960) The behavior of unicellular organisms in an electromagnetic field. *Experimental Cell Research,* 20 (3): 548–564.
50. Neumann E, Rosenheck K. (1972) Permeability changes induced by electric impulses in vesicular membranes. *J Membr Biol,* 10(3): 279-290.
51. Zimmermann U, Pilwat G, Riemann F. (1974) Dielectric breakdown of cell membranes. *Biophysical journal,* 14(11): 881-899.
52. Andocs G, Renner H, Balogh L, Fonyad L, Jakab C, Szasz A. (2009) Strong synergy of heat and modulated electromagnetic field in tumor cell killing. *Strahlentherapie und Onkologie,* 185(2): 120-126.
53. Datta NR, Rogers S, Ordóñez SG, Puric E, Bodis S. (2016) Hyperthermia and radiotherapy in the management of head and neck cancers: A systematic review and meta-analysis. *Int J Hyperthermia,* 32(1): 31-40.
54. Datta NR, Rogers S, Klingbiel D, Gómez S, Puric E, Bodis S. (2016) Hyperthermia and radiotherapy with or without chemotherapy in locally advanced cervical cancer: a systematic review with conventional and network meta-analyses. *Int J Hyperthermia,* 32(7): 809-821.
55. Masunaga S, Hiraoka M, Takahashi M, Jo S, Akuta K, Nishimura Y, Nagata Y, Abe M. (1990) Clinical results of thermoradiotherapy for locally advanced and/or recurrent breast cancer—comparison of results with radiotherapy alone. *International Journal of Hyperthermia,* 6(3): 487-497.
56. Moran CJ, Marchosky JA, Wippold FJ, 2nd, DeFord JA, Fearnot NE. (1995) Conductive interstitial hyperthermia in the treatment of intracranial metastatic disease. *J Neurooncol,* 26(1): 53-63.
57. Lee SY, Lee NR, Cho D-H, Kim JS. (2017) Treatment outcome analysis of chemotherapy combined with modulated electro-hyperthermia compared with chemotherapy alone for recurrent cervical cancer, following irradiation. *Oncology letters,* 14(1): 73-78.
58. Minnaar CA, Maposa I, Kotzen JA, Baeyens A. (2022) Effects of Modulated Electro-Hyperthermia (mEHT) on Two and Three Year Survival of Locally Advanced Cervical Cancer Patients. *Cancers (Basel),* 14(3).

59. Kondo M OH, Yoshikawa T. (2000) Therapeutic effects of chemoembolization using degradable starch microspheres and regional hyperthermia on unresectable hepatocellular carcinoma. *Select Pap Hypertherm,* 20: 85–98.
60. Kouloulias VE, Dardoufas CE, Kouvaris JR, Gennatas CS, Polyzos AK, Gogas HJ, Sandilos PH, Uzunoglu NK, Malas EG, Vlahos LJ. (2002) Liposomal doxorubicin in conjunction with reirradiation and local hyperthermia treatment in recurrent breast cancer: a phase I/II trial. *Clin Cancer Res,* 8(2): 374-382.
61. Ranieri G, Laface C, Laforgia M, De Summa S, Porcelli M, Macina F, Ammendola M, Molinari P, Lauletta G, Di Palo A, Rubini G, Ferrari C, Gadaleta CD. (2020) Bevacizumab Plus FOLFOX-4 Combined With Deep Electro-Hyperthermia as First-line Therapy in Metastatic Colon Cancer: A Pilot Study. *Front Oncol,* 10: 590707.
62. Cicero G, De Luca R, Dieli F. (2018) Progression-free survival as a surrogate endpoint of overall survival in patients with metastatic colorectal cancer. *OncoTargets and therapy,* 11: 3059-3063.
63. Sung H, Ferlay J, Siegel RL, Laversanne M, Soerjomataram I, Jemal A, Bray F. (2021) Global Cancer Statistics 2020: GLOBOCAN Estimates of Incidence and Mortality Worldwide for 36 Cancers in 185 Countries. *CA Cancer J Clin,* 71(3): 209-249.
64. Sinn H-P, Kreipe H. (2013) A Brief Overview of the WHO Classification of Breast Tumors, 4th Edition, Focusing on Issues and Updates from the 3rd Edition. *Breast care (Basel, Switzerland),* 8(2): 149-154.
65. Rakha EA, El-Sayed ME, Lee AH, Elston CW, Grainge MJ, Hodi Z, Blamey RW, Ellis IO. (2008) Prognostic significance of Nottingham histologic grade in invasive breast carcinoma. *J Clin Oncol,* 26(19): 3153-3158.
66. .
67. Foulkes WD, Smith IE, Reis-Filho JS. (2010) Triple-negative breast cancer. *N Engl J Med,* 363(20): 1938-1948.
68. Ahn SG, Kim SJ, Kim C, Jeong J. (2016) Molecular Classification of Triple-Negative Breast Cancer. *Journal of breast cancer,* 19(3): 223-230.
69. Gerratana L, Basile D, Buono G, De Placido S, Giuliano M, Minichillo S, Coinu A, Martorana F, De Santo I, Del Mastro L, De Laurentiis M, Puglisi F, Arpino G.

(2018) Androgen receptor in triple negative breast cancer: A potential target for the targetless subtype. *Cancer Treatment Reviews,* 68: 102-110.

70. Power EJ, Chin ML, Haq MM. (2018) Breast Cancer Incidence and Risk Reduction in the Hispanic Population. *Cureus,* 10(2): e2235.
71. Niklaus NJ, Tokarchuk I, Zbinden M, Schläfli AM, Maycotte P, Tschan MP. (2021) The Multifaceted Functions of Autophagy in Breast Cancer Development and Treatment. *Cells,* 10(6).
72. Park MK, Lee CH, Lee H. (2018) Mouse models of breast cancer in preclinical research. *Laboratory animal research,* 34(4): 160-165.
73. Aslakson CJ, Miller FR. (1992) Selective events in the metastatic process defined by analysis of the sequential dissemination of subpopulations of a mouse mammary tumor. *Cancer Res,* 52(6): 1399-1405.
74. Le MT, Hamar P, Guo C, Basar E, Perdigão-Henriques R, Balaj L, Lieberman J. (2014) miR-200-containing extracellular vesicles promote breast cancer cell metastasis. *J Clin Invest,* 124(12): 5109-5128.
75. Chen L, Huang T-G, Meseck M, Mandeli J, Fallon J, Woo SLC. (2007) Rejection of Metastatic 4T1 Breast Cancer by Attenuation of Treg Cells in Combination With Immune Stimulation. *Molecular Therapy,* 15(12): 2194-2202.
76. Schrörs B, Boegel S, Albrecht C, Bukur T, Bukur V, Holtsträter C, Ritzel C, Manninen K, Tadmor AD, Vormehr M, Sahin U, Löwer M. (2020) Multi-Omics Characterization of the 4T1 Murine Mammary Gland Tumor Model. *Frontiers in Oncology,* 10.
77. Dykxhoorn DM, Wu Y, Xie H, Yu F, Lal A, Petrocca F, Martinvalet D, Song E, Lim B, Lieberman J. (2009) miR-200 enhances mouse breast cancer cell colonization to form distant metastases. *PLoS One,* 4(9): e7181.
78. Korpal M, Ell BJ, Buffa FM, Ibrahim T, Blanco MA, Celià-Terrassa T, Mercatali L, Khan Z, Goodarzi H, Hua Y, Wei Y, Hu G, Garcia BA, Ragoussis J, Amadori D, Harris AL, Kang Y. (2011) Direct targeting of Sec23a by miR-200s influences cancer cell secretome and promotes metastatic colonization. *Nat Med,* 17(9): 1101-1108.
79. Tan SY, Yip A. (2018) Hans Selye (1907-1982): Founder of the stress theory. *Singapore Med J,* 59(4): 170-171.

80. Shanmugavelayudam SK, Rubenstein DA, Yin W. (2011) Effects of physiologically relevant dynamic shear stress on platelet complement activation. *Platelets,* 22(8): 602-610.
81. De Maio A. (1999) Heat shock proteins: facts, thoughts, and dreams. *Shock,* 11(1): 1-12.
82. Xu M, Wright WD, Higashikubo R, Roti JL. (1996) Chronic thermotolerance with continued cell proliferation. *Int J Hyperthermia,* 12(5): 645-660; discussion 661-642.
83. Chatterjee S, Burns TF. (2017) Targeting Heat Shock Proteins in Cancer: A Promising Therapeutic Approach. *Int J Mol Sci,* 18(9).
84. Csilla T, Oskar N, Gabriel K. The Use of Acute Phase Proteins as Biomarkers of Diseases in Cattle and Swine. In: Sabina J (szerk.), Acute Phase Proteins, doi:10.5772/55857. IntechOpen, Rijeka, 2013: Ch. 5.
85. Iwaniec J, Robinson GP, Garcia CK, Murray KO, de Carvalho L, Clanton TL, Laitano O. (2021) Acute phase response to exertional heat stroke in mice. *Experimental physiology,* 106(1): 222-232.
86. Roka B, Tod P, Kaucsar T, Vizovisek M, Vidmar R, Turk B, Fonovic M, Szenasi G, Hamar P. (2019) The Acute Phase Response Is a Prominent Renal Proteome Change in Sepsis in Mice. *Int J Mol Sci,* 21(1).
87. Arumugam TV, Shiels IA, Woodruff TM, Granger DN, Taylor SM. (2004) The role of the complement system in ischemia-reperfusion injury. *Shock,* 21(5): 401-409.
88. Gruys E, Toussaint MJ, Niewold TA, Koopmans SJ. (2005) Acute phase reaction and acute phase proteins. *J Zhejiang Univ Sci B,* 6(11): 1045-1056.
89. Lubbers R, van Essen MF, van Kooten C, Trouw LA. (2017) Production of complement components by cells of the immune system. *Clin Exp Immunol,* 188(2): 183-194.
90. Molmenti EP, Ziambaras T, Perlmutter DH. (1993) Evidence for an acute phase response in human intestinal epithelial cells. *J Biol Chem,* 268(19): 14116-14124.
91. Morgan BP, Gasque P. (1997) Extrahepatic complement biosynthesis: where, when and why? *Clin Exp Immunol,* 107(1): 1-7.

92. Janciauskiene S, Wrenger S, Günzel S, Gründing AR, Golpon H, Welte T. (2021) Potential Roles of Acute Phase Proteins in Cancer: Why Do Cancer Cells Produce or Take Up Exogenous Acute Phase Protein Alpha1-Antitrypsin? *Front Oncol,* 11: 622076.
93. Piñeiro M, Andrés M, Iturralde M, Carmona S, Hirvonen J, Pyörälä S, Heegaard PM, Tjørnehøj K, Lampreave F, Piñeiro A, Alava MA. (2004) ITIH4 (inter-alpha-trypsin inhibitor heavy chain 4) is a new acute-phase protein isolated from cattle during experimental infection. *Infect Immun,* 72(7): 3777-3782.
94. Roumenina LT, Daugan MV, Petitprez F, Sautes-Fridman C, Fridman WH. (2019) Context-dependent roles of complement in cancer. *Nat Rev Cancer,* 19(12): 698-715.
95. Merle NS, Church SE, Fremeaux-Bacchi V, Roumenina LT. (2015) Complement System Part I - Molecular Mechanisms of Activation and Regulation. *Front Immunol,* 6: 262.
96. Janeway CA Jr TP, Walport M, et al. The complement system and innate immunity. In: Immunobiology: The Immune System in Health and Disease. New York: Garland Science, 2001.
97. Ma YJ, Garred P. (2018) Pentraxins in Complement Activation and Regulation. *Frontiers in Immunology,* 9.
98. Merle NS, Noe R, Halbwachs-Mecarelli L, Fremeaux-Bacchi V, Roumenina LT. (2015) Complement System Part II: Role in Immunity. *Frontiers in Immunology,* 6.
99. Collard CD, Lekowski R, Jordan JE, Agah A, Stahl GL. (1999) Complement activation following oxidative stress. *Mol Immunol,* 36(13-14): 941-948.
100. Nayak A, Ferluga J, Tsolaki AG, Kishore U. (2010) The non-classical functions of the classical complement pathway recognition subcomponent C1q. *Immunol Lett,* 131(2): 139-150.
101. Kwan WH, van der Touw W, Heeger PS. (2012) Complement regulation of T cell immunity. *Immunol Res,* 54(1-3): 247-253.
102. Liszewski MK, Kolev M, Le Friec G, Leung M, Bertram PG, Fara AF, Subias M, Pickering MC, Drouet C, Meri S, Arstila TP, Pekkarinen PT, Ma M, Cope A, Reinheckel T, Rodriguez de Cordoba S, Afzali B, Atkinson JP, Kemper C. (2013)

Intracellular complement activation sustains T cell homeostasis and mediates effector differentiation. *Immunity,* 39(6): 1143-1157.

103. Arbore G, West EE, Spolski R, Robertson AAB, Klos A, Rheinheimer C, Dutow P, Woodruff TM, Yu ZX, O'Neill LA, Coll RC, Sher A, Leonard WJ, Köhl J, Monk P, Cooper MA, Arno M, Afzali B, Lachmann HJ, Cope AP, Mayer-Barber KD, Kemper C. (2016) T helper 1 immunity requires complement-driven NLRP3 inflammasome activity in $CD4^+$ T cells. *Science,* 352(6292): aad1210.
104. Markiewski MM, Daugherity E, Reese B, Karbowniczek M. (2020) The Role of Complement in Angiogenesis. *Antibodies (Basel),* 9(4).
105. Garlanda C, Bottazzi B, Magrini E, Inforzato A, Mantovani A. (2018) PTX3, a Humoral Pattern Recognition Molecule, in Innate Immunity, Tissue Repair, and Cancer. *Physiol Rev,* 98(2): 623-639.
106. Oren R, Laufer J, Goldberg I, Kopolovic J, Waldherr R, Passwell JH. (1995) C3, C4, factor B and HLA-DR alpha mRNA expression in renal biopsy specimens from patients with IgA nephropathy. *Immunology,* 86(4): 575-583.
107. Bukosza EN, Kornauth C, Hummel K, Schachner H, Huttary N, Krieger S, Nöbauer K, Oszwald A, Razzazi Fazeli E, Kratochwill K, Aufricht C, Szénási G, Hamar P, Gebeshuber CA. (2020) ECM Characterization Reveals a Massive Activation of Acute Phase Response during FSGS. *Int J Mol Sci,* 21(6).
108. Andrews PA, Zhou W, Sacks SH. (1995) Tissue synthesis of complement as an immune regulator. *Mol Med Today,* 1(4): 202-207.
109. Prins A. Proteases and Protease Inhibitors Involved in Plant Stress Response and Acclimation. University of Pretoria, Pretoria, South Africa,, 2008.
110. Silverman GA, Bird PI, Carrell RW, Church FC, Coughlin PB, Gettins PG, Irving JA, Lomas DA, Luke CJ, Moyer RW, Pemberton PA, Remold-O'Donnell E, Salvesen GS, Travis J, Whisstock JC. (2001) The serpins are an expanding superfamily of structurally similar but functionally diverse proteins. Evolution, mechanism of inhibition, novel functions, and a revised nomenclature. *J Biol Chem,* 276(36): 33293-33296.
111. Turner PC, Moyer RW. (2002) Poxvirus immune modulators: functional insights from animal models. *Virus Res,* 88(1-2): 35-53.

112. Gettins PG. (2002) Serpin structure, mechanism, and function. *Chem Rev,* 102(12): 4751-4804.
113. Law RHP, Zhang Q, McGowan S, Buckle AM, Silverman GA, Wong W, Rosado CJ, Langendorf CG, Pike RN, Bird PI, Whisstock JC. (2006) An overview of the serpin superfamily. *Genome Biology,* 7(5): 216.
114. Winkler IG, Hendy J, Coughlin P, Horvath A, Levesque JP. (2005) Serine protease inhibitors serpina1 and serpina3 are down-regulated in bone marrow during hematopoietic progenitor mobilization. *J Exp Med,* 201(7): 1077-1088.
115. Hunt LT, Dayhoff MO. (1980) A surprising new protein superfamily containing ovalbumin, antithrombin-III, and alpha 1-proteinase inhibitor. *Biochem Biophys Res Commun,* 95(2): 864-871.
116. Bao J, Pan G, Poncz M, Wei J, Ran M, Zhou Z. (2018) Serpin functions in host-pathogen interactions. *PeerJ,* 6: e4557-e4557.
117. Lord MS, Melrose J, Day AJ, Whitelock JM. (2020) The Inter-α-Trypsin Inhibitor Family: Versatile Molecules in Biology and Pathology. *Journal of Histochemistry & Cytochemistry,* 68(12): 907-927.
118. Zhuo L, Kimata K. (2008) Structure and function of inter-alpha-trypsin inhibitor heavy chains. *Connect Tissue Res,* 49(5): 311-320.
119. Okroj M, Holmquist E, Sjölander J, Corrales L, Saxne T, Wisniewski HG, Blom AM. (2012) Heavy chains of inter alpha inhibitor (IαI) inhibit the human complement system at early stages of the cascade. *J Biol Chem,* 287(24): 20100-20110.
120. Perlmutter DH, Cole FS, Kilbridge P, Rossing TH, Colten HR. (1985) Expression of the alpha 1-proteinase inhibitor gene in human monocytes and macrophages. *Proc Natl Acad Sci U S A,* 82(3): 795-799.
121. Perlmutter DH, Travis J, Punsal PI. (1988) Elastase regulates the synthesis of its inhibitor, alpha 1-proteinase inhibitor, and exaggerates the defect in homozygous PiZZ alpha 1 PI deficiency. *J Clin Invest,* 81(6): 1774-1780.
122. Mornex JF, Chytil-Weir A, Martinet Y, Courtney M, LeCocq JP, Crystal RG. (1986) Expression of the alpha-1-antitrypsin gene in mononuclear phagocytes of normal and alpha-1-antitrypsin-deficient individuals. *J Clin Invest,* 77(6): 1952-1961.

123. Knoell DL, Ralston DR, Coulter KR, Wewers MD. (1998) Alpha 1-antitrypsin and protease complexation is induced by lipopolysaccharide, interleukin-1beta, and tumor necrosis factor-alpha in monocytes. *Am J Respir Crit Care Med,* 157(1): 246-255.

124. Cohen AB. (1973) Interrelationships between the human alveolar macrophage and alpha-1-antitrypsin. *J Clin Invest,* 52(11): 2793-2799.

125. Clemmensen SN, Jacobsen LC, Rorvig S, Askaa B, Christenson K, Iversen M, Jorgensen MH, Larsen MT, van Deurs B, Ostergaard O, Heegaard NH, Cowland JB, Borregaard N. (2011) Alpha-1-antitrypsin is produced by human neutrophil granulocytes and their precursors and liberated during granule exocytosis. *Eur J Haematol,* 86(6): 517-530.

126. Bashir MS, Jones DB, Wright DH. (1992) Alpha-1 anti-trypsin and CD30 expression occur in parallel in activated T cells. *Clin Exp Immunol,* 88(3): 543-547.

127. Chen YH, Cheadle CE, Rice LV, Pfeffer PE, Dimeloe S, Gupta A, Bush A, Gooptu B, Hawrylowicz CM. (2021) The Induction of Alpha-1 Antitrypsin by Vitamin D in Human T Cells Is TGF-beta Dependent: A Proposed Anti-inflammatory Role in Airway Disease. *Front Nutr,* 8: 667203.

128. Montesinos-Rongen M, Brunn A, Bentink S, Basso K, Lim WK, Klapper W, Schaller C, Reifenberger G, Rubenstein J, Wiestler OD, Spang R, Dalla-Favera R, Siebert R, Deckert M. (2008) Gene expression profiling suggests primary central nervous system lymphomas to be derived from a late germinal center B cell. *Leukemia,* 22(2): 400-405.

129. Carlson JA, Rogers BB, Sifers RN, Hawkins HK, Finegold MJ, Woo SL. (1988) Multiple tissues express alpha 1-antitrypsin in transgenic mice and man. *J Clin Invest,* 82(1): 26-36.

130. Molmenti EP, Perlmutter DH, Rubin DC. (1993) Cell-specific expression of alpha 1-antitrypsin in human intestinal epithelium. *J Clin Invest,* 92(4): 2022-2034.

131. Ray MB, Desmet VJ, Gepts W. (1977) alpha-1-Antitrypsin immunoreactivity in islet cells of adult human pancreas. *Cell Tissue Res,* 185(1): 63-68.

132. Chelbi ST, Wilson ML, Veillard AC, Ingles SA, Zhang J, Mondon F, Gascoin-Lachambre G, Doridot L, Mignot TM, Rebourcet R, Carbonne B, Concordet JP,

Barbaux S, Vaiman D. (2012) Genetic and epigenetic mechanisms collaborate to control SERPINA3 expression and its association with placental diseases. *Hum Mol Genet,* 21(9): 1968-1978.

133. Gopalan SM, Wilczynska KM, Konik BS, Bryan L, Kordula T. (2006) Astrocyte-specific expression of the alpha1-antichymotrypsin and glial fibrillary acidic protein genes requires activator protein-1. *J Biol Chem,* 281(4): 1956-1963.
134. Biswas S, Chen E, Gao Y, Lee S, Hewlett I, Devadas K. (2022) Modulation of HIV Replication in Monocyte-Derived Macrophages (MDM) by Host Antiviral Factors Secretory Leukocyte Protease Inhibitor and Serpin Family C Member 1 Induced by Steroid Hormones. *Viruses,* 14(1).
135. Janssen U, Thomas G, Glant T, Phillips A. (2001) Expression of inter-alpha-trypsin inhibitor and tumor necrosis factor-stimulated gene 6 in renal proximal tubular epithelial cells. *Kidney Int,* 60(1): 126-136.
136. Zhang S, He H, Day AJ, Tseng SC. (2012) Constitutive expression of inter-α-inhibitor (IαI) family proteins and tumor necrosis factor-stimulated gene-6 (TSG-6) by human amniotic membrane epithelial and stromal cells supporting formation of the heavy chain-hyaluronan (HC-HA) complex. *J Biol Chem,* 287(15): 12433-12444.
137. Martin J, Midgley A, Meran S, Woods E, Bowen T, Phillips AO, Steadman R. (2016) Tumor Necrosis Factor-stimulated Gene 6 (TSG-6)-mediated Interactions with the Inter-α-inhibitor Heavy Chain 5 Facilitate Tumor Growth Factor β1 (TGFβ1)-dependent Fibroblast to Myofibroblast Differentiation. *J Biol Chem,* 291(26): 13789-13801.
138. Yoshihara Y, Plaas A, Osborn B, Margulis A, Nelson F, Stewart M, Rugg MS, Milner CM, Day AJ, Nemoto K, Sandy JD. (2008) Superficial zone chondrocytes in normal and osteoarthritic human articular cartilages synthesize novel truncated forms of inter-alpha-trypsin inhibitor heavy chains which are attached to a chondroitin sulfate proteoglycan other than bikunin. *Osteoarthritis Cartilage,* 16(11): 1343-1355.
139. Kim B, De La Monte S, Hovanesian V, Patra A, Chen X, Chen RH, Miller MC, Pinar MH, Lim YP, Stopa EG, Stonestreet BS. (2020) Ontogeny of inter-alpha

inhibitor protein (IAIP) expression in human brain. *J Neurosci Res,* 98(5): 869-887.

140. Schaer DJ, Vinchi F, Ingoglia G, Tolosano E, Buehler PW. (2014) Haptoglobin, hemopexin, and related defense pathways-basic science, clinical perspectives, and drug development. *Frontiers in physiology,* 5: 415-415.

141. Rifkind JM, Mohanty JG, Nagababu E. (2014) The pathophysiology of extracellular hemoglobin associated with enhanced oxidative reactions. *Front Physiol,* 5: 500.

142. Theilgaard-Monch K, Jacobsen LC, Nielsen MJ, Rasmussen T, Udby L, Gharib M, Arkwright PD, Gombart AF, Calafat J, Moestrup SK, Porse BT, Borregaard N. (2006) Haptoglobin is synthesized during granulocyte differentiation, stored in specific granules, and released by neutrophils in response to activation. *Blood,* 108(1): 353-361.

143. Lai IH, Tsao JH, Lu YP, Lee JW, Zhao X, Chien FL, Mao SJ. (2009) Neutrophils as one of the major haptoglobin sources in mastitis affected milk. *Vet Res,* 40(3): 17.

144. Huntoon KM, Russell L, Tracy E, Barbour KW, Li Q, Shrikant PA, Berger FG, Garrett-Sinha LA, Baumann H. (2013) A unique form of haptoglobin produced by murine hematopoietic cells supports B-cell survival, differentiation and immune response. *Mol Immunol,* 55(3-4): 345-354.

145. Huntoon KM, Wang Y, Eppolito CA, Barbour KW, Berger FG, Shrikant PA, Baumann H. (2008) The acute phase protein haptoglobin regulates host immunity. *J Leukoc Biol,* 84(1): 170-181.

146. Ito N, Yamada M, Morishita K, Nojima S, Motooka K, Sakata N, Asuka T, Otsu R, Takamatsu S, Kamada Y, Mori S, Akita H, Eguchi H, Morii E, Miyoshi E. (2021) Identification of fucosylated haptoglobin-producing cells in pancreatic cancer tissue and its molecular mechanism. *Glycoconj J,* 38(1): 45-54.

147. Skovgaard K, Cirera S, Vasby D, Podolska A, Breum S, Dürrwald R, Schlegel M, Heegaard PM. (2013) Expression of innate immune genes, proteins and microRNAs in lung tissue of pigs infected experimentally with influenza virus (H1N2). *Innate Immun,* 19(5): 531-544.

148. Li P, Gao XH, Chen HD, Zhang Y, Wang Y, Wang H, Wang Y, Xie Y. (2005) Localization of haptoglobin in normal human skin and some skin diseases. *Int J Dermatol,* 44(4): 280-284.
149. Wang H, Gao XH, Wang YK, Li P, He CD, Xie Y, Chen HD. (2005) Expression of haptoglobin in human keratinocytes and Langerhans cells. *Br J Dermatol,* 153(5): 894-899.
150. Tian FJ, Zhang YY, Liu LQ, Xiong Y, Wang ZS, Wang SZ. (2016) Haptoglobin protein and mRNA expression in psoriasis and its clinical significance. *Mol Med Rep,* 14(4): 3735-3742.
151. Smith GF. (1980) Fibrinogen-fibrin conversion. The mechanism of fibrin-polymer formation in solution. *The Biochemical journal,* 185(1): 1-11.
152. Ko Y-P, Flick MJ. (2016) Fibrinogen Is at the Interface of Host Defense and Pathogen Virulence in Staphylococcus aureus Infection. *Seminars in thrombosis and hemostasis,* 42(4): 408-421.
153. Lawrence SO, Simpson-Haidaris PJ. (2004) Regulated de novo biosynthesis of fibrinogen in extrahepatic epithelial cells in response to inflammation. *Thromb Haemost,* 92(2): 234-243.
154. Nguyen MD, Simpson-Haidaris PJ. (2000) Cell type-specific regulation of fibrinogen expression in lung epithelial cells by dexamethasone and interleukin-1beta. *Am J Respir Cell Mol Biol,* 22(2): 209-217.
155. Parrott JA, Whaley PD, Skinner MK. (1993) Extrahepatic expression of fibrinogen by granulosa cells: potential role in ovulation. *Endocrinology,* 133(4): 1645-1649.
156. Kemper C, Köhl J. (2018) Back to the future - non-canonical functions of complement. *Seminars in immunology,* 37: 1-3.
157. Reis ES, Mastellos DC, Ricklin D, Mantovani A, Lambris JD. (2018) Complement in cancer: untangling an intricate relationship. *Nat Rev Immunol,* 18(1): 5-18.
158. Markiewski MM, DeAngelis RA, Benencia F, Ricklin-Lichtsteiner SK, Koutoulaki A, Gerard C, Coukos G, Lambris JD. (2008) Modulation of the antitumor immune response by complement. *Nat Immunol,* 9(11): 1225-1235.

159. Bulla R, Tripodo C, Rami D, Ling GS, Agostinis C, Guarnotta C, Zorzet S, Durigutto P, Botto M, Tedesco F. (2016) C1q acts in the tumour microenvironment as a cancer-promoting factor independently of complement activation. *Nature communications,* 7: 10346-10346.

160. Ajona D, Zandueta C, Corrales L, Moreno H, Pajares MJ, Ortiz-Espinosa S, Martínez-Terroba E, Perurena N, de Miguel FJ, Jantus-Lewintre E, Camps C, Vicent S, Agorreta J, Montuenga LM, Pio R, Lecanda F. (2018) Blockade of the Complement C5a/C5aR1 Axis Impairs Lung Cancer Bone Metastasis by CXCL16-mediated Effects. *American journal of respiratory and critical care medicine,* 197(9): 1164-1176.

161. Wang H, Li Y, Shi G, Wang Y, Lin Y, Wang Q, Zhang Y, Yang Q, Dai L, Cheng L, Su X, Yang Y, Zhang S, Li Z, Li J, Wei Y, Yu D, Deng H. (2020) A Novel Antitumor Strategy: Simultaneously Inhibiting Angiogenesis and Complement by Targeting VEGFA/PIGF and C3b/C4b. *Mol Ther Oncolytics,* 16: 20-29.

162. Kosni NN, Ganti N, Noor MH, Razak IS, Ajat MM, Omar AR. (2016) Expression of complement C5a receptor and the viability of 4T1 tumor cells following agonist-antagonist treatment. *J Cancer Res Ther,* 12(2): 590-596.

163. Maher SG, McDowell DT, Collins BC, Muldoon C, Gallagher WM, Reynolds JV. (2011) Serum proteomic profiling reveals that pretreatment complement protein levels are predictive of esophageal cancer patient response to neoadjuvant chemoradiation. *Ann Surg,* 254(5): 809-816; discussion 816-807.

164. Ajona D, Pajares MJ, Corrales L, Perez-Gracia JL, Agorreta J, Lozano MD, Torre W, Massion PP, de-Torres JP, Jantus-Lewintre E, Camps C, Zulueta JJ, Montuenga LM, Pio R. (2013) Investigation of complement activation product c4d as a diagnostic and prognostic biomarker for lung cancer. *Journal of the National Cancer Institute,* 105(18): 1385-1393.

165. Doni A, Stravalaci M, Inforzato A, Magrini E, Mantovani A, Garlanda C, Bottazzi B. (2019) The Long Pentraxin PTX3 as a Link Between Innate Immunity, Tissue Remodeling, and Cancer. *Frontiers in Immunology,* 10.

166. Thomas C, Henry W, Cuiffo BG, Collmann AY, Marangoni E, Benhamo V, Bhasin MK, Fan C, Fuhrmann L, Baldwin AS, Perou C, Vincent-Salomon A,

Toker A, Karnoub AE. (2017) Pentraxin-3 is a PI3K signaling target that promotes stem cell-like traits in basal-like breast cancers. *Sci Signal,* 10(467).

167. Chang X, Li D, Liu C, Zhang Z, Wang T. (2021) Pentraxin 3 is a diagnostic and prognostic marker for ovarian epithelial cancer patients based on comprehensive bioinformatics and experiments. *Cancer Cell International,* 21(1): 193.
168. Ajona D, Castaño Z, Garayoa M, Zudaire E, Pajares MJ, Martinez A, Cuttitta F, Montuenga LM, Pio R. (2004) Expression of complement factor H by lung cancer cells: effects on the activation of the alternative pathway of complement. *Cancer Res,* 64(17): 6310-6318.
169. Tai CS, Lin YR, Teng TH, Lin PY, Tu SJ, Chou CH, Huang YR, Huang WC, Weng SL, Huang HD, Chen YL, Chen WL. (2017) Haptoglobin expression correlates with tumor differentiation and five-year overall survival rate in hepatocellular carcinoma. *PLoS One,* 12(2): e0171269.
170. Tabassum U, Reddy O, Mukherjee G. (2012) Elevated serum haptoglobin is associated with clinical outcome in triple-negative breast cancer patients. *Asian Pac J Cancer Prev,* 13(9): 4541-4544.
171. Chen J, Cheuk IW-Y, Siu M-T, Yang W, Cheng AS, Shin VY, Kwong A. (2020) Human haptoglobin contributes to breast cancer oncogenesis through glycolytic activity modulation. *American journal of cancer research,* 10(9): 2865-2877.
172. Cao LL, Pei XF, Qiao X, Yu J, Ye H, Xi CL, Wang PY, Gong ZL. (2018) SERPINA3 Silencing Inhibits the Migration, Invasion, and Liver Metastasis of Colon Cancer Cells. *Dig Dis Sci,* 63(9): 2309-2319.
173. Yang G-D, Yang X-M, Lu H, Ren Y, Ma M-Z, Zhu L-Y, Wang J-H, Song W-W, Zhang W-M, Zhang R, Zhang Z-G. (2014) SERPINA3 promotes endometrial cancer cells growth by regulating G2/M cell cycle checkpoint and apoptosis. *International journal of clinical and experimental pathology,* 7(4): 1348-1358.
174. Zhou J, Cheng Y, Tang L, Martinka M, Kalia S. (2017) Up-regulation of SERPINA3 correlates with high mortality of melanoma patients and increased migration and invasion of cancer cells. *Oncotarget,* 8(12): 18712-18725.
175. Poddar NK, Maurya SK, Saxena V. Role of Serine Proteases and Inhibitors in Cancer. In: Chakraborti S, Dhalla NS (szerk.), Proteases in Physiology and

Pathology, doi:10.1007/978-981-10-2513-6_12. Springer Singapore, Singapore, 2017: 257-287.

176. A. T. Phlegmatia Alba Dolens. In: fils J-BBe (szerk.), Clinique Médicale de L'hôtel-dieu de Paris Vol. 3, Paris, France, 1865: 654–712.

177. Simpson-Haidaris PJ, Rybarczyk B. (2001) Tumors and fibrinogen. The role of fibrinogen as an extracellular matrix protein. *Ann N Y Acad Sci,* 936: 406-425.

178. Weisel JW, Litvinov RI. (2017) Fibrin Formation, Structure and Properties. *Sub-cellular biochemistry,* 82: 405-456.

179. Staton CA, Brown NJ, Lewis CE. (2003) The role of fibrinogen and related fragments in tumour angiogenesis and metastasis. *Expert Opin Biol Ther,* 3(7): 1105-1120.

180. Costantini V, Zacharski LR, Memoli VA, Kisiel W, Kudryk BJ, Rousseau SM. (1991) Fibrinogen deposition without thrombin generation in primary human breast cancer tissue. *Cancer Res,* 51(1): 349-353.

181. Rybarczyk BJ, Simpson-Haidaris PJ. (2000) Fibrinogen assembly, secretion, and deposition into extracellular matrix by MCF-7 human breast carcinoma cells. *Cancer Res,* 60(7): 2033-2039.

182. Liu Y-L, Yan Z-X, Xia Y, Xie X-Y, Zhou K, Xu L-L, Shi Y-L, Wang Q, Bi J-W. (2020) Ligustrazine reverts anthracycline chemotherapy resistance of human breast cancer by inhibiting JAK2/STAT3 signaling and decreasing fibrinogen gamma chain (FGG) expression. *American journal of cancer research,* 10(3): 939-952.

183. Palumbo JS, Kombrinck KW, Drew AF, Grimes TS, Kiser JH, Degen JL, Bugge TH. (2000) Fibrinogen is an important determinant of the metastatic potential of circulating tumor cells. *Blood,* 96(10): 3302-3309.

184. Yoon YJ, Kim JA, Shin KD, Shin DS, Han YM, Lee YJ, Lee JS, Kwon BM, Han DC. (2011) KRIBB11 inhibits HSP70 synthesis through inhibition of heat shock factor 1 function by impairing the recruitment of positive transcription elongation factor b to the hsp70 promoter. *J Biol Chem,* 286(3): 1737-1747.

185. Antonietti P, Linder B, Hehlgans S, Mildenberger IC, Burger MC, Fulda S, Steinbach JP, Gessler F, Rödel F, Mittelbronn M, Kögel D. (2017) Interference with the HSF1/HSP70/BAG3 Pathway Primes Glioma Cells to Matrix

Detachment and BH3 Mimetic-Induced Apoptosis. *Mol Cancer Ther,* 16(1): 156-168.

186. Pulaski BA, Ostrand-Rosenberg S. (2001) Mouse 4T1 breast tumor model. *Curr Protoc Immunol,* Chapter 20: Unit 20 22.

187. Schvarcz CA, Danics L, Krenacs T, Viana P, Beres R, Vancsik T, Nagy A, Gyenesei A, Kun J, Fonovic M, Vidmar R, Benyo Z, Kaucsar T, Hamar P. (2021) Modulated Electro-Hyperthermia Induces a Prominent Local Stress Response and Growth Inhibition in Mouse Breast Cancer Isografts. *Cancers (Basel),* 13(7).

188. Danics L, Schvarcz CA, Viana P, Vancsik T, Krenacs T, Benyo Z, Kaucsar T, Hamar P. (2020) Exhaustion of Protective Heat Shock Response Induces Significant Tumor Damage by Apoptosis after Modulated Electro-Hyperthermia Treatment of Triple Negative Breast Cancer Isografts in Mice. *Cancers (Basel),* 12(9).

189. Dank M, Balogh A, Benedek A, Besztercei B, Danics L, Forika G, Garay T, Hamar P, Karászi Á, Kaucsár T, Kiss É, Krenács T, Major E, Mohácsi R, Portörõ I, Ruisanchez É, Schvarcz C, Szász MA, Mbuotidem TJ, Vancsik T, Zolcsák Z, Benyó Z. (2019) [Preclinical and clinical investigation and development of electromagnetic oncological device - experience with solid tumors]. *Magy Onkol,* 63(4): 354-358.

190. Szasz AM, Minnaar CA, Szentmártoni G, Szigeti GP, Dank M. (2019) Review of the Clinical Evidences of Modulated Electro-Hyperthermia (mEHT) Method: An Update for the Practicing Oncologist. *Frontiers in oncology,* 9: 1012-1012.

191. Taesig Jeung SYM, Ji Hoon Choi, Jae Sang Yu, Sangwook Lim , Oliver Szasz. (2014) Modulated electro-hyperthermia applied as monotherapy for various cases having no other options *Oncothermia Journal,* 11: 92-92.

192. Thomas MJ, Major E, Benedek A, Horváth I, Máthé D, Bergmann R, Szász AM, Krenács T, Benyó Z. (2020) Suppression of Metastatic Melanoma Growth in Lung by Modulated Electro-Hyperthermia Monitored by a Minimally Invasive Heat Stress Testing Approach in Mice. *Cancers (Basel),* 12(12).

193. Tsang Y-W, Chi K-H, Huang C-C, Chi M-S, Chiang H-C, Yang K-L, Li W-T, Wang Y-S. (2019) Modulated electro-hyperthermia-enhanced liposomal drug uptake by cancer cells. *International journal of nanomedicine,* 14: 1269-1279.

194. Tsang YW, Huang CC, Yang KL, Chi MS, Chiang HC, Wang YS, Andocs G, Szasz A, Li WT, Chi KH. (2015) Improving immunological tumor microenvironment using electro-hyperthermia followed by dendritic cell immunotherapy. *BMC Cancer,* 15: 708.

195. Qin W, Akutsu Y, Andocs G, Suganami A, Hu X, Yusup G, Komatsu-Akimoto A, Hoshino I, Hanari N, Mori M, Isozaki Y, Akanuma N, Tamura Y, Matsubara H. (2014) Modulated electro-hyperthermia enhances dendritic cell therapy through an abscopal effect in mice. *Oncol Rep,* 32(6): 2373-2379.

196. Jeon TW, Yang H, Lee CG, Oh ST, Seo D, Baik IH, Lee EH, Yun I, Park KR, Lee YH. (2016) Electro-hyperthermia up-regulates tumour suppressor Septin 4 to induce apoptotic cell death in hepatocellular carcinoma. *Int J Hyperthermia,* 32(6): 648-656.

197. Cha J, Jeon TW, Lee CG, Oh ST, Yang HB, Choi KJ, Seo D, Yun I, Baik IH, Park KR, Park YN, Lee YH. (2015) Electro-hyperthermia inhibits glioma tumorigenicity through the induction of E2F1-mediated apoptosis. *Int J Hyperthermia,* 31(7): 784-792.

198. Gadaleta-Caldarola G, Infusino S, Galise I, Ranieri G, Vinciarelli G, Fazio V, Divella R, Daniele A, Filippelli G, Gadaleta CD. (2014) Sorafenib and locoregional deep electro-hyperthermia in advanced hepatocellular carcinoma: A phase II study. *Oncol Lett,* 8(4): 1783-1787.

199. Minnaar CA, Kotzen JA, Naidoo T, Tunmer M, Sharma V, Vangu M-D-T, Baeyens A. (2020) Analysis of the effects of mEHT on the treatment-related toxicity and quality of life of HIV-positive cervical cancer patients. *International Journal of Hyperthermia,* 37(1): 263-272.

200. Vancsik T, Kovago C, Kiss E, Papp E, Forika G, Benyo Z, Meggyeshazi N, Krenacs T. (2018) Modulated electro-hyperthermia induced loco-regional and systemic tumor destruction in colorectal cancer allografts. *J Cancer,* 9(1): 41-53.

201. Meggyeshazi N, Andocs G, Balogh L, Balla P, Kiszner G, Teleki I, Jeney A, Krenacs T. (2014) DNA fragmentation and caspase-independent programmed cell death by modulated electrohyperthermia. *Strahlenther Onkol,* 190(9): 815-822.

202. Serganova I, Rizwan A, Ni X, Thakur SB, Vider J, Russell J, Blasberg R, Koutcher JA. (2011) Metabolic imaging: a link between lactate dehydrogenase A, lactate, and tumor phenotype. *Clin Cancer Res,* 17(19): 6250-6261.

203. Krenács T, Meggyesházi N, Kõvágó C, Kiss É, Forika G, Balogh A, Vancsik T. (2019) [Mechanism of action of modulated electro- hyperthermia (mEHT) induced tumor damage in colorectal adenocarcinoma models]. *Magy Onkol,* 63(4): 359-364.

204. Vancsik T, Forika G, Balogh A, Kiss E, Krenacs T. (2019) Modulated electro-hyperthermia induced p53 driven apoptosis and cell cycle arrest additively support doxorubicin chemotherapy of colorectal cancer in vitro. *Cancer Med,* 8(9): 4292-4303.

205. Vancsik T, Mathe D, Horvath I, Varallyaly AA, Benedek A, Bergmann R, Krenacs T, Benyo Z, Balogh A. (2021) Modulated Electro-Hyperthermia Facilitates NK-Cell Infiltration and Growth Arrest of Human A2058 Melanoma in a Xenograft Model. *Front Oncol,* 11: 590764.

206. Besztercei B, Vancsik T, Benedek A, Major E, Thomas MJ, Schvarcz CA, Krenacs T, Benyo Z, Balogh A. (2019) Stress-Induced, p53-Mediated Tumor Growth Inhibition of Melanoma by Modulated Electrohyperthermia in Mouse Models without Major Immunogenic Effects. *Int J Mol Sci,* 20(16).

207. Hance MW, Nolan KD, Isaacs JS. (2014) The double-edged sword: conserved functions of extracellular hsp90 in wound healing and cancer. *Cancers (Basel),* 6(2): 1065-1097.

208. Pio R, Ajona D, Lambris JD. (2013) Complement inhibition in cancer therapy. *Semin Immunol,* 25(1): 54-64.

209. Cuenca AG, Cuenca AL, Winfield RD, Joiner DN, Gentile L, Delano MJ, Kelly-Scumpia KM, Scumpia PO, Matheny MK, Scarpace PJ, Vila L, Efron PA, LaFace DM, Moldawer LL. (2014) Novel role for tumor-induced expansion of myeloid-derived cells in cancer cachexia. *Journal of immunology (Baltimore, Md. : 1950),* 192(12): 6111-6119.

10. Bibliography of the candidate's publications

Publications used in the thesis:

Schvarcz, C. A., Danics, L., Krenács, T., Viana, P., Béres, R., Vancsik, T., Nagy, Á., Gyenesei, A., Kun, J., Fonovič, M., Vidmar, R., Benyó, Z., Kaucsár, T., Hamar, P. (2021) Modulated electro-hyperthermia induces a prominent local stress response and growth inhibition in mouse breast cancer isografts. *Cancers (Basel).* 13(7):1744. Impact factor: 6.575

Danics, L., **Schvarcz, C. A.**, Viana, P., Vancsik, T., Krenács, T., Benyó, Z., Kaucsár, T., Hamar, P. (2020) Exhaustion of Protective Heat Shock Response Induces Significant Tumor Damage by Apoptosis after Modulated Electro-Hyperthermia Treatment of Triple Negative Breast Cancer Isografts in Mice. *Cancers (Basel).* 12(9):2581. Impact factor: 6.639

Publications, related to but not included in the thesis:

Bencze, N., **Schvarcz, C.A.**, Kriszta, G., Danics, L., Szőke, É., Balogh, P., Szállási, Á., Hamar, P., Helyes, Zs., Botz, B. (2021) Desensitization of Capsaicin-sensitive Afferents Accelerates Early Tumor Growth via Increased Vascular Leakage in a Murine Model of Triple Negative Breast Cancer. *Frontiers in Oncology*. 11:685297 Impact factor: 5.738

Dank, M., Balogh, A., Benedek, A., Besztercei, B., Danics, L., Forika, G., Garay,T., Hamar, P., Karászi, Á., Kaucsár, T., Kiss, É., Krenács, T., Major, E., Mohácsi, R., Portörő, I., Ruisanchez, É., **Schvarcz, Cs.**, Szász, A.M., Thomas, J.M., Vancsik, T., Zolcsák, Z., Benyó, Z. (2019) Elektromágneses daganatterápiás készülék preklinikai és klinikai vizsgálatai, valamint műszaki továbbfejlesztése: tapasztalatok szolid tumorokkal. *Magyar Onkológia*. 63(4):354-358.

Besztercei, B., Vancsik, T.*, Benedek, A., Major, E., Thomas, M.J., Schvarcz, C.A., Krenács, T., Benyó, Z., Balogh, A. (2019) Stress-induced, p53-mediated Tumor Growth Inhibition of Melanoma by Modulated Electrohyperthermia in Mouse Models without Major Immunogenic Effects. *International Journal of Molecular Sciences*. 20(16):4019 Impact factor: 4.556

11. Acknowledgement

I would like to thank my supervisor, Professor Péter Hamar for his support and trust he provided to me from the start of my PhD studies. His professional advice and guidance helped me a lot to get a perspective on making research processes, scientific writing and research attitude in general.

I want to express my highest gratitude to Professor Zoltán Benyó for providing the opportunity to conduct my research at the Institute of Translational Medicine of Semmelweis University and for his professional advice and advocateship during my PhD studies.

I am particularly thankful to Lea Danics, my colleague and friend, with whom we started our research carrier together in 2017. I could always count on her and her support helped me a lot during my PhD.

I would like to thank Tamás Kaucsár for being one of my most influential mentors, who introduced me to the field of research. His professional guidance formed a lot in my work towards the right way.

I would like to thank Tamás Vancsik, my colleague and friend for his help in our group's work. Without his help, we wouldn't have achieved the results serving as the basis of our publications and this dissertation.

I would like to thank for my lab teammates: Pedro Leroy, Mahak Zahra, Nino Giunashvili, Kenan Aloss, Gábor Szénási, Pál Tod, Beáta Róka, Ibolya Pintér, Dániel Bócsi, Zoltán Koós and all of the former members of our workgroup.

I am thankful for Enikő Major, Balázs Besztercei, Andrea Balogh, Ildikó Murányi, Anna Szabó and all the coworkers of the Institute of Translational Medicine. I am also thankful for Gertrúd Forika, Éva Mátrainé Balogh, Rita Uzseka, Zsófia Zsibai from the Department of Pathology and Experimental Cancer Research for all of their help and the employees of Oncotherm Ltd. for their technical support. I would like to express my sincere gratitude to all my co-authors for their effort and help in our publications.

I am grateful to Professor Tibor Krenács and Professor András Szász for reviewing my manuscript and the present dissertation and their professional help during my PhD studies.

Finally, I am most thankful for my parents, sisters, grandparents, whole family, and especially my son and wife. She supported me under all circumstances, without her encouragement, this work could not have been accomplished.